JAERI-Research
2002-028

NEUTRON AND PROTON NUCLEAR DATA EVALUATION FOR ^{235}U AND ^{238}U AT ENERGIES UP TO 250 MeV

December 2002

A. Yu. Konobeyev, Tokio FUKAHORI and Osamu IWAMOTO

日本原子力研究所
Japan Atomic Energy Research Institute

本レポートは，日本原子力研究所が不定期に公刊している研究報告書です。
入手の問合わせは，日本原子力研究所研究情報部研究情報課（〒319-1195　茨城県那珂郡東海村）あて，お申し越しください。なお，このほかに財団法人原子力弘済会資料センター（〒319-1195　茨城県那珂郡東海村日本原子力研究所内）で複写による実費頒布をおこなっております。

This report is issued irregularly.
Inquiries about availability of the reports should be addressed to Research Information Division, Department of Intellectual Resources, Japan Atomic Energy Research Institute, Tokai-mura, Naka-gun, Ibaraki-ken, 319-1195, Japan.

編集兼発行　　日本原子力研究所

JAERI-Research 2002-028

Neutron and Proton Nuclear Data Evaluation for ^{235}U and ^{238}U at Energies up to 250 MeV

A.Yu. Konobeyev, Tokio FUKAHORI and Osamu IWAMOTO

Department of Nuclear Energy System

Tokai Research Establishment

Japan Atomic Energy Research Institute

Tokai-mura, Naka-gun, Ibaraki-ken

(Received October 7, 2002)

Basic features of nuclear data evaluation for uranium isotopes ^{235}U and ^{238}U at intermediate energies are described. The coupled channel optical model was used to obtain total cross section, reaction cross section, angular distributions and transmission coefficients. The direct, pre-compound and evaporation models were used to describe neutron and charged particles emission from excited nuclei. The neutron data evaluated were combined with JENDL-3.3 data below 20 MeV to obtain a full data set in the whole energy range between 10^{-5} eV and 250 MeV. Evaluation of the proton data has been done at energies from 1 to 250 MeV

Keywords: Nuclear Data, Evaluation, Intermediate Energy, Neutron, Proton, Cross Section, Fission, Pre-equilibrium Model, Statistical Model, ^{235}U, ^{238}U

^{235}U と ^{238}U に対する 250MeV までの中性子と陽子核データの評価

日本原子力研究所東海研究所エネルギーシステム研究部

A.Yu. Konobeyev・深堀　智生・岩本　修

(2002 年 10 月 7 日受理)

中間エネルギーにおけるウラン同位体 ^{235}U と ^{238}U の核データ評価の基本的な内容を述べる。チャンネル結合光学モデルを使用し全断面積、反応断面積、散乱断面積の角度分布及び透過係数を求めた。励起原子核からの中性子と荷電粒子放出を直接、前平衡、蒸発モデルを用いて求めた。評価した中性子データは 20 MeV 以下のデータの JENDL-3.3 と合わせることにより、10^{-5} eV から 250 MeV までの全エネルギー領域でのデータセットが得られた。陽子データの評価は 1 から 250 MeV まで行った。

東海研究所：〒319-1195 茨城県那珂郡東海村白方白根 2-4

Contents

1. Introduction 1

2. Brief Description of the Nuclear Models and Codes Used in the Present Work 1

3. Neutron Nuclear Data Evaluation for ^{238}U 5

4. Neutron Nuclear Data Evaluation for ^{235}U 10

5. Proton Nuclear Data Evaluation for ^{238}U 14

6. Proton Nuclear Data Evaluation for ^{235}U 17

7. Conclusion 19

Acknowledgements 19

References 20

目 次

1. 緒言 1

2. 本研究で使用した核反応モデル及びコードの概要 1

3. ^{238}U の中性子核データの評価 5

4. ^{235}U の中性子核データの評価 10

5. ^{238}U の陽子核データの評価 14

6. ^{235}U の陽子核データの評価 17

7. 結論 19

謝辞 19

参考文献 20

This is a blank page.

1. Introduction

Nuclear data evaluation at intermediate energies has a principal meaning for the increasing of accuracy of data used in different applications. Such applications include the development of concept of an accelerator-driven waste incineration system, radiation therapy, isotope production for medicine, material research using accelerators and others.

In the data evaluation a special attention should be given for incident particle energies below 250 MeV, where application of codes based on the intranuclear cascade evaporation model and the QMD-model is rather questionable due to the physical limitations or deviation of calculated and measured nuclear reaction characteristics.

This work is devoted to nuclear data evaluation for uranium isotopes ^{235}U and ^{238}U irradiated by neutrons and protons at energies up to 250 MeV. Theoretical nuclear models, available experimental data and systematics were used for the evaluation.

The neutron data were obtained mainly in the energy region from 20 to 250 MeV. Below 20 MeV data from JENDL-3.3 library for ^{235}U [1] and ^{238}U [2] were considered as the standard and were included completely in the final file prepared from 10^{-5} eV to 250 MeV. The proton data were prepared at energies from 1 to 250 MeV.

2. Brief Description of the Nuclear Models and Codes Used in the Present Work

Coupled-channel optical model has been used to provide total cross section, angular distributions for elastic and inelastic neutron scattering, to calculate the transmission coefficients for neutrons and charged particles. The optimal set of the coupled channel optical model parameters has been derived from analyses of available experimental data to perform the calculations up to 250 MeV. The numerical calculations were carried out with ECIS96 code [3].

The Hauser-Feshbach statistical model and the pre-compound model realized in GNASH code [4] were used for the calculation of particle emission spectra and nuclide production cross sections.

Nuclear level density was obtained on the basis of generalized superfluid model with parameters fitted to cumulative number of low-lying levels and observed neutron resonance densities [5]. The expression for nuclear level density is written as follows

$$\rho(U,J,\pi) = \rho_{qp}(U',J,\pi)\,K_{vib}(U')\,K_{rot}(U'), \qquad (1)$$

where $\rho_{qp}(U',J,\pi)$ is the density of quasi-particle nuclear excitation [6], $K_{vib}(U')$ and $K_{rot}(U')$ are the vibrational and rotational enhancement factors at the effective energy of excitation U'. The vibrational enhancement coefficient $K_{vib}(U')$ was calculated according to Ref.[5].

For the inner saddle and axially symmetric saddle deformation the rotational enhancement factors were obtained as follows $K_{rot}(U') = \sigma_{\perp}^2$, for the asymmetric saddle point $K_{rot}(U') = 2\sqrt{2\pi}\,\sigma_{\perp}^2\,\sigma_{II}$, and for the outer saddle $K_{rot}(U') = 2\sigma_{\perp}^2$ [7], where $\sigma_{\perp}$ and σ_{II} are perpendicular and parallel spin cutoff functions, respectively.

The attenuation of the rotational enhancement with the excitation energy growth was considered according to Refs.[5,8].

The nuclear level density parameters are calculated according to the following expression [5,6]

$$a(U) = \begin{cases} \tilde{a}\left(1+\delta W\,\varphi(U'-E_{cond})/(U'-E_{cond})\right), & \text{if } U' > U_{cr} \\ a(U_{cr}), & \text{if } U' \le U_{cr} \end{cases}, \qquad (2)$$

where the asymptotic value of level density parameter is equal to $\tilde{a} = A(\alpha+\beta A^{-1/3})$, $\alpha=0.073$, $\beta = 0.115$, $\varphi(U) = 1-\exp(-\gamma U)$, $\gamma=0.4/A^{1/3}$ MeV^{-1}, δW is the shell correction.

The effective energy of excitation U', critical energy of the phase transition U_{cr} and the condensation energy E_{cond} were defined according to Refs.[5,6].

For the ground state the shell corrections δW_{gs} in Eq.(2) were calculated on the basis of Myers, Swiatecky approach [9]. For the inner and outer saddle points the values of δW_s^A and δW_s^B were taken from Ref.[7] considering the difference between types of the saddle symmetry.

The fission barriers were considered as spin-dependent and described as follows [10],

$$B_f^i(J) = C^i B_{ld}(J) + f(T)\, g(J)\,(\delta W_s^i - \delta W_{gs}), \quad (3)$$

where $B_{ld}(J)$ is the spin-dependent barrier calculated according to Sierk liquid-droplet model [11], δW_{gs} and δW_s^i are the shell corrections for ground state and the i-th saddle point, respectively, C^i is the adjustment factor, f(T) and g(J) are temperature and spin fade-out functions.

Factors C^i were defined in the present work to provide the agreement between calculations and available experimental data for neutron interactions with uranium isotopes.

The nuclear temperature (T) fade-out function f(T) in Eq.(3) was calculated according to Ref.[10]

$$f(T) = \begin{cases} 1, & \text{for } T \le 1.65\,\text{MeV} \\ 5.809\exp(-1.066\,T), & \text{for } T > 1.65\,\text{MeV} \end{cases}, \quad (4)$$

The function g(J) was defined according to the following expression [10]

$$g(J) = \frac{1}{1+\exp(J - J_{1/2})/\Delta J}, \quad (5)$$

where the parameters $J_{1/2}$ and ΔJ are equal to $J_{1/2}$=24, ΔJ=2.5 [12].

Nuclear dissipation effects resulting in the reduction of the fission width with the growth of the excitation energy were taken into consideration based on the results of Refs.[13,14].

The pre-equilibrium nucleon spectra were calculated with the exciton model taking account of multiple pre-compound emission. Value of the averaged squared matrix element for two body interactions was obtained from Ref.[15], where the parameterization of $<|M|^2>$ has been done as the function of E/n (where E is the excitation energy and "n" is the number of excitons). A description of the pre-compound model including angular momentum effects can be found in Refs.[4,16].

Examples of the (n,xn) and (n,f) reaction cross sections calculation by the GNASH with the global set of model parameters are shown in Figs.1 and 2.

The model used in the original GNASH code [4] to describe the pre-compound spectra of the composite particles contains noticeable shortcomings. An example is given in Fig.3. This figure shows an α-particle spectrum for p+^{209}Bi reaction at a primary energy E_p=90 MeV, calculated on the basis of

the approach described in Ref.[4] and with pre-equilibrium model described below. The calculations with GNASH code are not in the agreement with the available experimental data [17]. It should be noted that any variation of the main parameters of pre-equilibrium model [4] could not provide a reasonable agreement with the experimental data for complex particles emission from the heavy nuclei. The shortcomings of the GNASH algorithm [4] for description of the pre-compound emission for particles with $A \geq 2$ were pointed out also in Ref.[18].

In the present work the pre-equilibrium α-particle emission spectra were calculated in the framework of coalescence pick-up model [19] combined with the knock-out model as shown in Refs.[20,21]. The multiple pre-equilibrium emission was taken into consideration. For deuteron, triton and ^{3}He spectra calculation the exciton pick-up model [22] was applied. The contribution of the direct mechanism to the deuteron emission was considered on the basis of phenomenological approach [23]. All approaches considered above were tested using the available experimental data in the intermediate energy region of primary particles.

Fission neutron- and γ-spectra were obtained on the basis of the model described in Ref.[24]. This model is a refined Fong approach [25] adjusted to experimental data for the fission fragment yields and other fission characteristics in a wide energy range of primary particles. The algorithm described in Ref.[24] was used before as a part of the intranuclear cascade evaporation code [26]. In the present work to increase the accuracy of obtained results this algorithm was introduced in ALICE code [27,28], which is at the same time a modified and extended version of the original Blann code [29]. Application of this code (ALICE/ASH) allows to use more sophisticated models, such as optical model for inverse cross sections and superfluid model for nuclear level density calculations, comparing with the approaches usually used in the codes based on the INC model. Figure 4 shows an example of the fission product yields calculation using ALICE/ASH code for the neutron interactions with ^{235}U at the different primary energies.

3. Neutron Nuclear Data Evaluation for ^{238}U

Neutron scattering and absorption

To obtain total cross sections, angular distributions of scattered neutrons at primary energies up to 250 MeV the coupled channel optical model parameters has been derived from the analyses of the experimental data. For calculations at energies below 100 MeV the parameters from Ref.[30] were adopted. The set of the CC optical model parameters is shown in Table 1.

The calculated total cross section is presented in Fig.5 with the experimental data [31-40] and the results obtained with various sets of optical model parameters taken from Refs.[30,41,42]. The experimental data at energies up to 250 MeV are cited by the compilation [43] and Ref.[30]. Only limited number of measured data below 20 MeV is presented in Fig.5, which shows also values predicted by the systematics. The systematics was obtained in Ref.[44] from an analysis of experimental data for a wide range of nuclei at energies between 14 MeV and 1 TeV.

A good agreement is observed between the result of the present calculations, available experimental data and systematics values. It should be noted that the parameter sets from Refs.[30,41,42] used for the comparison were obtained at energies below 100 MeV demonstrating at these energies good agreement with the experimental data.

There are no experimental data for elastic and reaction cross section for n+^{238}U interactions at energies above 20 MeV. These cross sections obtained with the CC optical model and parameters from Table 1 and Refs.[30,41,42] are shown in Figs.6 and 7, which also show the cross sections calculated at energies below 20 MeV with the optical potential from Ref.[45] used for JENDL-3.3 file preparation.

The elastic scattering cross section calculated with different sets of optical model parameters are in good agreement at energies below 100 MeV. At the higher energies the present calculations are close to the systematics values [44]. For the reaction cross sections (Fig.7) results of the various calculations differ noticeably. The calculation with the optical model parameters from Table 1 is in the agreement with JENDL-3.3 at 20 MeV data and with the systematics [44] at energies above 100 MeV.

Figures 8 and 9 illustrate calculated angular distribution for elastic and inelastic scattering for the lowest 2^+, 4^+ and 6^+ collective levels at primary neutron energies equal to 50 and 200 MeV.

Fission

The fission-evaporation competition was considered for more than two hundred residual nuclei included in the calculation.

The fission of uranium, protactinium and thorium isotopes gives the most contribution in the total fission cross section for n+^{238}U interactions. The other nuclides give less than 7 % of the total fission cross sections. The relative contribution of different elements for ^{238}U fission cross sections calculated by GNASH code is shown in Fig.10.

The fission cross sections calculated with GNASH code is compared in Fig.11 with available experimental data above 20 MeV [46-48]. Measured ratios of the fission cross sections for ^{238}U and ^{235}U from Refs.[46,48] were transformed to the absolute values using the fission cross sections for ^{235}U obtained from the analysis of different experiments.

There is a reasonable agreement between the GNASH calculations and the experimental data (Fig.11). Nevertheless, the final evaluation of (n,f) cross section has been performed based on the statistical analysis of the available experimental data and theoretical calculations. The result is shown in Fig.11 and signed as "JENDL/HE". The fission cross section calculated with ALICE/ASH code is compared with the experimental data in Fig.12.

Neutron production

The neutron production in n+^{238}U interactions has contributions from reactions without fission (e.g. (n,2n)), the emission preceding the fission (e.g. (n,2nf) reaction) and the emission from excited fission fragments.

In the first two cases the neutron spectra have pre-compound tails and noticeable anisotropy in the angular distribution. Such spectra were calculated with GNASH code and the angular distribution was obtained by Kalbach systematics [49]. Examples of neutron spectra calculated at primary particle energies equal to 50 and 200 MeV is shown in Fig.13.

Figure 14 shows the neutron production cross section and the contribution of pre-fission neutron emission calculated by GNASH code. Also the pre-fission neutron yield measured in Ref.[50] is shown. The small correction of the data [50] was made for the comparison with the present calculations. The data were measured in Ref.[50] for p+^{238}U interactions and include the contribution of low energy neutrons[1]. The correction was made to take account of the contribution of the pre-compound neutron emission and the difference between the fission cross sections for proton and neutron induced reactions.

The neutron production cross sections calculated with GNASH code are in good agreement with JENDL-3.3 data at the energy equal to 20 MeV and with the experimental data [50].

The average number of neutrons emitted from the fission fragments and fission neutron spectra were calculated with ALICE/ASH code. The calculations with ALICE/ASH code were performed under assumption [14] that the ratio of the neutron and fission widths is not energy dependent at small excitation energies. Parameters of the models realized in this code [27] were chosen to achieve a general agreement with GNASH calculations and the experimental data.

Figure 15 shows the evaluated average number of prompt neutrons per fission <ν> together with available experimental data above 20 MeV [50,51]. The number of the post-fission neutrons was obtained with ALICE/ASH code; the pre-fission contribution was calculated using GNASH code. Small correction has been made to achieve the agreement with the experimental data [51] below 30 MeV. Calculated normalized fission neutron spectra are shown in Fig.16 for the energy of primary neutrons equal to 30, 60 and 250 MeV. Also the Maxwellian fission spectra are shown here with the temperature

[1] The "best" measured result for 155 MeV-protons on ^{238}U according to Ref.[50] is 5.8 ± 1.0 neutrons per fission for the pre-fission evaporation and 5.1 ± 0.5 neutrons for the post-fission events. The neutron energy is detected below 9 MeV.

Θ defined from the calculated fission spectra maximum location. It is seen, that at the relatively small energies the calculated fission spectra are approximated by Maxwellian shape with a good accuracy. At the high primary particle energies the calculated spectra differs from the Maxwellian ones at the high-energy tail of the spectra.

Charge particle emission

Models to obtain the charged particle emission spectra and yields were described above. Angular distributions for all channels were estimated with Kalbach systematics [49].

Due to the lack of experimental data above 14.5 MeV the calculated charged particle yields are compared with the systematics values at 62, 90 and 160 MeV. The systematics were obtained in the present work based on measured data for charge particle yields in proton induced reactions. These data were taken from Ref.[52] at 62 MeV (8 nuclei from ^{12}C to ^{209}Bi), Ref.[17] at 90 MeV (4 nuclei from ^{27}Al to ^{209}Bi) and from a compilation of the measured data in Ref.[53] around 160 MeV (number of measurements: deuterons: 9 from ^{12}C to ^{208}Pb; tritons: 17 from ^{12}C to ^{232}Th; ^{3}He: 15 from ^{12}C to ^{232}Th; α-particles: 13 from ^{12}C to ^{232}Th). The data and the systematics trends are shown in Figs.17-19.

The obtained formulas to estimate deuteron (σ_d), triton (σ_t), ^{3}He (σ_h) and α-particle (σ_α) production cross sections are the following

<u>62 MeV:</u> <u>90 MeV:</u>

σ_d=61.894 S+79.095, σ_d=290.285 S+98.8155,

σ_t=86.538 S+6.342, σ_t=185.809 S+5.70936,

σ_h= 15.1404 exp(−9.2863 S), σ_h= −16.1045 S+12.0636,

σ_α=183.049 exp(−7.578 S), σ_α=245.854 exp(−4.95716 S),

<u>160 MeV:</u>

σ_d=265.529 S+65.3466,

σ_t=143.391 S+3.96263,

σ_h= −14.1149 S+14.0019,

σ_α= −147.131 S+125.526,

here the cross sections are given in mb, S=(A−2Z)/A, Z,A are atomic and mass numbers of the target nucleus.

Figure 20 shows the calculated total proton production cross section and the contribution of the post-fission evaporation. The experimental data from Ref.[54] at 14.8 MeV and the systematics prediction at 14.5 MeV [55] are also shown. There is a good agreement of the calculated and systematics values at 14.5 MeV. The experimental data from Ref.[54] seem to be too high comparing with other measurements for heavy nuclei (see Ref.[56]).

Calculated total deuteron production cross sections are shown in Fig.21 together with the systematics predictions at 14.5, 62, 90 and 160 MeV. For 14.5 MeV the systematics from Ref.[55] was used. The systematics value [55] was corrected to exclude possible (n,np) reaction contribution from the measured sums of the cross sections for (n,d) and (n,np) reactions.

Figures 22 and 23 show the triton and the ^{3}He–production cross sections. The systematics value for (n,t) reaction at 14.5 MeV was obtained from Ref.[57].

The calculated α-production cross section is presented in Fig.24 together with the experimental data [54,58] and the systematics predictions. The systematics value at 14.5 MeV was obtained according to Ref.[59]. The production of the α-particles from the excited fission fragments is also shown in Fig.24.

γ-emission

Photon emission spectra from excited nuclei, except for the fission fragments, were calculated with GNASH code. The post-fission emission was treated by ALICE/ASH code.

Fig.25 shows the calculated total γ-production cross section and the contribution of the emission from the excited fission fragments. Below 20 MeV data from JENDL-3.3 are shown. There is a good agreement between the values calculated above 20 MeV and those contained in JENDL-3.3 file.

4. Neutron Nuclear Data Evaluation for ^{235}U

Neutron scattering and absorption

The total cross section calculated with ECIS code for ^{235}U is shown in Fig.26 together with available experimental data [34,60,61]. In comparison with ^{238}U there is quite limited number of experimental data for ^{235}U above 20 MeV, which do not cover all energy region under investigation. Also Fig.26 shows the total cross section values taken from intermediate energy file prepared in the Institute of Nuclear Power Engineering (INPE) [62,63]. Evaluated data from Ref.[62] are based mainly on the systematics values from Ref.[44], which are not shown here. A good agreement is observed for two different evaluations.

Figure 27 shows the elastic cross sections for ^{235}U evaluated in the present work and in Ref.[62]. There is no experimental data for the considered cross sections above several MeV's. For the elastic scattering cross section, there is a reasonable agreement between two evaluations.

The present calculations for the elastic angular distribution are compared with the data from Ref.[62] in Fig.28. In general, a good agreement is obtained up to primary neutron energy equal to 50 MeV. Above 50 MeV the evaluation [62] is based on semi-empirical systematics from Ref.[64] for elastic angular distribution and the agreement between different data sets is seen only for low scattering angles.

The direct inelastic scattering cross sections were calculated for the members of the ground state rotational band: $9/2^-$ (46.2 keV), $11/2^-$ (103 keV), $13/2^-$ (170.7 keV) and $15/2^-$ (249.1 keV) levels. It should be noted that JENDL-3.3 evaluation considers the direct components for two of the first levels mentioned here, which give the most contribution to the total direct inelastic scattering cross section. Fig.29 shows the calculated direct inelastic scattering cross sections at energies from 0.1 to 250 MeV.

The inelastic scattering angular distribution with the excitation of the level $9/2^-$ (46.2 keV) evaluated by different authors is compared in Fig.30 for a neutron energy equal to 20 MeV. All evaluations except BROND-2.2 are in reasonable agreement for angles below 30^0. At large scattering angles the difference of the data is more noticeable. A good agreement is achieved between the present calculations and JENDL-3.3 data.

Fission

As for n+^{238}U interactions, the fission of uranium, protactinium and thorium isotopes gives the most contribution in the total fission cross section for ^{235}U. The relative contribution of the different elements to the (n,f) cross section is similar to those for ^{238}U (see Fig.10 and Fig.31). The nuclei with atomic number $Z \leq 89$ give less than 9 % of the total fission cross sections (Fig.31). The recommended evaluated fission cross section for ^{235}U is shown in Fig.32 with the experimental data from Refs.[65,66].

The ratio of the (n,f) cross sections calculated by GNASH code and evaluated values is shown in Fig.33 together with the results obtained using ALICE/ASH code. In general the deviation of the calculated and recommended cross sections is less than 5 % and never exceeds 10 %.

Neutron production

The yields of the neutrons emitted before the fission calculated with GNASH code is shown in Fig.34, as well as the data from JENDL-3.3 and neutron yields preceding the fission. There is a good agreement between results of the present calculations and JENDL-3.3 data as for the total, as for the pre-fission neutron production cross section at the energy equal to 20 MeV.

The neutron production cross sections obtained using GNASH and ALICE/ASH codes are compared in Fig.35. The deviation of the different calculations is less than 10% at the primary neutron

energies below 100 MeV, is equal to 16 % at 150 MeV and 24 % at 250 MeV. The final data included in JENDL-HE file are based on the results obtained with GNASH code. For the illustration the calculated (n,xn) reaction cross sections with the "x" value up to 8 are shown in Fig.36.

Figure 37 shows an example of the angle integrated neutron spectra calculated by GNASH and ALICE/ASH codes at 50 and 250 MeV. There is a good agreement in the shape of the spectra calculated by the different codes except for the high-energy tail, where the direct inelastic scattering with the excitation of the discrete levels plays the dominant role.

The averaged number of prompt fission neutrons <ν> is shown in Fig.38 together with experimental data [51,67]. The pre-fission part of the <ν> was calculated by GNASH code and the post-fission contribution was obtained using ALICE/ASH code. The calculated values are in an excellent agreement with JENDL-3.3 and measured data [51,67].

Figure 39 shows an example of the normalized fission neutron spectrum calculated in the present work at a primary neutron energy equal to 200 MeV. Also the evaluated data from Ref.[62] and the Maxwellian spectrum are shown. The observed deviation of the standard Maxwellian spectrum from the one calculated by the theoretical approach one was discussed above for ^{238}U. The difference between present calculations and data from Ref.[62] is due to the different models used for the spectra calculations. Evaluation [62] is based on the using of the intranuclear cascade evaporation model. The advantage of the model used in the present work and implemented in ALICE/ASH code was discussed above in the Section 2.

Charge particle emission

Proton production cross section calculated using GNASH and ALICE/ASH codes are compared in Fig.35. The difference of the results is about 26 % at the primary neutron energy equal to 250 MeV. An example of the proton spectra calculation at 50 and 250 MeV is shown in Fig.40.

Figure 41 shows a comparison of the evaluated proton production cross section, experimental data [58], systematics value [55] and data from FENDL/A-2 library. Present evaluation is in the agreement with FENDL/A-2 data at energies below 15 MeV. At higher energies difference between two data sets is noticeable.

Evaluated deuteron, triton, ^{3}He and α-particle production cross sections are presented in Figs.42-45 together with FENDL/A-2 data and cross sections estimated using the systematics at energies around 14.5, 62, 90 and 160 MeV.

Deuteron and triton evaluated yields are in the agreement with the systematics values at 14.5 MeV [55] and 14.6 MeV [57]. For (n,α) reaction the systematics prediction [59] at 14.5 MeV seems to be too low. A reasonable agreement is obtained between the evaluated data and FENDL/A-2 at this energy (Fig.45). At the same time the difference between the results of the present evaluation and data from FENDL/A-2 is significant in many cases (Figs.41-45). In this connection it should be noted that the data from FENDL/A-2 for ^{235}U were prepared with THRES code [68] based on rough and simplified description of the reaction mechanism.

The yields of charged particles due to fission fragments de-excitation calculated using ALICE/ASH code are shown in Fig.46. Comparison of the data presented in Fig.46 with the total charged particle production cross sections (Figs.36, 41-45) shows that the post-fission evaporation gives only small contributions to the total particle yields.

γ-emission

Calculated γ-production cross section for ^{235}U is shown in Fig.47 together with JENDL-3.3 data. Also the γ-yield for the post-fission evaporation is shown. An example of the calculated γ-spectrum is given in Fig.48 for the primary neutron energy equal to 250 MeV.

5. Proton Nuclear Data Evaluation for ^{238}U

Scattering angular distribution and reaction cross section

Calculations were performed with the coupled channel model. Parameters of the optical potential were chosen to provide an agreement between experimental and calculated proton angular distributions, reaction cross section and to obtain reasonable energy dependence of the inelastic scattering cross sections at energies up to 250 MeV. Below 65 MeV the parameters of the optical potential from Ref.[30] were used. The available experimental data for elastic and inelastic scattering differential cross sections [69-72] are limited by the energy range up 65 MeV and the using of the optical model parameters from Ref.[30] provides the best agreement with the experimental data comparing with other calculations. Comprehensive illustrations are given in Ref.[30] and are not reproduced in the present work.

Figure 49 shows examples of the calculated elastic angular distributions at energies 150 and 250 MeV where experimental data are not available. The present results are located between the curves obtained using the optical parameters from Ref.[30] and Ref.[42].

Reaction cross section at energies up to 250 MeV were measured for ^{238}U in Refs.[69,73-76]. Fig.50 shows the experimental data and reaction cross sections calculated using different CC model parameters and the systematics from Ref.[44]. The cross sections calculated with the parameters from Refs.[41,42] seem to be too high at energies above 100 MeV. The most reasonable results comparing with the measured data are obtained in the present work.

Figure 51 shows the calculated direct inelastic scattering cross sections for 2^+, 4^+ and 6^+ states of ^{238}U at energies up to 250 MeV.

Fission

Fission cross sections at energies up to 250 MeV were measured for ^{238}U and natural mixture of uranium isotopes in Refs.[69,74,77-102]. Both data for ^{238}U and for natural uranium [78-81,86,95,98] are used in the present work for the comparison with the calculated cross sections. The big number of the data has been obtained 40-50 years ago. For many cases such data differ noticeably from the results of the later measurements.

Figure 52 shows the experimental data and calculated fission cross sections for ^{238}U. The calculations were performed with GNASH and ALICE/ASH codes. The fission cross section predicted by the systematics [103] is also presented in Fig.52. Part of the data measured below 20 MeV is not shown not to "overload" the picture. It is seen that the calculated cross sections and systematics values are close to the measured data from Ref.[92] and [102].

Neutron production

There is the lack of the experimental information for this one of the most important characteristics of the proton interactions with ^{238}U. Despite of the absence of the directly measured neutron production cross section (σ_n), the data from Refs.[50,104,105] can be used for the comparison with the calculated cross sections after some treatment.

Neutron double differential cross sections measured for ^{238}U in Refs.[104,105] at the primary proton energies 113 and 256 MeV were converted in the total neutron production cross section. It was done after the integration by the energy of the measured $d^2\sigma/d\varepsilon d\Omega$ distributions and based on the general dependency of $d\sigma/d\Omega$ [17] from the angle of the emitted particle. The dominating contribution in the neutron production for ^{238}U is due to isotropic low energy neutron emission occurring in the different stages of the reaction. This fact simplifies the recovery of the σ_n values based on the measured $d^2\sigma/d\varepsilon d\Omega$ distributions available at the limited number of angles.

Data from Ref.[50] were measured for pre-fission and post-fission neutron emission at the energy of outgoing neutrons from 0.5 to 9 MeV. These data were transformed to the total σ_n values after the estimation of the contribution of the neutrons not detected in Ref.[50].

Figure 53 shows the evaluated total neutron production cross section and the values recovered from the measured data as discussed above. The contribution of the post-fission neutrons is also shown in Fig.53. There is a reasonable agreement between calculated and measured data.

The part of the total neutron production cross section corresponding to the pre-fission and (p,xn)-emission calculated with GNASH and ALICE/ASH codes is shown in Fig.54. The deviation of the different results at energies above 100 MeV is about 14-17 %.

For an illustration calculated and measured neutron double differential cross sections are shown in Fig.55 for the primary proton energy equal to 113 MeV.

Charged particle production

The proton production cross sections calculated with GNASH and ALICE codes are shown in Fig.54. The main difference between two different calculations is in the energy range below 40 MeV. As in the case of the n+^{238}U interactions the contribution of the post-fission protons emitted are negligible comparing with the total proton production.

The obtained deuteron, triton, ^{3}He and α-particle production cross sections are shown in Fig.56 together with the systematics predictions at 62, 90 and 160 MeV.

Examples of spectra calculated for the charged particle emission are presented in Fig.57 for the primary proton energy equal to 100 MeV.

Isotope production cross sections

The yields of the individual nuclides in the reactions excepting fission at energies below 250 MeV was measured in Refs.[78,81,106-114]. The data can be optionally divided in two groups including the measurements performed in 1954-1961 years and in 1983-1994 years. The quality of the old measurements is quite questionable and sometimes the deviation of the measured values for the same nuclide are considerable (see e.g. data for ^{227}Pa production in Ref.[106] and [107]).

The noticeable part of the measurements is for (p,n) reaction cross section. The experimental data and the evaluated curve for this reaction are shown in Fig.58.

The special attention of experimentalists was devoted to (p,3n) reaction. The yield of ^{236}Np produced in this reaction was measured as for the meta-stable [108-112], as for the ground [111,112] state of the nucleus. Fig.59 shows the evaluated (p,3n) reaction cross sections corresponded to the sum of the ^{236m}Np and ^{236g}Np yields. Data from Ref.[110] corresponding to ^{236m}Np production were transformed to the total ^{236}Np yields based on the isomeric ratio measured in Ref.[111]. Figure 60 shows the (p,xn) reaction cross sections together with the experimental data from Ref.[109].

γ-production

The calculated total γ-production cross section for p+^{238}U interaction is shown in Fig.61. The yield of γ-rays from post-fission evaporation is also shown.

Figure 62 shows the (p,γ) reaction cross section for ^{238}U and single available experimental point at 200 MeV from Ref.[109].

6. Proton Nuclear Data Evaluation for ^{235}U

Scattering angular distribution and reaction cross section

Considerably less amount of experimental data is available for the proton induced reaction characteristics for ^{235}U comparing with ^{238}U.

Figure 63 shows the reaction cross section for ^{235}U calculated using different sets of the coupled channel optical model, estimated according to the systematics [44] and measured in Ref.[69].

The comparison of the calculated elastic angular distribution and single available experimental data [69] at a primary proton energy equal to 22.8 MeV is shown in Fig.64. A good agreement is observed for all range of the detected angles.

The energy dependence of the direct inelastic scattering cross sections is presented in Fig.65 for the members of the ground state rotational band: $9/2^-$ (46.2 keV), $11/2^-$ (103 keV), $13/2^-$ (170.7 keV) and $15/2^-$ (249.1 keV).

Fission

Fission cross section at energies below 250 MeV for ^{235}U was measured in Refs.[77,78,82,92,94,99,102,115-117]. The data obtained by authors of Ref.[116] are cited by Refs.[118,119].

Figure 66 shows the experimental data, the fission cross section calculated by GNASH code, ALICE/ASH code and obtained with systematics [103]. Also the data of the recent fission cross section evaluation [118] are shown. Some measured data presented in Fig.66 are cited by Ref.[120].

There is a reasonable agreement between (p,f) reaction cross sections calculated in the present work, the measured data (excepting data from Ref.[82]), systematics predictions and independent evaluation from Ref.[118].

Neutron production

Evaluated neutron production cross section is shown for ^{235}U in Fig.67 in comparison with the data obtained for ^{238}U.

The evaluated (p,xn) reaction cross section are presented in Fig.68 together with the experimental data from Ref.[109].

Charged particle and γ-ray production

The energy dependence of the charged particle and γ-production cross sections and the shapes of the corresponding spectra are similar for both of uranium isotopes, ^{235}U and ^{238}U. These data were discussed for ^{238}U above. The absolute values of the cross sections differ slightly for ^{238}U and ^{235}U and can be found in the evaluated data files.

7. Conclusion

The description of the new data evaluation in the intermediate energy region for ^{238}U and ^{235}U is presented here. For the first time the evaluated data for ^{238}U and ^{235}U were obtained for neutron and proton induced reactions at energies up to 250 MeV (see Table 2).

The evaluation includes the application of the theoretical models and the experimental data analysis. The coupled channel optical model, pre-compound and equilibrium models were used for nuclear reaction characteristics calculation. The neutron data obtained at energies above 20 MeV were combined with JENDL-3.3 data file to obtain full data set at energies from 10^{-5} eV to 250 MeV. The proton data evaluation has been performed at energies from 1 to 250 MeV.

Acknowledgements

Authors are grateful to Dr. S. Chiba, Research Group of Hadron Science, and members of Nuclear Data Center, for their valuable discussions. The author, A.Yu. Konobeyev, also thank Japan Atomic Energy Research Institute, for giving the opportunity to perform this work.

References

[1] H.Matsunobu, T.Kawano, T.Ohsawa, JENDL-3.3 data file for ^{235}U, Evaluation: March 2000, revision: 31 July 2000.

[2] T.Kawano et al. JENDL-3.3 Data File for ^{238}U, Evaluation: March 2000, Revision: 9 January 2001,

[3] J.Raynal, ECIS96 code, unpublished

[4] P.G.Young, E.D.Arthur, M.B.Chadwick, Comprehensive Nuclear Model Calculations: Theory and Use of GNASH code, Proc. Int. Atomic Energy Agency Workshop on Nuclear Reaction Data and Nuclear Reactors, April 15-May 17, 1996, v.1, p.227; Report LANL, LA-12343-MS (1992).

[5] A.V.Ignatyuk, Level Densities, In: Handbook for Calculations of Nuclear Rèaction Data, IAEA-TECDOC-1034 (1998) p.65

[6] A.V.Ignatyuk, K.K.Istekov, G.N.Smirenkin, *Yadernaja Fizika* **29** (1979) 875.

[7] V.M.Maslov, Fission Level Densities, Handbook for Calculations of Nuclear Reaction Data, IAEA-TECDOC-1034 (1998) p.81

[8] G.Hansen, A.Jensen, *Nucl. Phys.* **A406** (1983) 236.

[9] W.O.Myers, W.J.Swiatecky, *Ark. Fysik* **36** (1967) 343.

[10] A.D.Arrigo, G.Giardina, M.Herman, A.V.Ignatyuk, A.Taccone, *J. Phys. G: Nucl. Part. Phys.* **20** (1994) 365.

[11] A.Sierk, *Phys. Rev.* **C 33** (1986) 2039.

[12] M.Herman, EMPIRE-II Statistical Model Code for Nuclear Reaction Calculations (v.2.13 Trieste), April 5, 2000, unpublished.

[13] E.M.Rastopchin, S.I.Mulgin, Yu.V.Ostapenko, V.V.Pashkevich et al, *Sov. J. Nucl. Phys.* **53** (1991) 741.

[14] A.V.Ignatyuk, G.A.Kudyaev, A.R.Junghans, M.deJong et al, *Nucl. Phys.* **A593** (1995) 519.

[15] C.Kalbach, *Phys. Rev.* **C32** (1985) 1157.

[16] M.B.Chadwick, P.G.Young, P.Oblozinsky, A.Marcinkowski, *Phys. Rev.* **C49** (1994) R2885.

[17] J.R.Wu, C.C.Chang, H.D.Holmgren, *Phys. Rev.* **C19** (1979) 698.

[18] A.V.Ignatyuk, V.P.Lunev, Yu.N.Shubin, E.V.Gai, N.N.Titarenko, A.Ventura, W.Gudowski, *Nucl. Sci. Eng.* **136** (2000) 340.

[19] A.Iwamoto, K.Harada, *Phys. Rev.* **C26** (1982) 1821.

[20] A.Yu.Konobeyev, V.P.Lunev, Yu.N.Shubin, Pre-equlibrium Emission of Clusters, Report IPPE-2465, 1995

[21] A.Yu.Konobeyev, V.P.Lunev, Yu.N.Shubin, *Acta Physica Slovaca* **45** (1995) 705.

[22] N.Sato, A.Iwamoto, K.Harada, *Phys. Rev.* **C28** (1983) 1527.

[23] A.Yu.Konobeyev, Yu.A.Korovin, *Kerntechnik* **61** (1996) 45.

[24] A.Yu.Konobeyev, Yu.A.Korovin, M.Vecchi, *Kerntechnik* **64** (1999) 216.

[25] P.Fong "Statistical Theory of Nuclear Fission", (Gordon and Breach Science Publ., NY), 1969; P.Fong, *Phys. Rev.* **135B** (1964) 1338.

[26] V.S.Barashenkov, A.Yu.Konobeyev, Yu.A.Korovin, V.N.Sosnin, *Atomnaja Energija* **87** (1999) 283.

[27] A.Yu.Konobeyev, Yu.A.Korovin, P.E.Pereslavtsev, Code "ALICE/ASH" for Calculation of Excitation Functions, Energy and Angular Distributions of Emitted Particles in Nuclear Reactions, Report INPE, Obninsk, February 1997

[28] A.I.Dityuk, A.Yu.Konobeyev, V.P.Lunev, Yu.N.Shubin, New Advanced Version of Computer Code ALICE-IPPE, Report IAEA INDC(CCP)-410, 1998

[29] Blann "ALICE 87 (Livermore) Precompound Nuclear Model Code", Report IAEA-NDS-93 REV.O, 1988.

[30] E.Sh.Sukhovitskii, S.Chiba, O.Iwamoto, T.Fukahori, ^{238}U Optical Potential up to 100 MeV Incident Nucleon Enegies, Report JAERI-Research 99-040, 1999; *Nucl. Sci. Technol.* **37** (2000) 120.

[31] J. de Juren, N.Knable, *Phys. Rev.* **77** (1950) 606.

[32] J. de Juren, B.J.Moyer, *Phys. Rev.* **81** (1951) 919.

[33] D.J.Hughes, R.B.Schwartz, Neutron Cross sections, 2d ed., BNL, Upton-New-York, 1958.

[34] J.M.Peterson, A.Bratenahl, J.P.Stoering, *Phys. Rev.* **120** (1960) 521.

[35] P.H.Bowen, J.P.Scanlon, G.H.Stafford et al., *Nucl. Phys.* **22** (1961) 640.

[36] R.J.Schneider, A.M.Cormack, *Nucl. Phys.* **A119** (1968) 197.

[37] S.H.Hayers, P.Stoler, J.M.Clement et al., *Nucl. Sci. Eng.* **50** (1973) 243.

[38] R.B.Schwartz, R.A.Schrack, H.T.Heaton, *Nucl. Sci. Eng.* **54** (1974) 322.

[39] J.Franz, H.P.Gratz, L.Lehman et al., *Nucl Phys.* **A490** (1988) 667.

[40] Shutt et al., 1988, cited by [30].

[41] P.G.Young, Report IAEA INDC(NDS)-335 (1995) p.109.

[42] P.G.Young, Experience at Los Alamos with Use of the Optical Model for Applied Nuclear Data Calculations, In: Handbook for Calculations of Nuclear Reaction Data, IAEA-TECDOC-1034 (1998) p.131.

[43] V.S.Barashenkov "Cross sections of Interactions of Particle and Nuclei with Nuclei", JINR, Dubna, 1993; http://www.nea.fr/html/dbdata/bara.html

[44] V.S.Barashenkov, A.Polanski, Electronic Guide for Nuclear Cross sections, JINR, Dubna, 1995

[45] G.Haouat, J.Lachkar, Ch.Lagrange, J.Jary, J.Sigaud, Y.Patin, *Nucl. Sci. Eng.* **81** (1982) 491.

[46] P.W.Lisowski, A.Gavron, W.E.Parker, S.J.Balestrini et al, Proc. Int. Conf. for Nuclear Science and Technology, Jülich, May 13-17 (1991) p. 732.

[47] V.P.Eismont, A.V.Prokofyev, A.N.Smirnov, K.Elmgren et al, *Phys. Rev.* **C53** (1996) 2911.

[48] A.Yu.Donets, A.V.Evdokimov, A.V.Fomichev, T.Fukahori et al, VII Int. Seminar on Iteraction of Neutrons with Nuclei, Dubna, May 25-28, 1999, p. 357.

[49] C.Kalbach, *Phys. Rev.* **C37** (1988) 2350.

[50] E.Cheifetz, Z.Fraenkel, J.Galin, M.Lefort, J.Peter, X.Tarrago, *Phys. Rev.* **C2** (1970) 256.

[51] J.Frehaut, EXFOR 21685, 1980.

[52] F.E.Bertrand, R.W.Peelle, *Phys. Rev.* **C8** (1973) 1045.

[53] V.S.Barashenkov, V.D.Toneev, Interaction of High Energy Particles and Nuclei with Nuclei (Atomizdat, Moscow, 1972), [English translation: FTD-ID(RS)T-1069-77, Wright-Patterson Air Force Base, Foreign Technology Division, Dayton, Ohio (1977)]

[54] N.Trautmann, R.Denig,G.Herrmann, *Radiochimica Acta* **11** (1969) 168.

[55] A.Yu.Konobeyev, Yu.A.Korovin, *Atomic Energy* **85** (1998) 556 (translated from Russian Journal "*Atomnaja Energija*").

[56] A.Yu.Konobeyev, Yu.A.Korovin, *Nucl. Instr. Meth. Phys. Res.* **B103** (1995) 15.

[57] A.Yu.Konobeyev, V.P.Lunev, Yu.N.Shubin, *Nuovo Cimento* **111A** (1998) 445.

[58] R.F.Coleman, B.E.Hawker, L.P.O'connor, J.L.Perkin, *Proceedings of the Physical Society (London)* **73** (1959) 215

[59] A.Yu.Konobeyev, V.P.Lunev, Yu.N.Shubin, *Nucl. Instr. Meth. Phys. Res.* **B108** (1996) 233.

[60] A.Langsford, P.H.Bowen, G.C.Cox, M.J.M.Saltmarsh, C.M.Newstead, A.E.R.E. Harwell Reports, AERE-PR/NP-9, N36, 1966; EXFOR 20911.

[61] F.L.Green, K.A.Nadolny, P.Stoler, Report USNDC-9, N170 1973; EXFOR 10588.

[62] A.Yu.Konobeyev, Yu.A.Korovin, A.Yu.Stankovsky, Evaluated Neutron Data File for ^{235}U up to 300 MeV, INPE, December 1997.

[63] Yu.A.Korovin, A.Yu.Konobeyev, P.E.Pereslavtsev, A.Yu.Stankovsky, Proc. Int. Conf. for Nuclear Science and Technology, Trieste, May 19-24, 1997, p. 851.

[64] V.S.Sichev, E.K.Gelfand, B.V.Manko, A.Ya.Serov, *Vestsi Akademii Navuk Belaruskai SSR (Ser. Fiz.-Energ.)* [*Transactions of Byelorussian Academy of Sciences (Phys. and Energ. Series)*] **2** (1987) 13.

[65] V.I.Goldanskiy, E.Z.Tarumov, V.S.Penkina, *Doklady Akademii Nauk,* **101** (1955) 1027; EXFOR 41212.

[66] P.W.Lisowski, A.Gavron, W.E.Parker, J.L.Ullmann, S.J.Balestrini et al, Proc. Spec. Meeting on Neutron Cross section Standards for the Energy Region above 20 MeV, Uppsala, Sweden, May 21-23, 1991, p.177.

[67] R.E.Howe, *Nucl. Sci. Eng.* **86** (1984) 157.

[68] J.Kopecky, H.Gruppelaar, Proc. Int. Conf. for Nuclear Science and Technology, Mito, May 30-June 3, 1988, p. 245.

[69] C.B.Fulmer, *Phys. Rev.* **116** (1959) 418.

[70] C.H.King, J.E.Finck, G.M.Crawley, Jr.J.A.Nolen, R.M.Ronningen, *Phys. Rev.* **C20** (1979) 2084.

[71] L.F.Hansen, I.D.Proctor, D.W.Heikkinen, V.A.Madsen, *Phys. Rev.* **C25** (1982) 189.

[72] Y.Takeuchi, H.Sakaguchi, M.Nakamura, T.Ichihara et al., *Phys. Rev.* **C34** (1986) 493.

[73] G.P.Millburn, W.Birnbaum, W.E.Crandall, L. Schecter, *Phys. Rev.* **95** (1954) 1268.

[74] G.L.Bate, J.R.Huizenga, *Phys. Rev.* **B133** (1964) 1471.

[75] P.Kirkby, W.T.Link, *Canadian J. Phys.* **44** (1966) 1847.

[76] A.J.Kirschbaum, Ph.D. Thesis, Report UCRL-1967, Berkeley, 1967.

[77] J.Jungerman, *Phys. Rev.* **79** (1950) 632.

[78] G.H.Mccormick, B.L.Cohen, *Phys. Rev.* **96** (1954) 722.

[79] H.G.Hicks, R.S.Gilbert, *Phys. Rev.* **100** (1955) 1286.

[80] G.N.Harding, cited by Ref.[79].

[81] A.Kjelberg, A.C.Pappas, *Nucl. Phys.* **1** (1956) 322.

[82] H.M.Steiner, J.A.Jungerman, *Phys. Rev.* **101** (1956) 807.

[83] N.S.Ivanova, *Soviet Physics JETP* **4** (1957) 365.

[84] P.C.Stevenson, H.G.Hicks, W.E.Nervik, D.R.Nethaway, *Phys. Rev.* **111** (1958) 886.

[85] G.R.Choppin, J.R.Meriwether, J.D.Fox, *Phys. Rev.* **131** (1963) 2149.

[86] L.Kowalski, C.Stephan, *Journal De Physique* **24** (1963) 901.

[87] A.C.Pappas et al, taken from Table 2.27 in E.Hyde, I.Perlman, G.Seaborg, The Nuclear Properties of the Heavy Elements; III Fission Phenomena, (Englwood Cliffs, N.J.), 1964.

[88] G.R.Choppin, E.F.Meyer, *J. Inorg. Nucl. Chem.* **28** (1966) 1509.

[89] A.C.Pappas, E.Hagebo, *J. Inorg. Nucl. Chem.* **28** (1966) 1769.

[90] S.Baba, H.Umezawa, H.Baba, *Nucl. Phys.* **A175** (1971) 177.

[91] V.S.Bychenkov, M.F.Lomanov, A.I.Obukhov, N.A.Perfilov et al., Preprint ITEP, Moscow, N965, 1972.

[92] O.E.Shigaev, V.S.Bychenkov, M.F.Lomanov, A.I.Obukhov et al, Report Khlopin Radiev. Inst., Leningrad, Ri-17, 1973; M.F.Lomanov, G.G.Shimchuk, R.M.Yakovlev, *Health Phys.* **37** (1979) 677.

[93] V.S.Bychenkov, M.F.Lomanov, A.I.Obukhov, N.A.Perfilov et al, *Sov. J. Nucl. Phys.* **17** (1973) 496.

[94] J.R.Boyce, T.D.Hayward, R.Bass, H.W.Newson et al., *Phys. Rev.* **C10** (1974) 231.

[95] A.Calboreanu, Em.Cincu, C.Pencea, O.Salagean, I.Manzatu, *Revue Roumaine De Physique* **21** (1976) 69.

[96] A.T.Kandil, *J. Inorg. Nucl. Chem.* **38** (1976) 37.

[97] V.N.Kononov, E.D.Poletaev, P.P.D'jachenko, *Sov. J. Nucl. Phys.* **27** (1978) 162.

[98] F.D.Bechetti, J.Janecke, P.Lister, K.Kwiatkowski, H.Karwowski, S.Zhou, *Phys. Rev.* **C28** (1983) 276.

[99] N.N.Ajitanand, K.N.Iyengar, R.P.Anand, D.M.Nadkarni, A.K.Mohanty, *Phys. Rev. Let.* **58** (1987) 1520.

[100] J.C.Gehring, B.B.Back, R.R.Betts, P.B.Fernandez et al., EXFOR O0642, C0088.

[101] E.Karttunen, M.Brenner, V.A.Rubchenya, S.A.Egorov et al, *Nucl. Sci. Eng.* **109** (1991) 350.

[102] A.N.Smirnov, I.Yu.Gorshkov, A.V.Prokofiev, V.P.Eismont, Proc. 21st Intern. Symp. on Nuclear Phys., Gaussig, Germany, November 4-8, 1991, p.214; V.P.Eismont, A.V.Prokofiev, A.N.Smirnov, Proc. Int. Conf. for Nuclear Science and Technology, Gatlinburg, May 9-13, 1994, p.397.

[103] T.Fukahori, S.Pearlstein, Report BNL-45200 (1991).

[104] M.M.Meier, D.A.Clark, C.A.Goulding, J.B.McClelland et al., EXFOR C0171

[105] M.M.Meier, W.B.Amian, C.A.Goulding, G.L.Morgan, C.E.Moss, EXFOR C0168

[106] M.Lindner, R.N.Osborne, *Phys. Rev.* **103** (1956) 378.

[107] W.W.Meinke, G.C.Wick, G.T.Seaborg, *J. Inorg. Nucl. Chem.* **3** (1956) 69.

[108] M.Lefort, *Comptes Rendus* **B253** (1961) 2221.

[109] Y.Y.Chu, M.L.Zhou, *IEEE Transactions on Nuclear Science* **30** (1983) 1153.

[110] V.A.Ageev, V.Ya.Golovnya, E.A.Gromova, S.A.Egorov et al., *Yadernaja Fizika* **46** (1987) 700; Exfor 83026.

[111] S.S.Kovalenko, Yu.A.Selitsky, V.B.Funshtein, S.V.Khlebnikov, V.A.Yakov- lev, Proc. Int. Conf. for Nuclear Science and Technology, Mito, May 30-June 3, 1988, p.995.

[112] J.Aaltonen, M.Brenner, S.A.Egorov, A.M.Fridkin et al, *Phys. Rev.* **C41** (1990) 513.

[113] B.Ya.Guzhovskii, S.N.Abramovich, A.G.Zvenigorodskii, V.S.Rudnev, S.V. Trusillo, Proc. Int. Conf. for Nuclear Science and Technology, Gatlinburg, May 9-13, 1994, p.390.

[114] A.Yokoyama, N.Takahashi, N.Nitani, H.Baba et al., *Z. Phys.* **A356** (1996) 55.

[115] V.A.Konshin, E.S.Matusevich, V.I.Regushevski, *Yadernaja Fizika* **2** (1965) 682; [Translation: *Sov. J. Nucl. Phys.* **2** (1966) 489].

[116] V.S.Bychenkov, M.F.Lomanov, A.I.Obukhov, G.G.Shimchuk, R.M.Yakovlev, 1989, 1992, cited by [118,119].

[117] T.Ohtsuki, Y.Nagame, K.Tsukada, N.Shinohara et al, *Phys. Rev.* **C44** (1991) 1405.

[118] S.Yavshits, O.Grudzevich, G.Boykov, V.Ippolitov, Proc. of the 2000 Symposium on Nuclear Data, Nov. 16-17, 2000, Tokai, Japan, JAERI-Conf 2001-006, INDC(JPN)-188/U, March 2001, p.277.

[119] V.A.Konshin, Report JAERI-Research 95-036, June 1995, p.76

[120] T.Fukahori, Compilation of Experimental Data for Fission Cross sections.

[121] P.G.Young, E.D.Arthur, M.Bozoian, T.R.England et al, Report LA-11753-MS, UC-000, July 1990.

Table 1. Optical model parameters for neutron interactions with ^{238}U at energies up to 250 MeV. (Potentials and energy are given in MeV, radii and diffuseness in fm)

Parameter	Energy range
V_R=46.65 – 0.307E+0.001 E^2 – 5.0 (A-2Z)/A,	E ≤ 100
V_R =64.214 – 0.47352 E+ 0.0009088 E^2– 5.0 (A-2Z)/A,	E > 100
W_D=4.49+0.491 E–9.0 (A-2Z)/A,	E ≤ 11.2
W_D=9.99–0.071 (E–11.2) –9.0 (A-2Z)/A,	11.2 < E ≤ E_{max}
W_D =0.0,	E > E_{max}
W_V=0.0,	E ≤ 11.2
W_V= 0.1000 (E-11.2),	11.2 < E < 150
W_V =13.88,	E ≥ 150
V_{SO}=6.02,	
r_R=1.2616,	
a_R=0.643,	
r_D=1.2331,	
a_D=0.567+0.0022 E,	E ≤ 11.2
a_D=0.5916,	E > 11.2
r_V=1.245,	
a_V=0.324,	
r_{SO}=1.12,	
a_{SO}=0.59-0.002 E,	E ≤ 100
a_{SO}=0.39,	E > 100
β_{20}=0.219, β_{40}=0.053, β_{60}=–0.0065,	
E_{max} = 126.761 (1.1984–(A-2Z)/A).	

Table 2. Staus of intermediate nuclear data evaluation for ^{238}U and ^{235}U.

Organization	Year	Primary particle	Maximal primary energy	Basic data below 20 MeV for neutron data file	Reference
U-238					
LANL	1988, 1989	neutrons, protons	100 MeV	ENDF/B-V	[121]
INPE, FZK	1995	neutrons	50 MeV	ENDF/B-VI, partially JENDL-3.2	[63]
IPPE, ENEA, RIT	1999	neutrons	150 MeV	ENDF/B-VI	[18]
JAERI	2001	neutrons, protons	250 MeV	JENDL-3.3	This work
U-235					
INPE, FZK	1997	neutrons	300 MeV	ENDF/B-VI	[63]
JAERI	2001	neutrons, protons	250 MeV	JENDL-3.3	This work

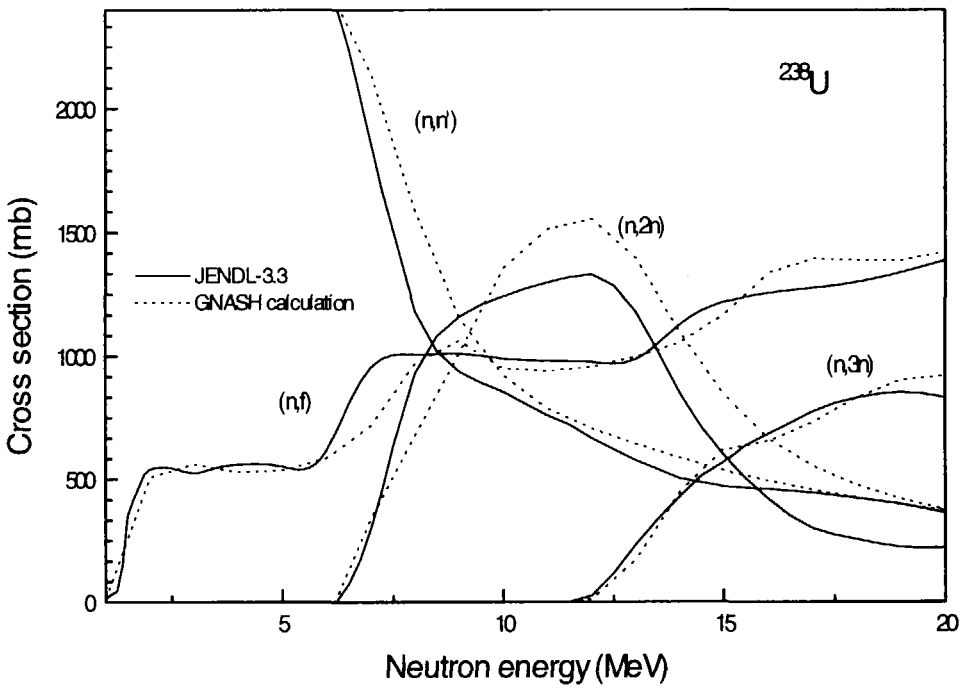

Fig.1 Example of GNASH code calculation (dotted line) with the global set of model parameters for (n,xn) and (n,f) reaction cross sections for ^{238}U as well as JENDL-3.3 (solid line).

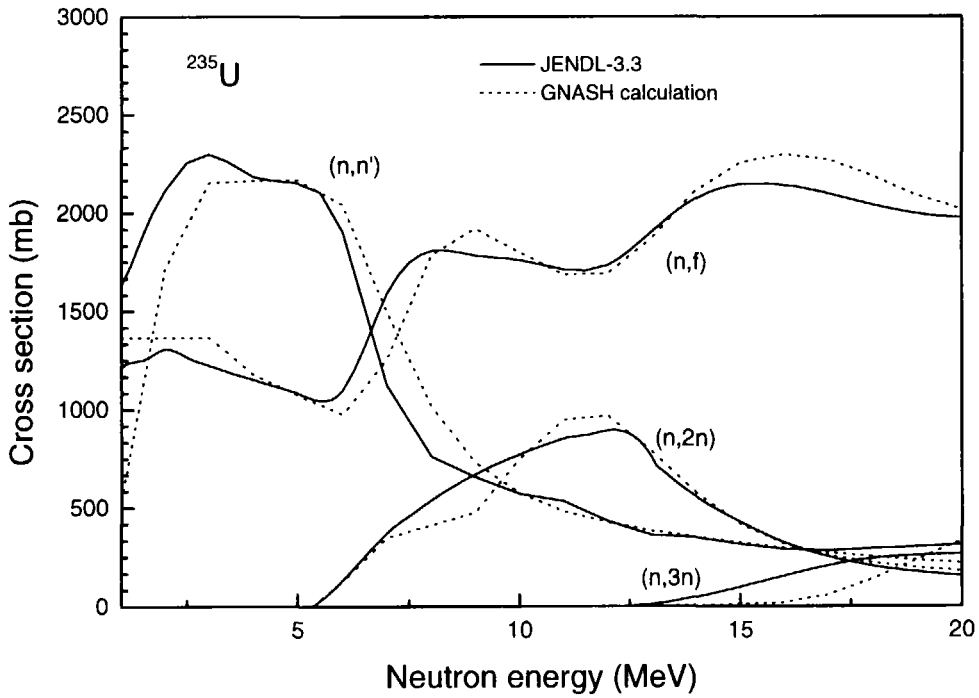

Fig.2 The example of GNASH code calculation (dotted line) with the global set of the model parameters for (n,xn) and (n,f) reaction cross sections for ^{235}U as well as JENDL-3.3 (solid line).

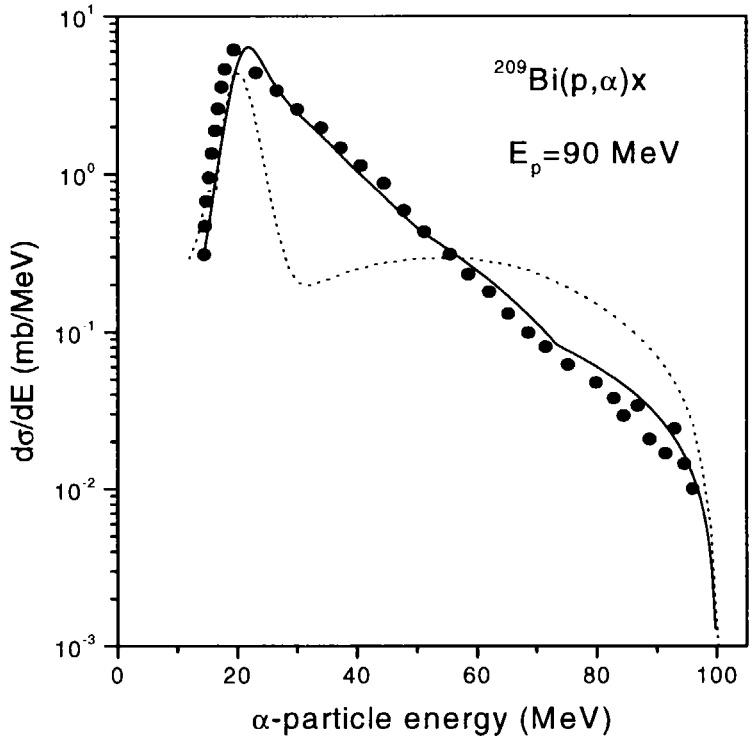

Fig.3 An α-particle spectrum for p+^{209}Bi reaction at E_p=90 MeV calculated using the pre-compound model for complex particle emission of GNASH [4] (dotted line) and with approach described in the present work (solid line). The experimental data are from Ref.[17].

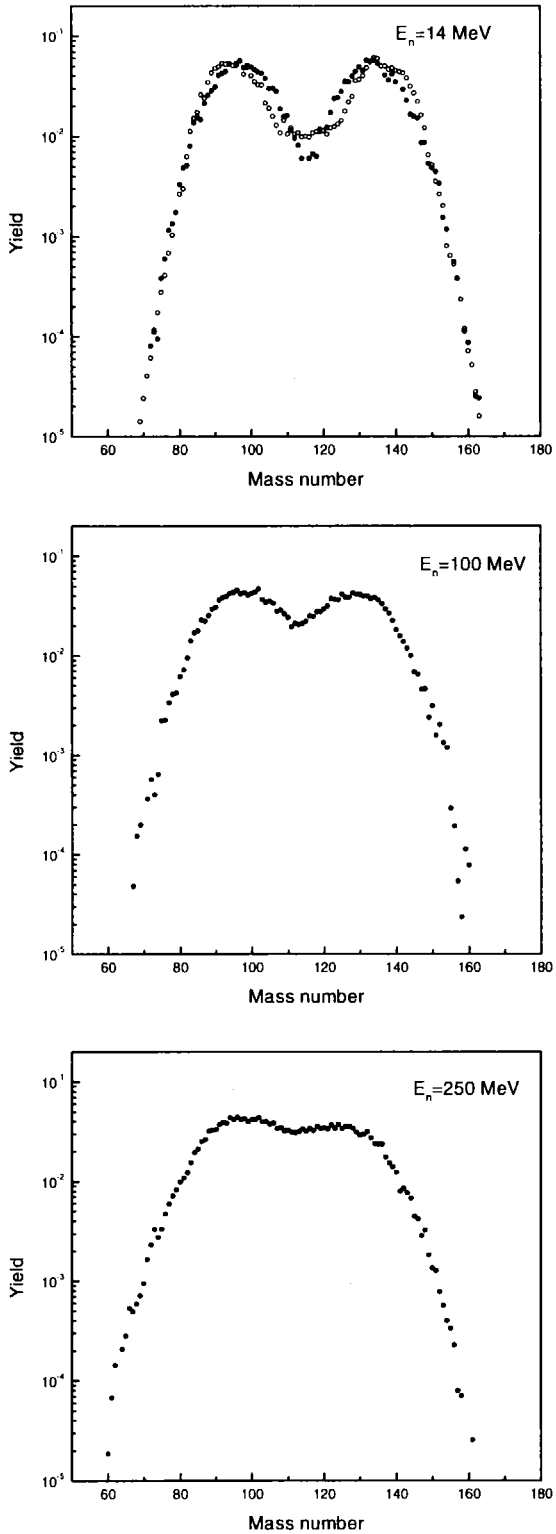

Fig.4 Fission product yields for the neutron interactions with ^{235}U at energies of 14, 100 and 250 MeV calculated using ALICE/ASH code (•). Data for 14 MeV-neutrons taken from JENDL-3.2 file are shown in the top figure (o).

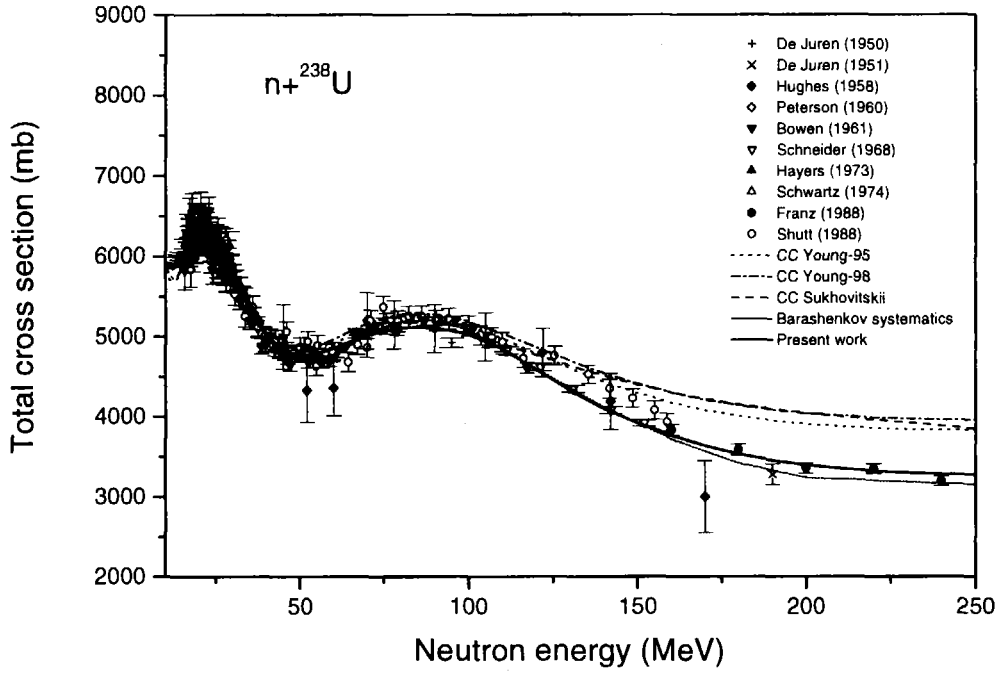

Fig.5 Total neutron cross section for ^{238}U calculated using different sets of coupled channel optical model parameters. Measured data are taken from Ref.[31-40].

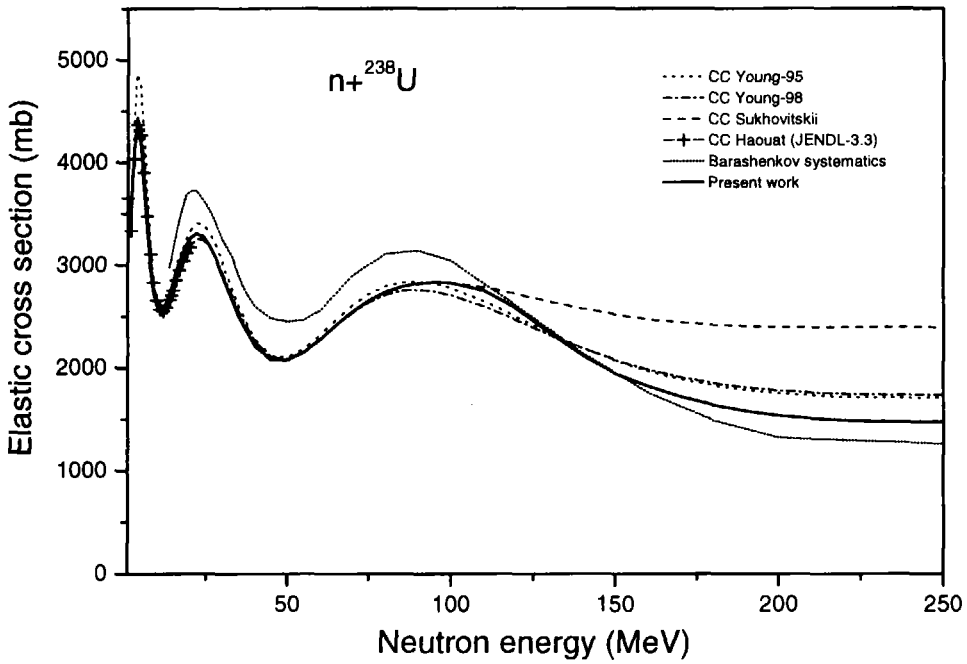

Fig.6 Elastic neutron cross section for ^{238}U calculated using different sets of coupled channel optical model parameters.

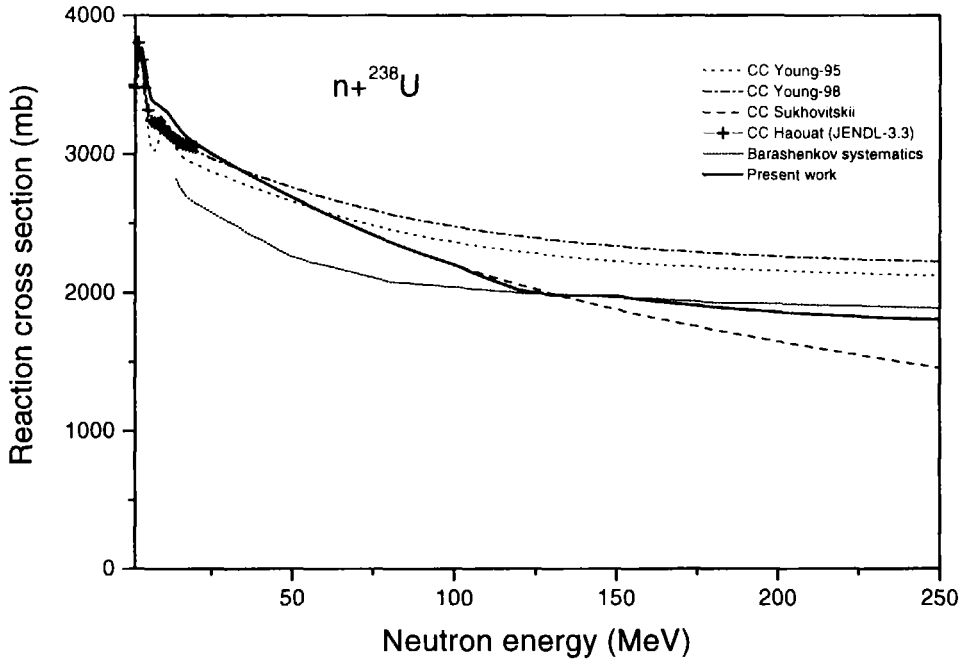

Fig.7 Reaction neutron cross section for ^{238}U calculated using different sets of the coupled channel optical model parameters.

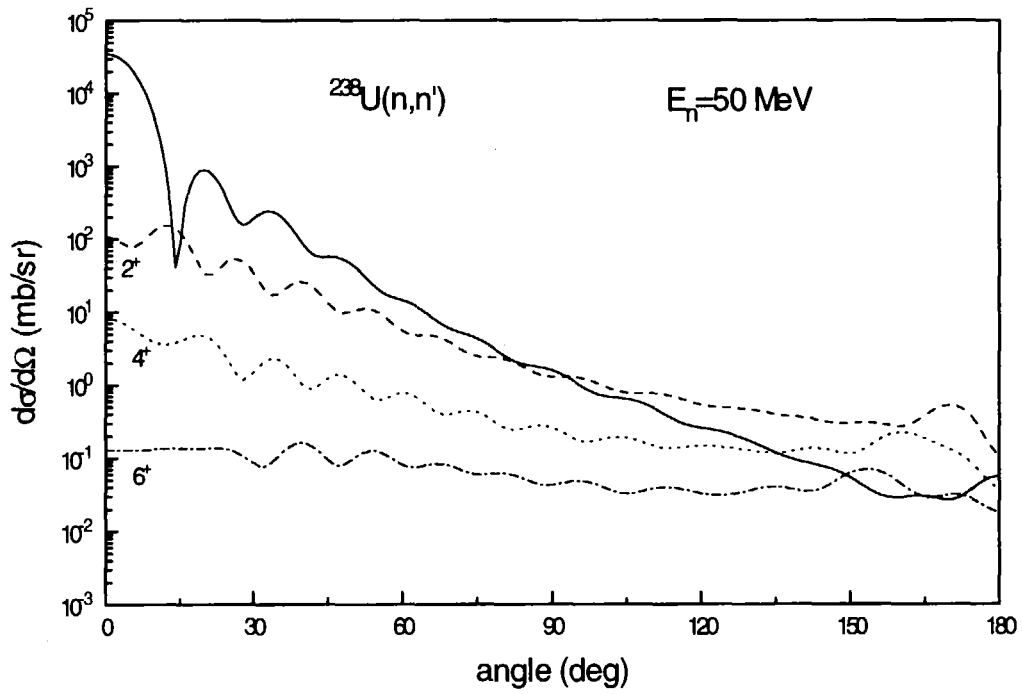

Fig.8 Angular distribution for elastic and inelastic neutron scattering at the incident neutron energy equal to 50 MeV obtained in the present work.

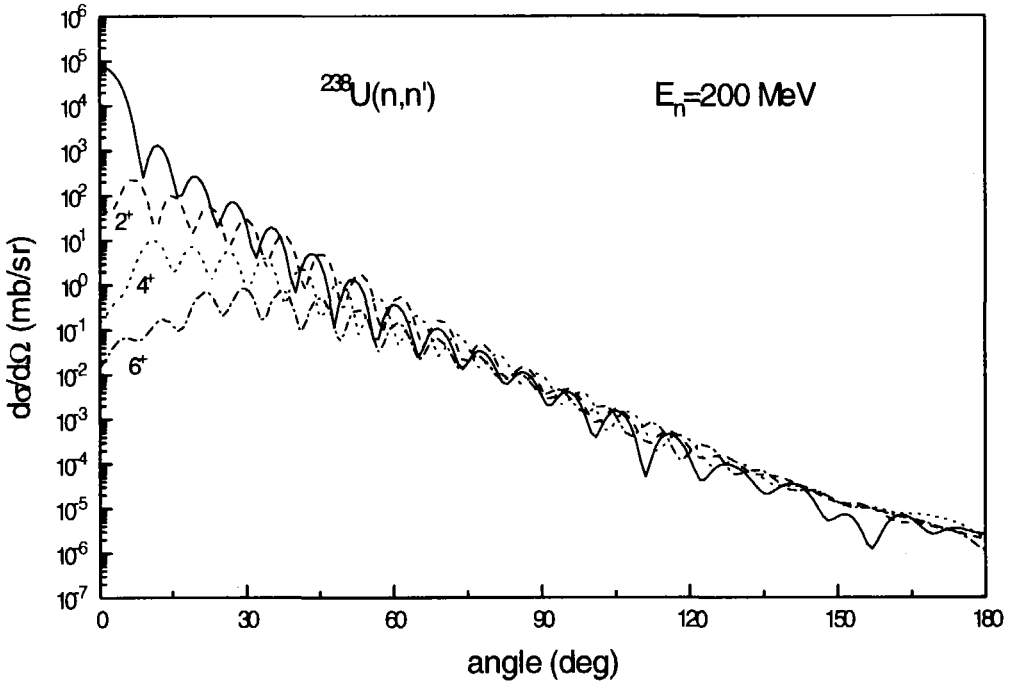

Fig.9 Angular distribution for elastic and inelastic neutron scattering at the incident neutron energy equal to 200 MeV obtained in the present work.

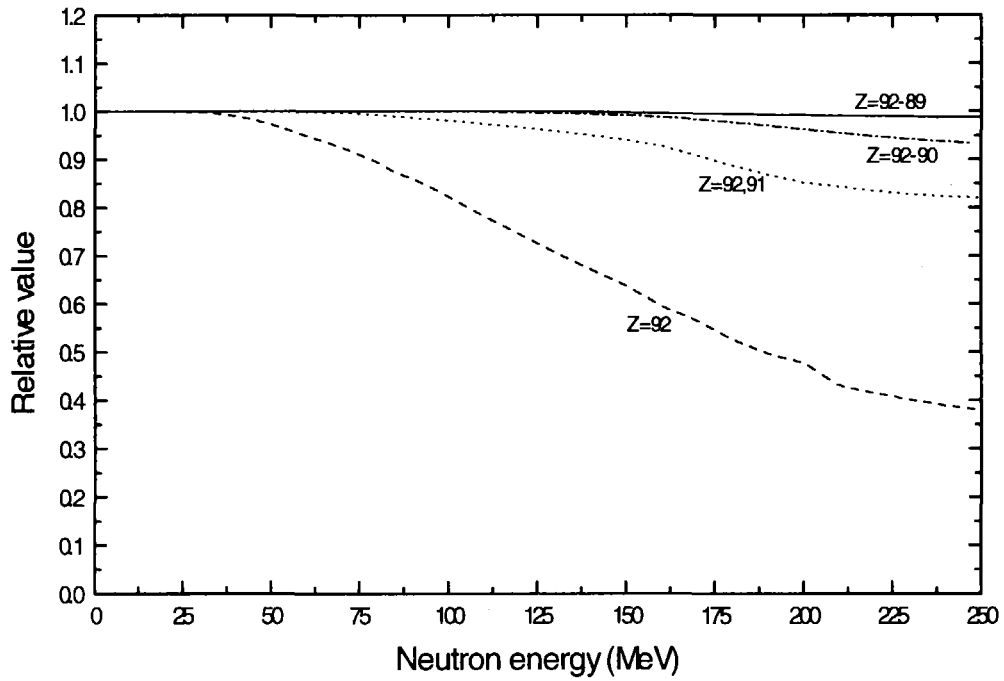

Fig.10 The relative contribution of the nuclei with the different atomic number in the total fission cross section for ^{238}U calculated by GNASH code.

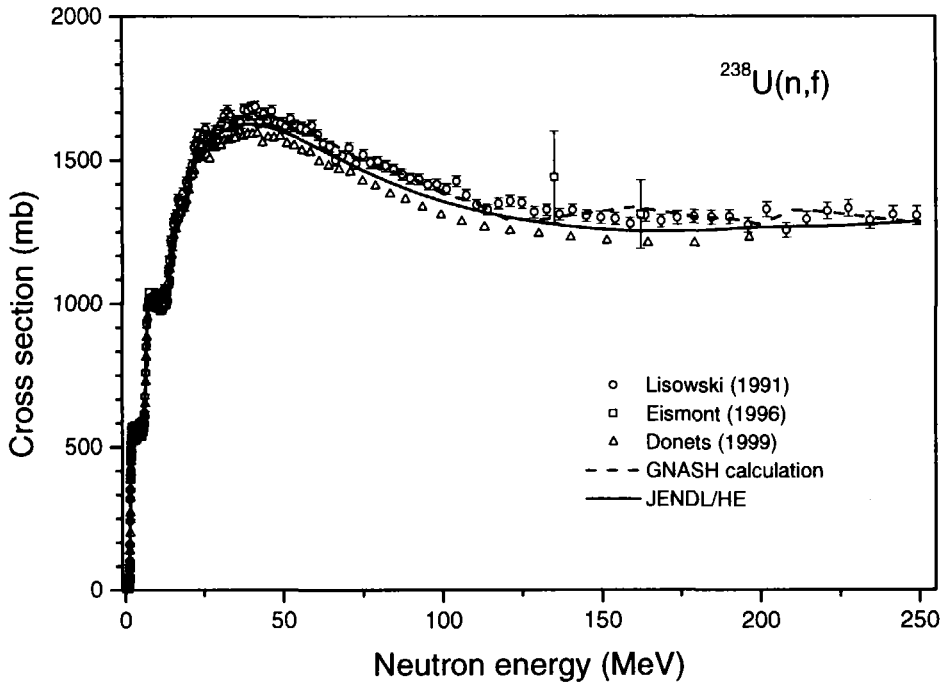

Fig.11 Fission cross section for ^{238}U calculated by GNASH code (dashed line), evaluated based on the results of calculations and experimental data (solid line) and experimental data from Ref.[46-48].

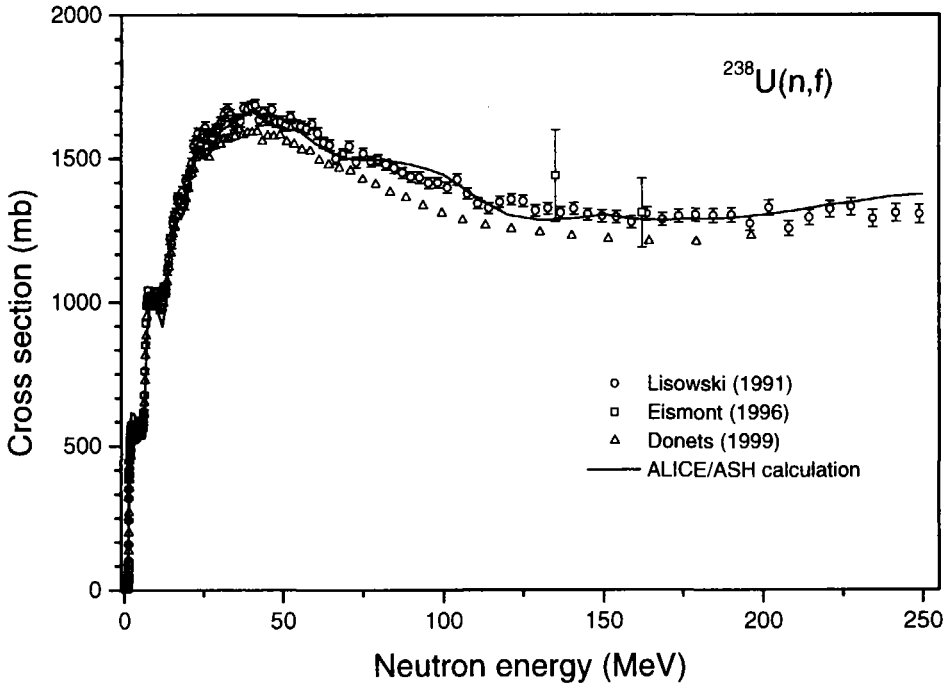

Fig.12 Fission cross section for ^{238}U calculated by ALICE/ASH code (solid line).

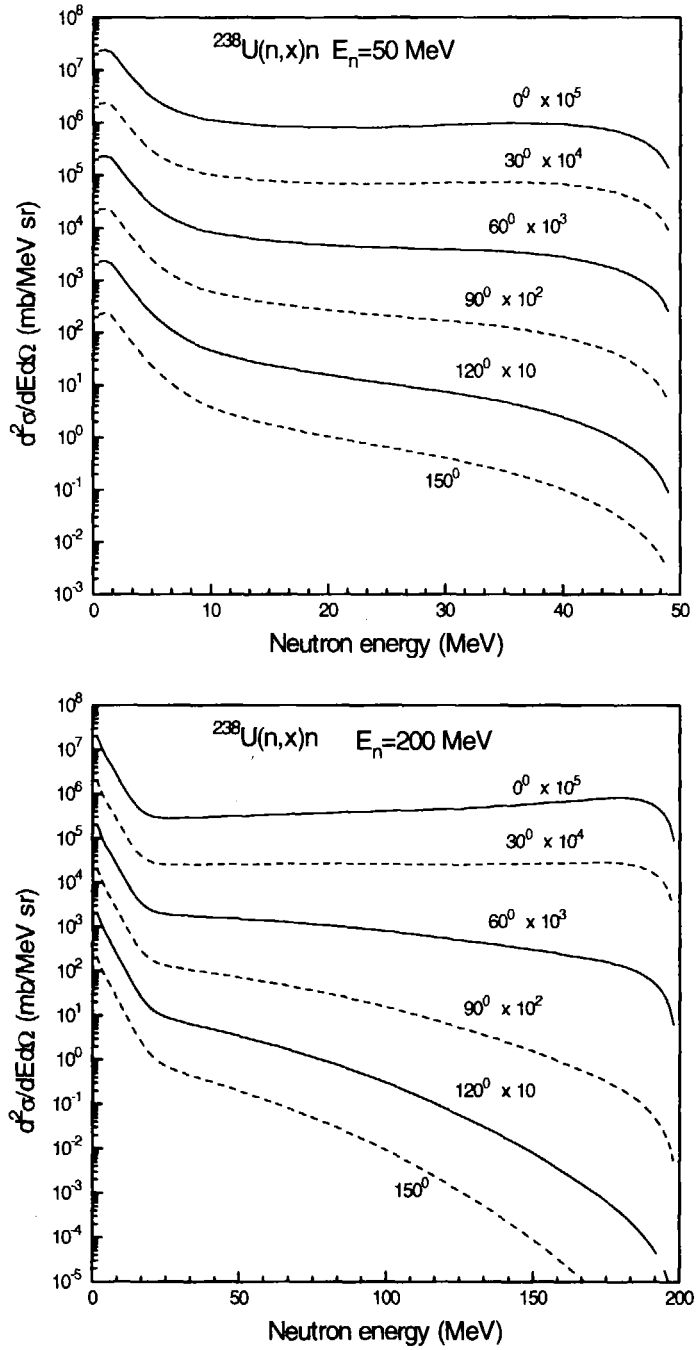

Fig.13 Examples of neutron double differential cross sections calculated with GNASH code and Kalbach systematics [49] for ^{238}U at incident neutron energy equal to 50 and 200 MeV.

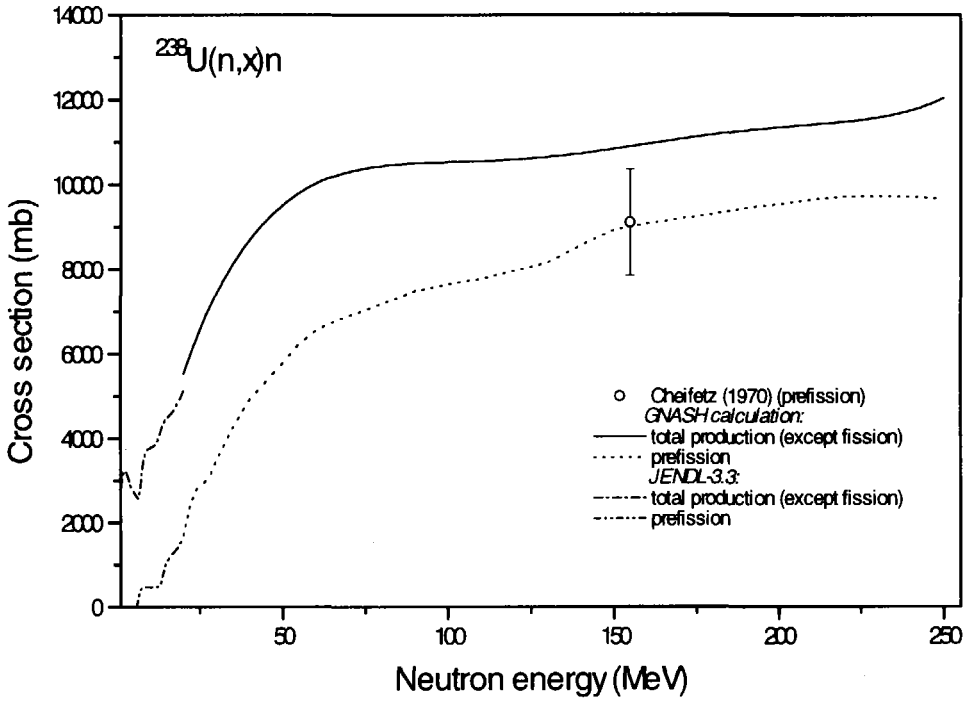

Fig.14 Neutron production cross section with and without the contribution from the post-fission evaporation calculated by GNASH code for ^{238}U and taken from JENDL-3.3 file.

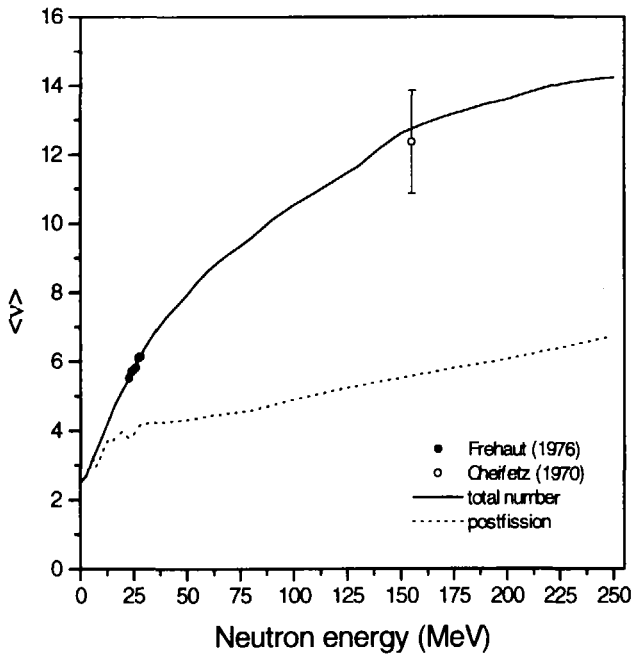

Fig.15 Total number of prompt fission neutrons and the neutrons emitted from excited fission fragments evaluated in the present work for ^{238}U. Experimental data are from Refs.[50,51].

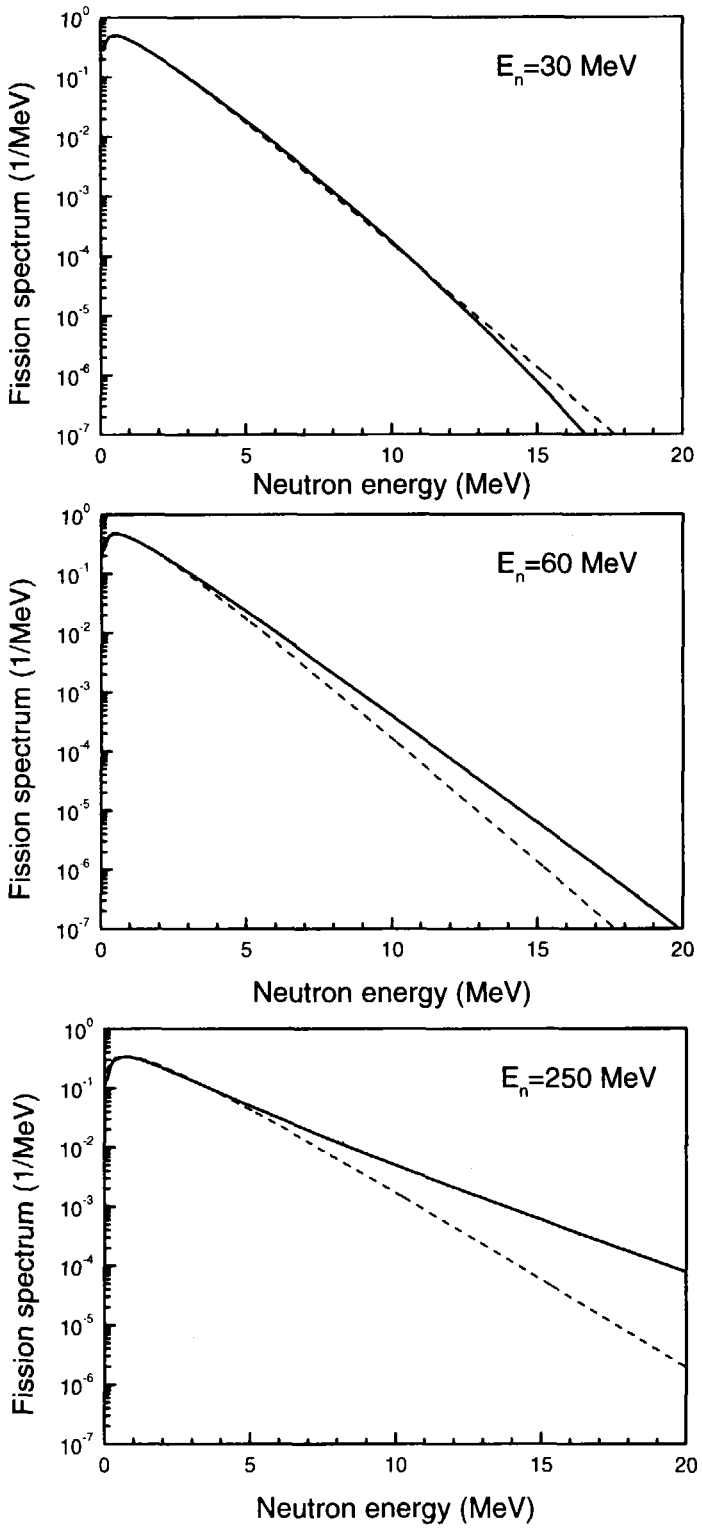

Fig.16 Normalized fission neutron spectra calculated in the present work for ^{238}U (solid line) and Maxwellian spectra (dashed line) for the primary neutron energies equal to 30, 60 and 250 MeV

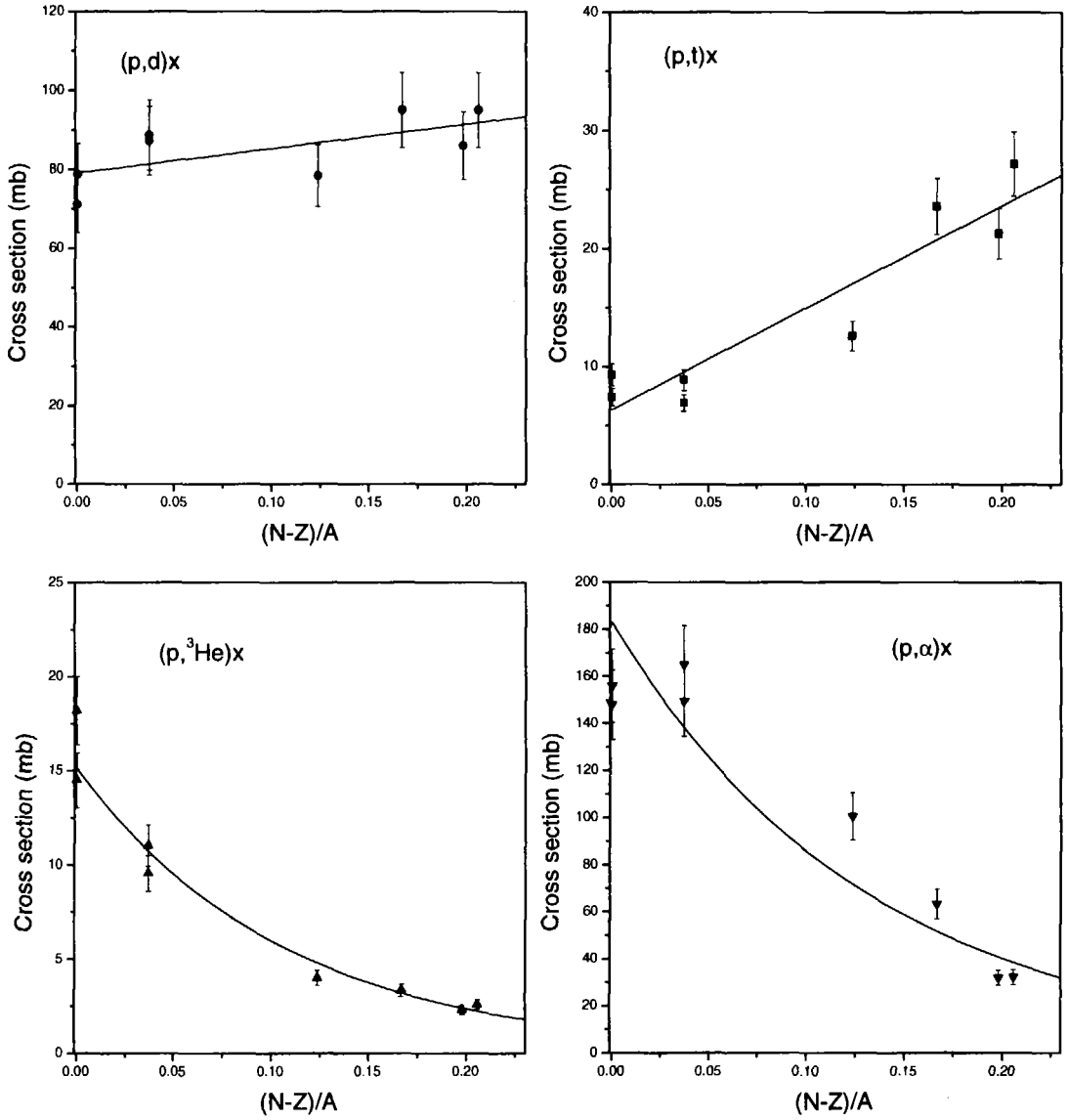

Fig.17 Experimental deuteron, triton, ^{3}He and α-particle production cross sections for 62 MeV-proton induced reactions [52] and the systematics trends (solid line).

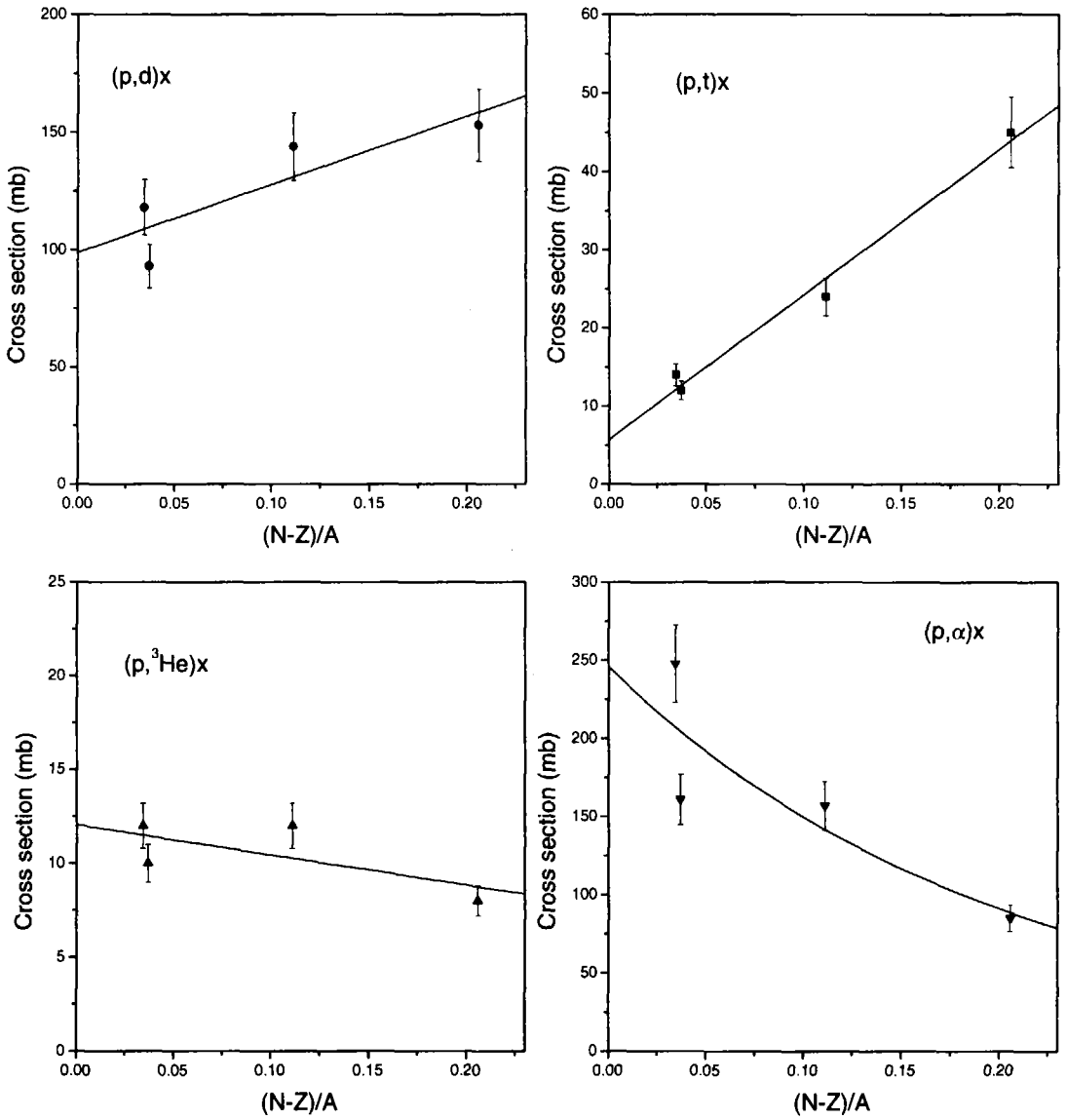

Fig.18 Experimental deuteron, triton, ^{3}He and α-particle production cross sections for 90 MeV-proton induced reactions [17] and the systematics trends (solid line).

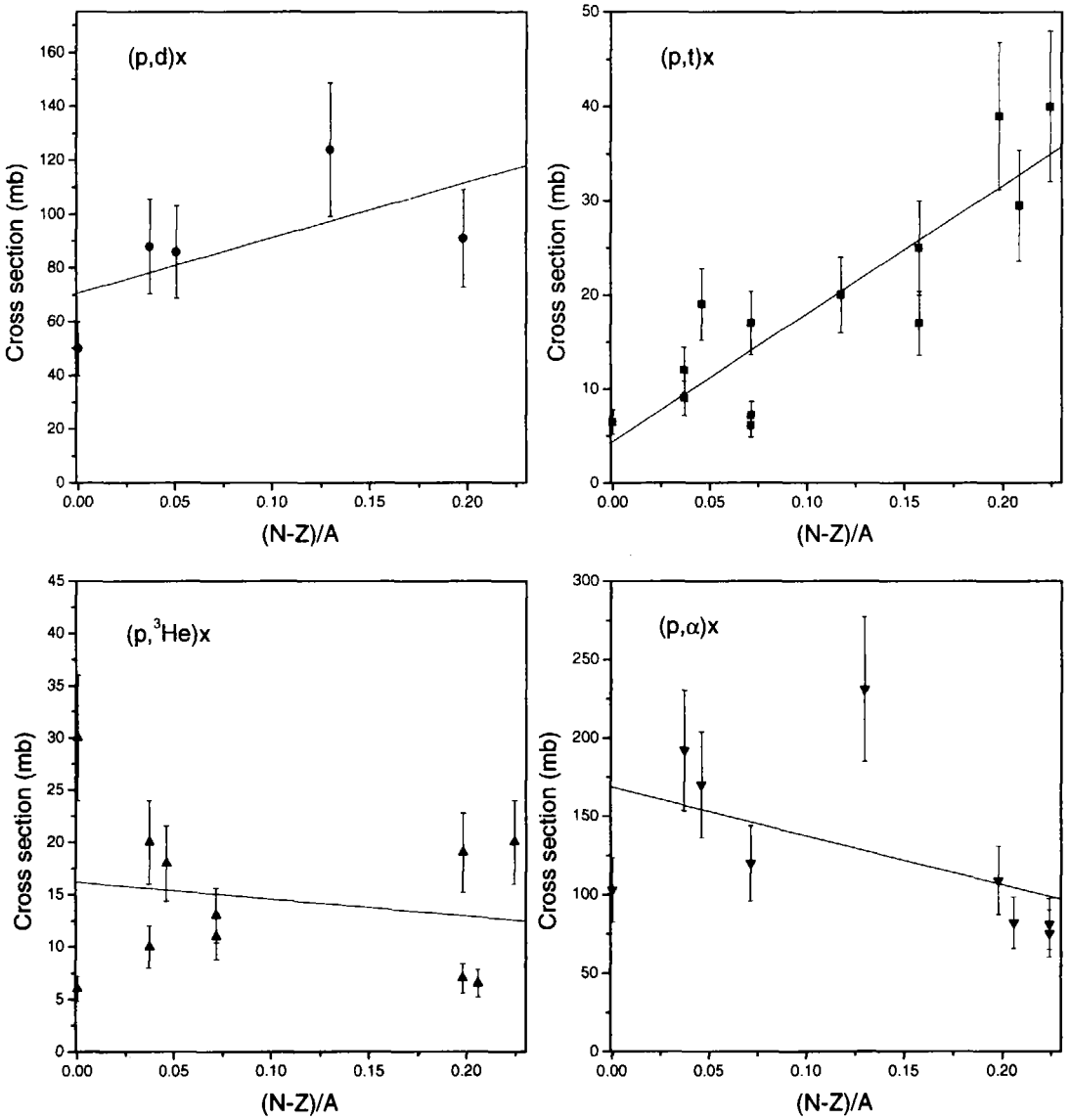

Fig.19 Experimental deuteron, triton, ^{3}He and α-particle production cross sections for the proton induced reactions at the primary energy around 160 MeV [53] and the systematics trends (solid line).

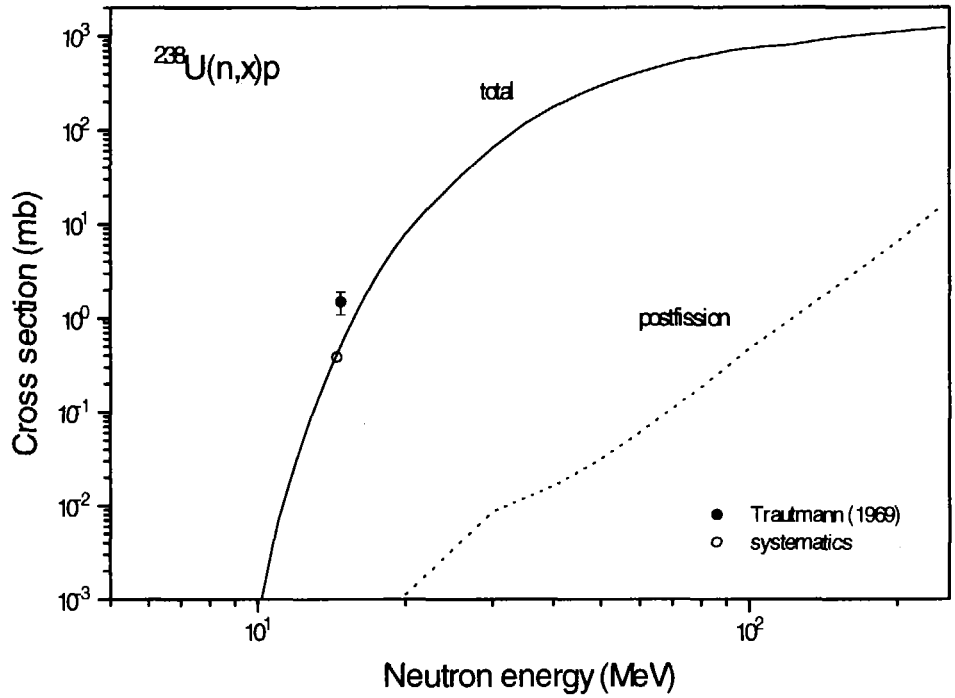

Fig.20 Evaluated total proton production cross section (solid line), post-fission evaporation contribution (dotted line), systematics [55] and measured [54] data for ^{238}U.

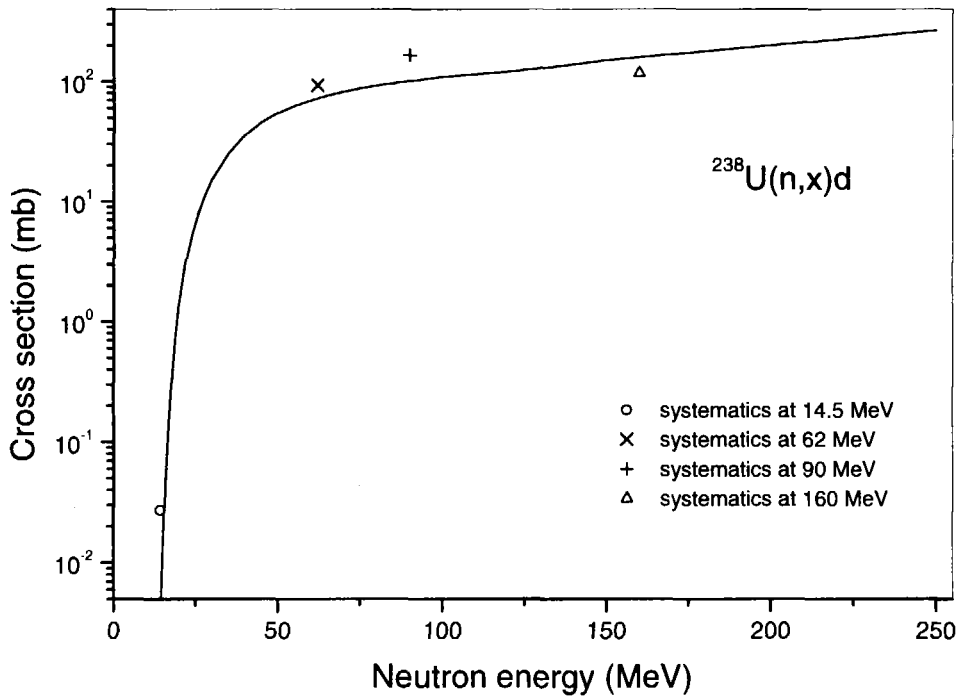

Fig.21 Evaluated deuteron production cross section and the systematics predictions for ^{238}U.

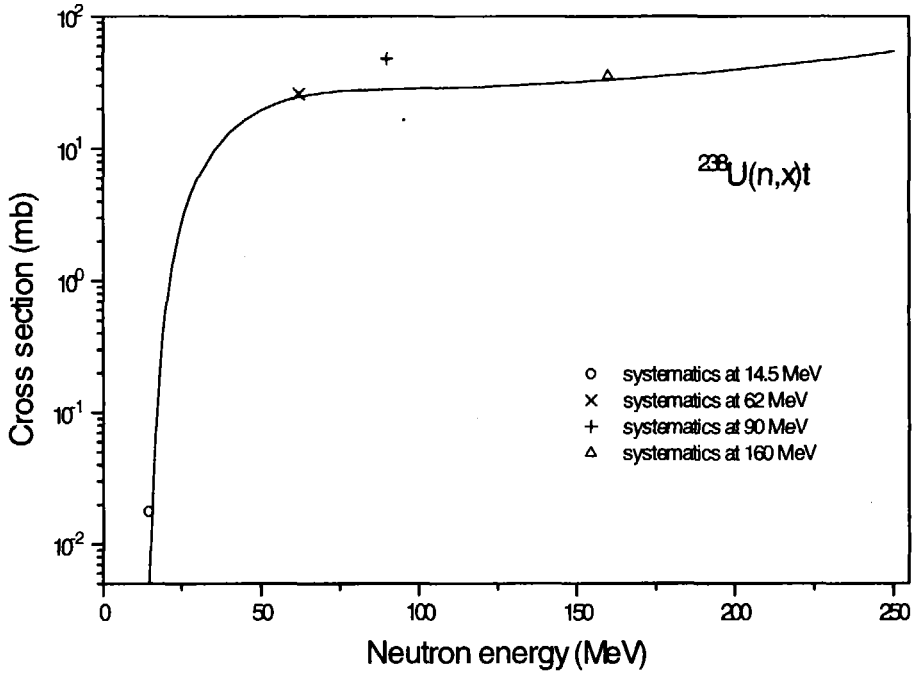

Fig.22 Evaluated triton production cross section (solid line) and the systematics predictions for ^{238}U (symbols).

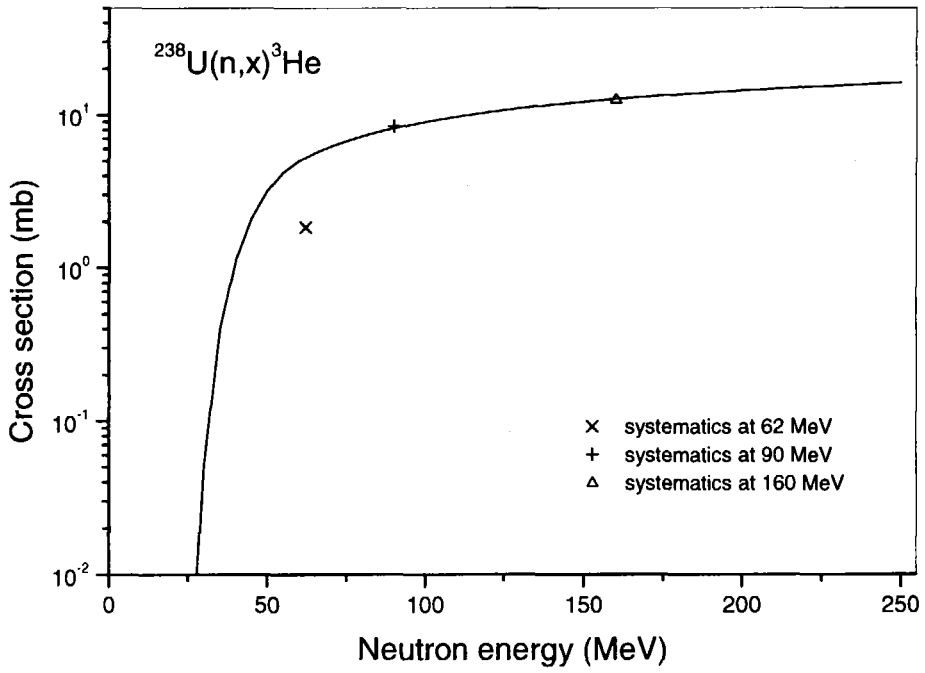

Fig.23 Evaluated ^{3}He production cross section (solid line) and the systematics predictions for ^{238}U (symbols).

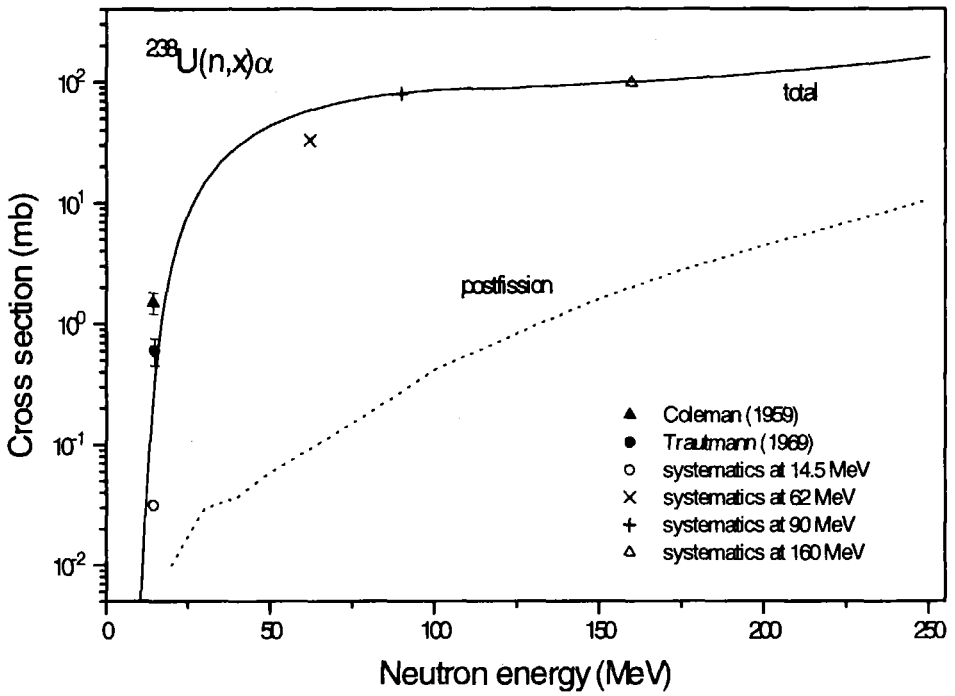

Fig.24 Evaluated total α-production cross section (solid line), post-fission evaporation contribution (dottedline), systematics and measured [54,58] data (symbols) for ^{238}U.

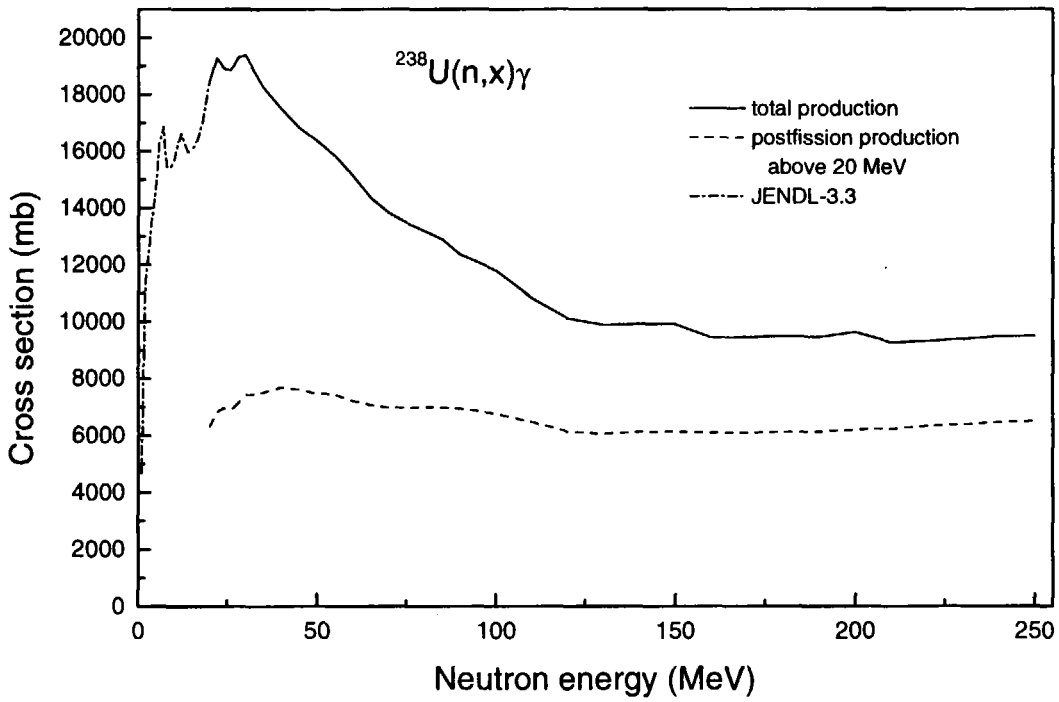

Fig.25 Total γ-production cross section, contribution of the post-fission emission and JENDL-3.3 data for ^{238}U.

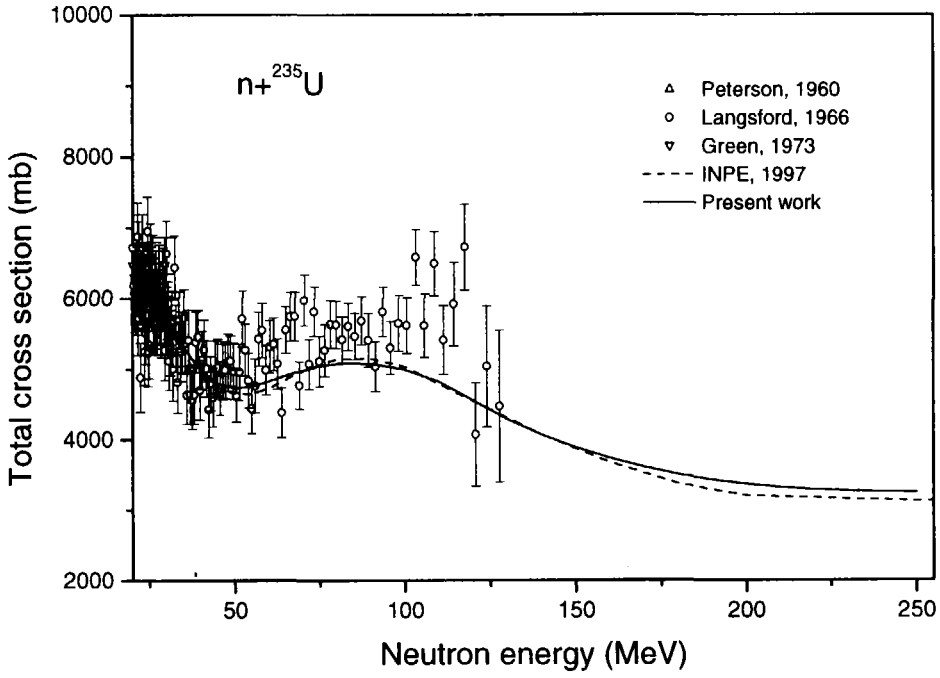

Fig.26 Total neutron cross section for ^{235}U obtained in Ref.[62] and evaluated in the present work. Experimental data are taken from Ref.[34,60,61].

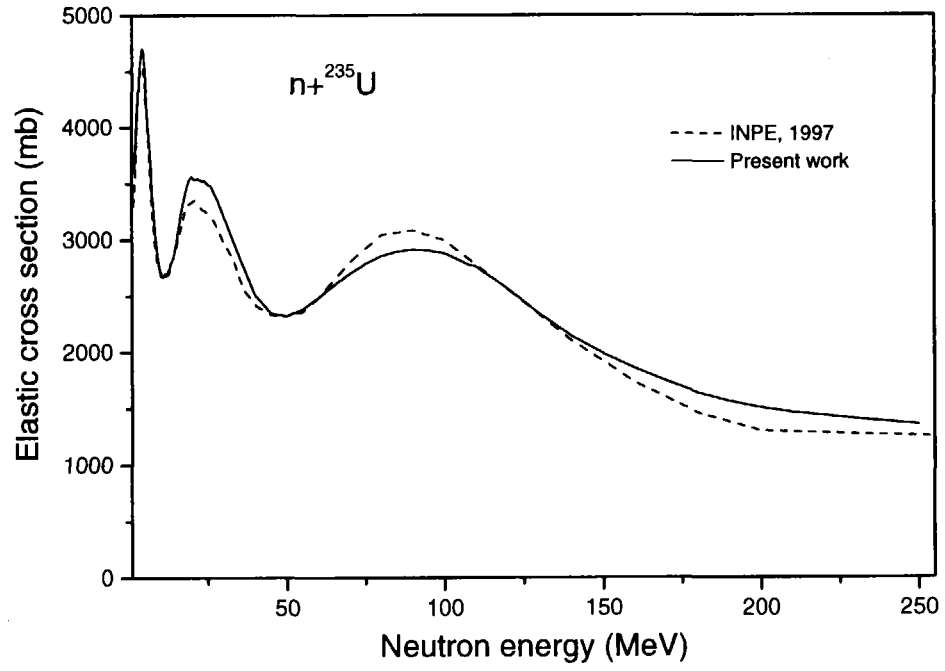

Fig.27 Elastic neutron cross section for ^{235}U obtained in Ref.[62] and evaluated in the present work.

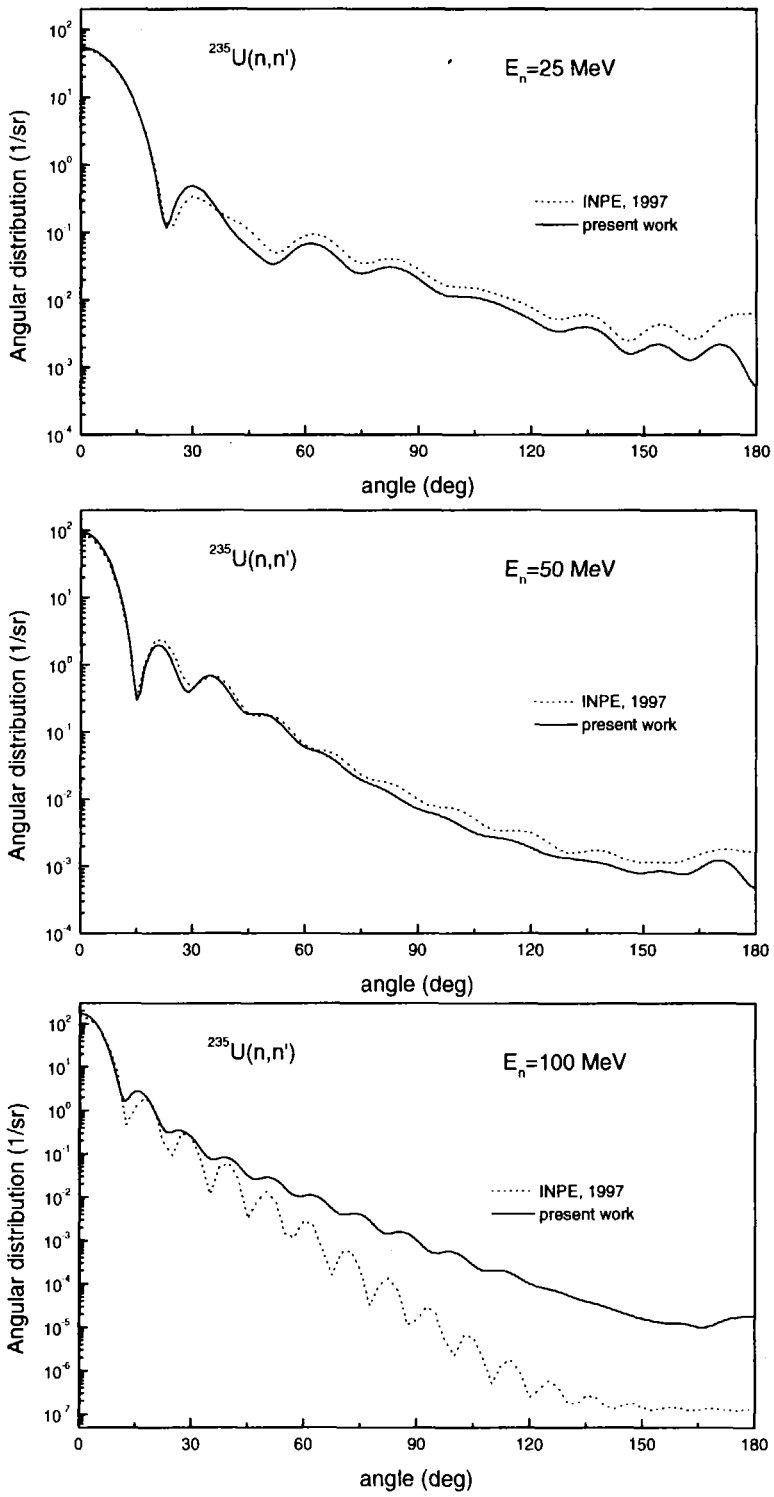

Fig.28 Normalized elastic neutron angular distribution for ^{235}U at the different primary energies obtained in Ref.[62] and calculated in the present work.

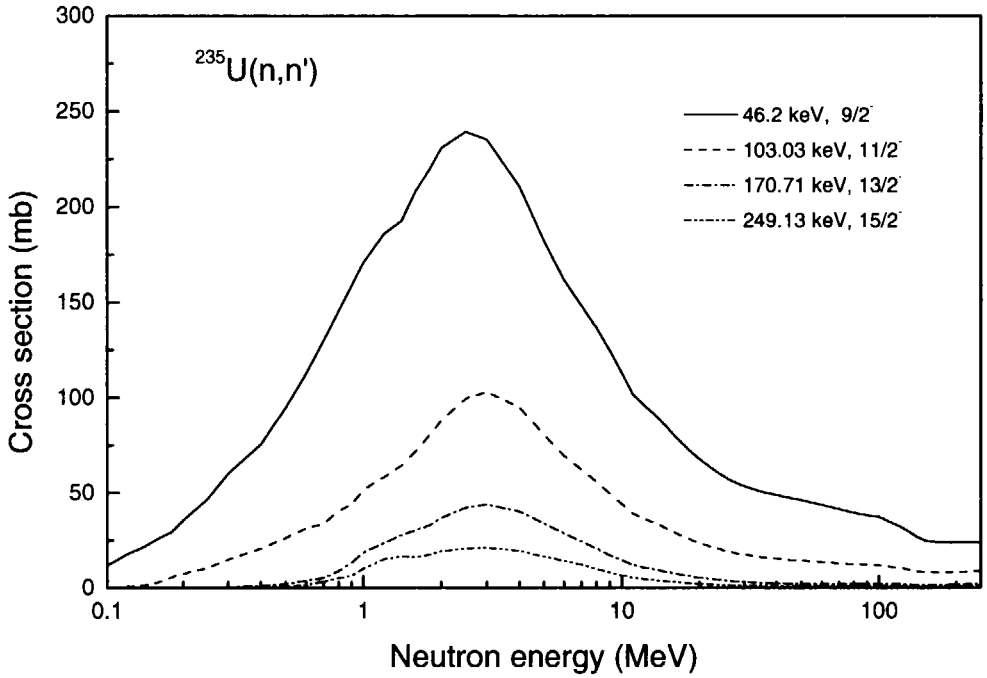

Fig.29 Direct neutron inelastic scattering cross sections for the excited levels $9/2^-$, $11/2^-$, $13/2^-$ and $15/2^-$ which are members of the ground-state rotational band.

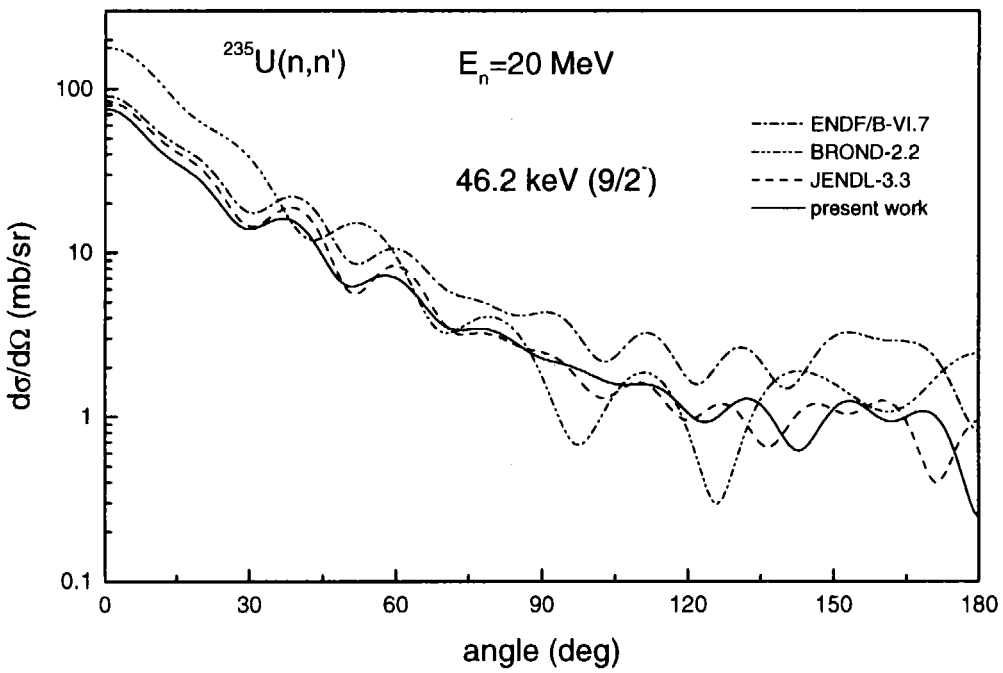

Fig.30 Comparison of the angular distribution for inelastic neutron scattering to the level at 46.2 keV, $9/2^-$, taken from the different data libraries and calculated in the present work.

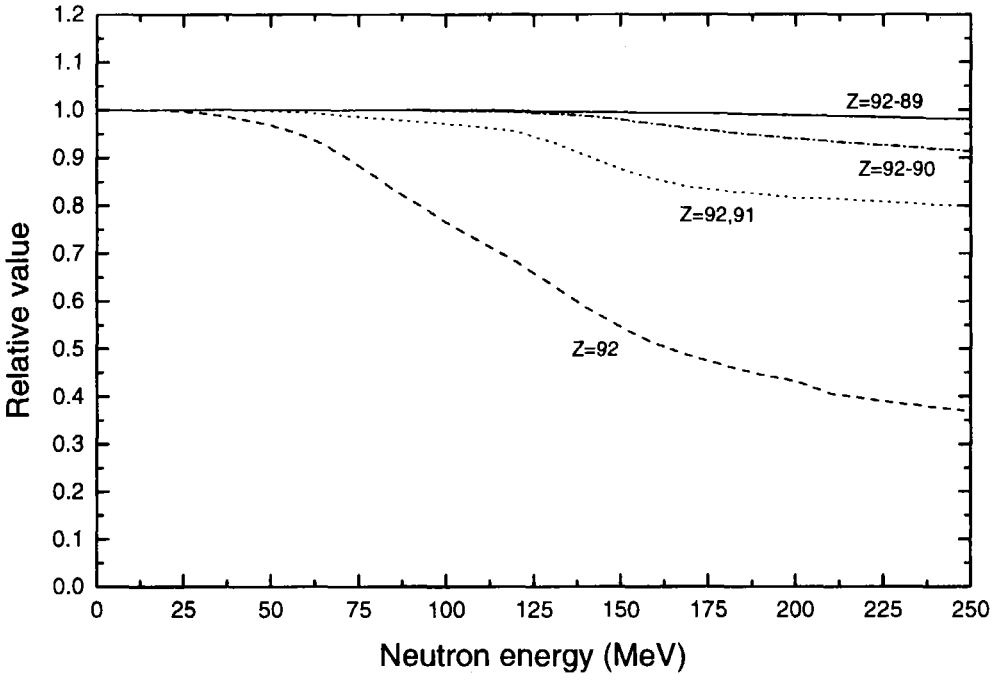

Fig.31 The relative contribution of the nuclei with different atomic number in the total fission cross section for ^{235}U calculated by GNASH code.

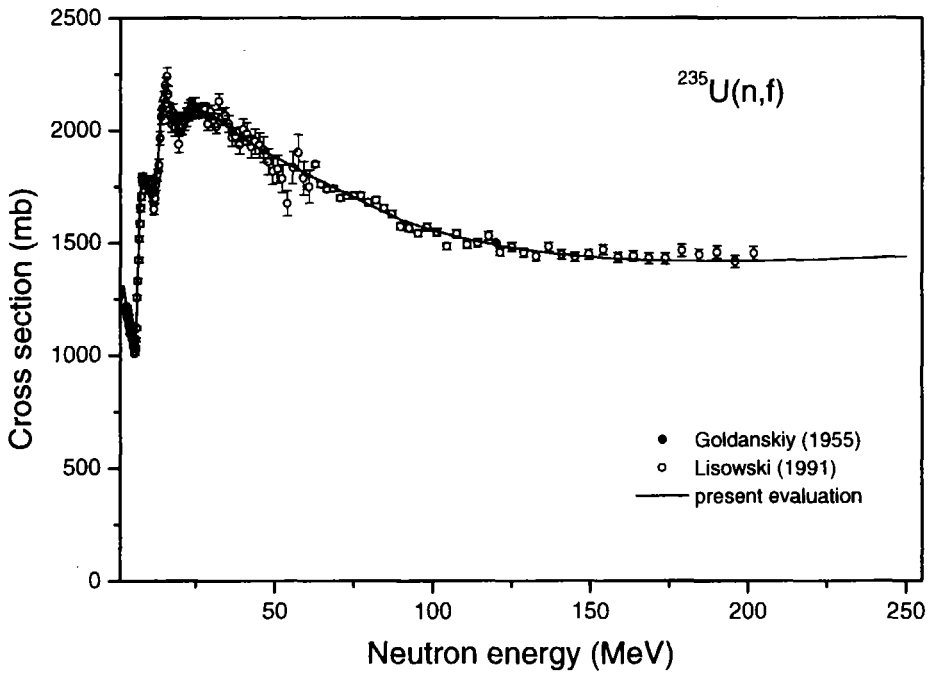

Fig.32 Recommended fission cross section for ^{235}U (solid line) and the experimental data from Refs.[65,66].

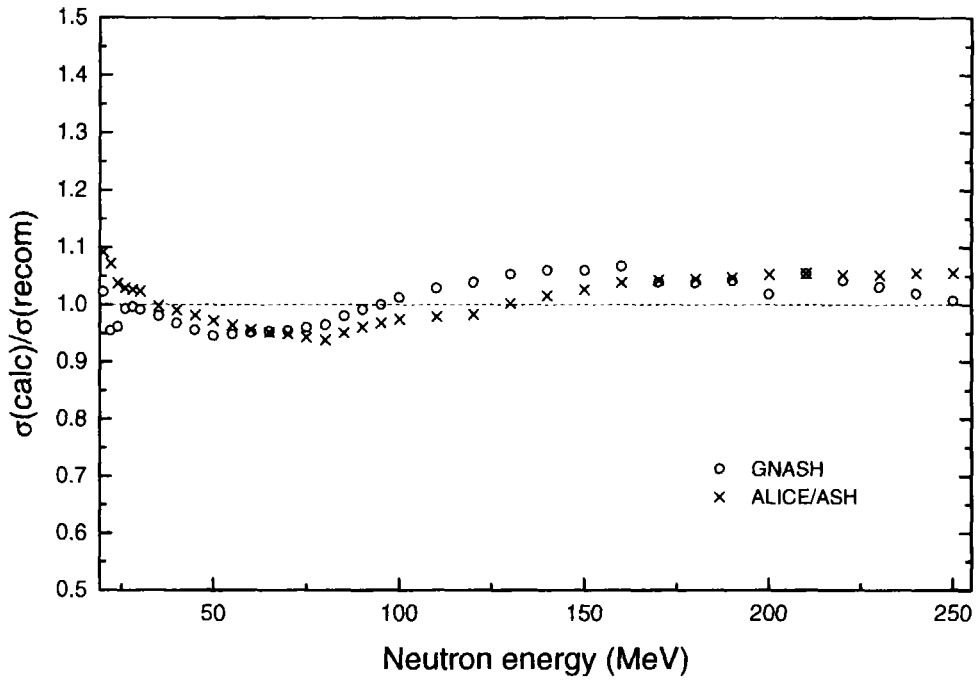

Fig.33 The ratio of the calculated fission cross section for ^{235}U with GNASH and ALICE/ASH codes and the recommended values for the fission cross section.

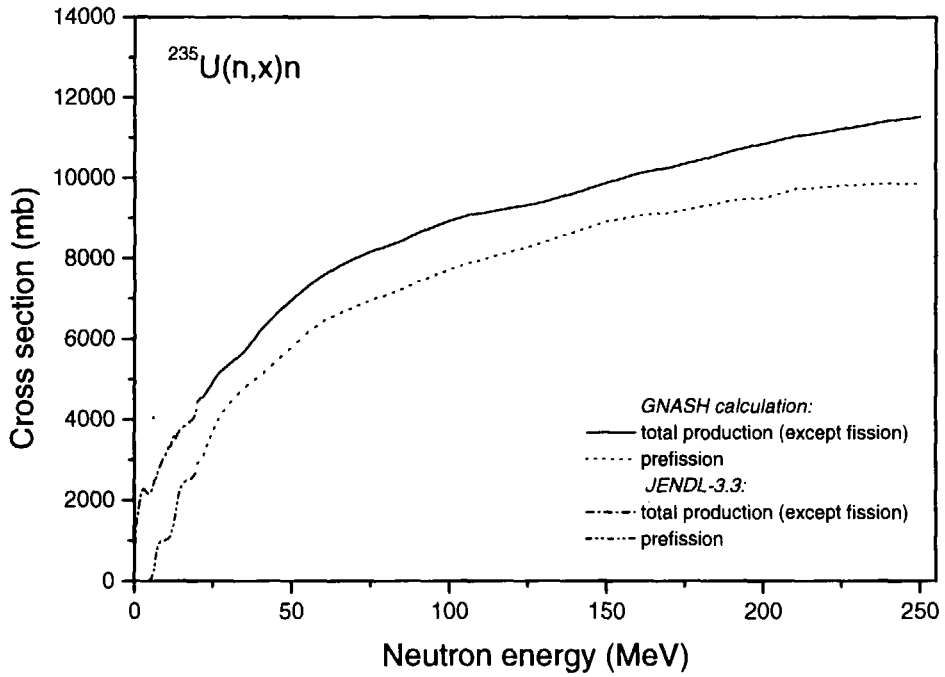

Fig.34 Neutron production cross section with and without the contribution from the post-fission evaporation calculated by GNASH code for ^{235}U and taken from JENDL-3.3 file.

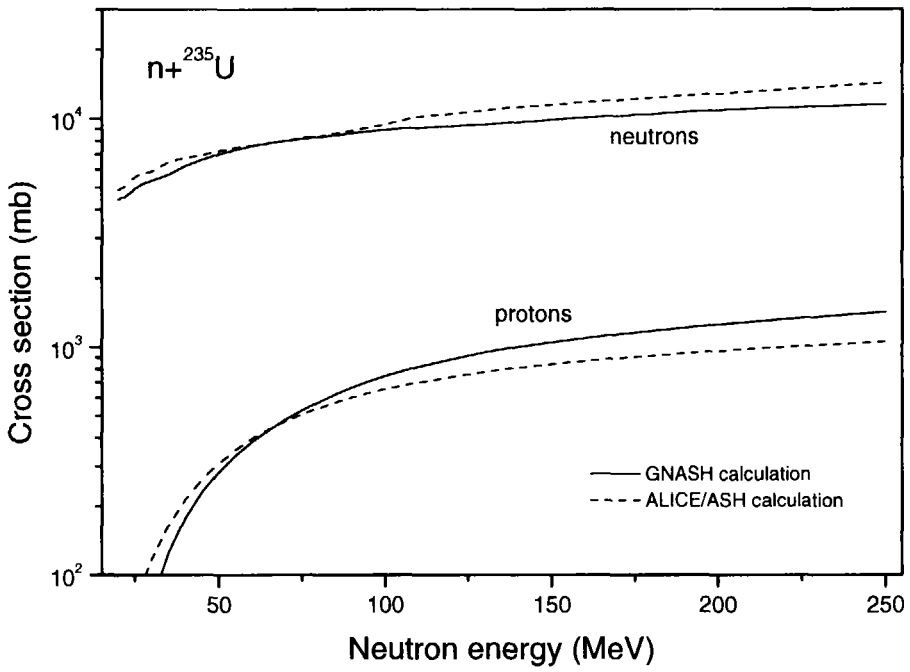

Fig.35 Comparison of the neutron and proton production cross sections calculated with GNASH and ALICE/ASH codes without the contribution from the post-fission evaporation.

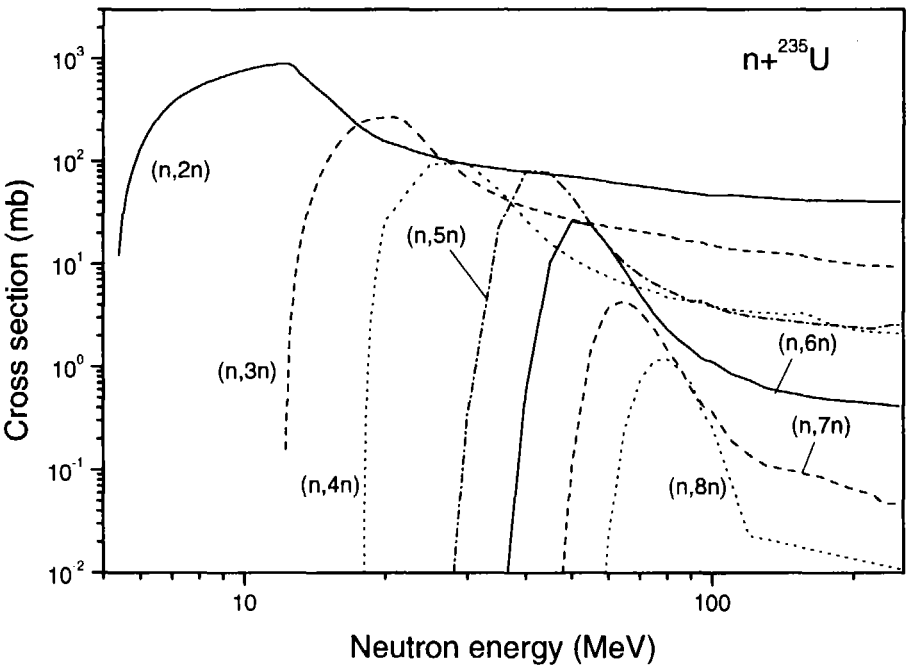

Fig.36 Evaluated (n,xn) reaction cross sections for ^{235}U.

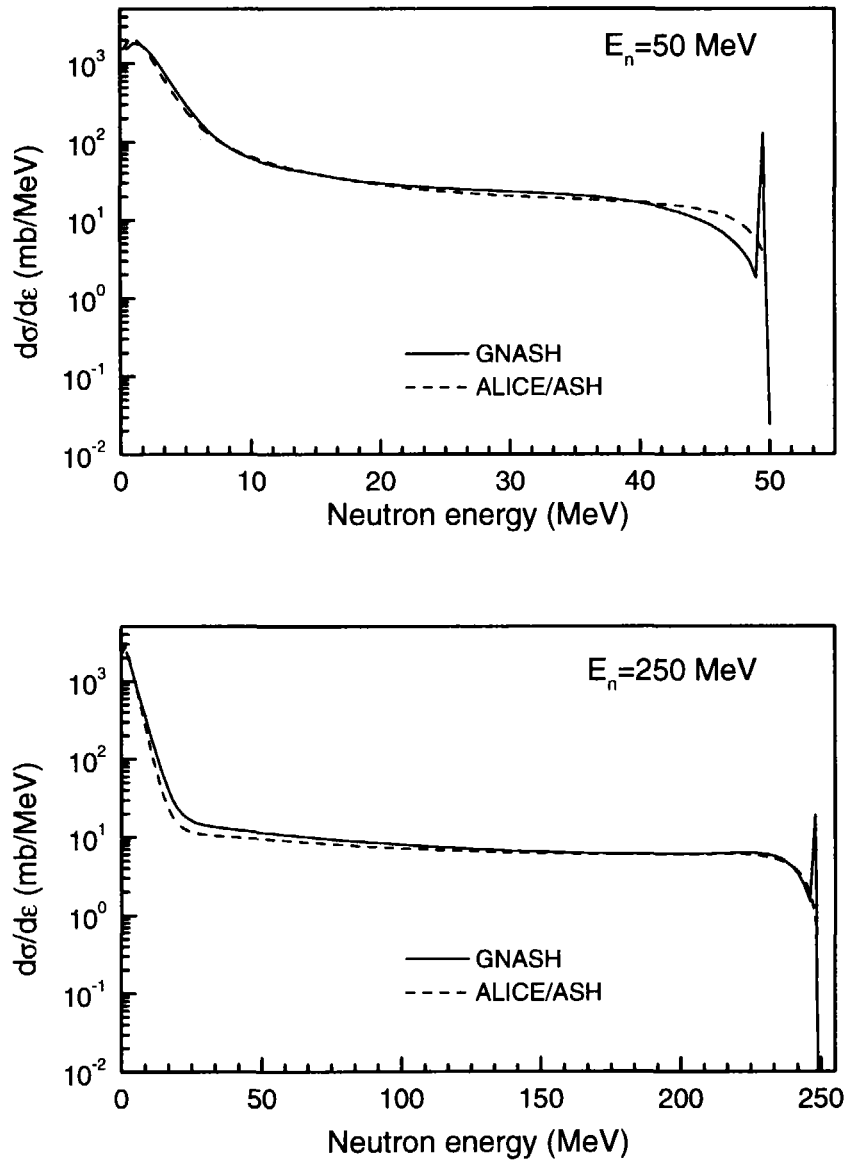

Fig.37 An example of neutron angle integrated spectra calculated using GNASH and ALICE/ASH codes for ^{235}U at incident neutron energies equal to 50 and 250 MeV.

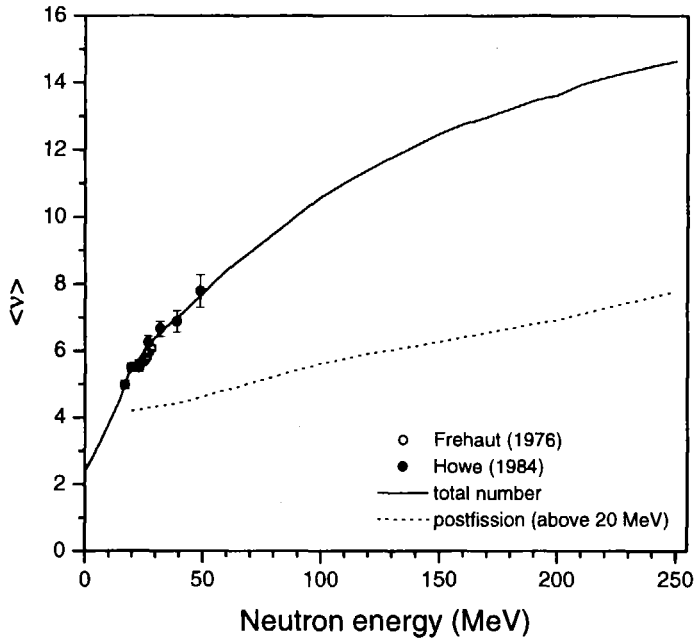

Fig.38 Total number of prompt fission neutrons and the neutrons emitted from the excited fission fragments evaluated in the present work for ^{235}U. The experimental data are from Refs.[51,67]

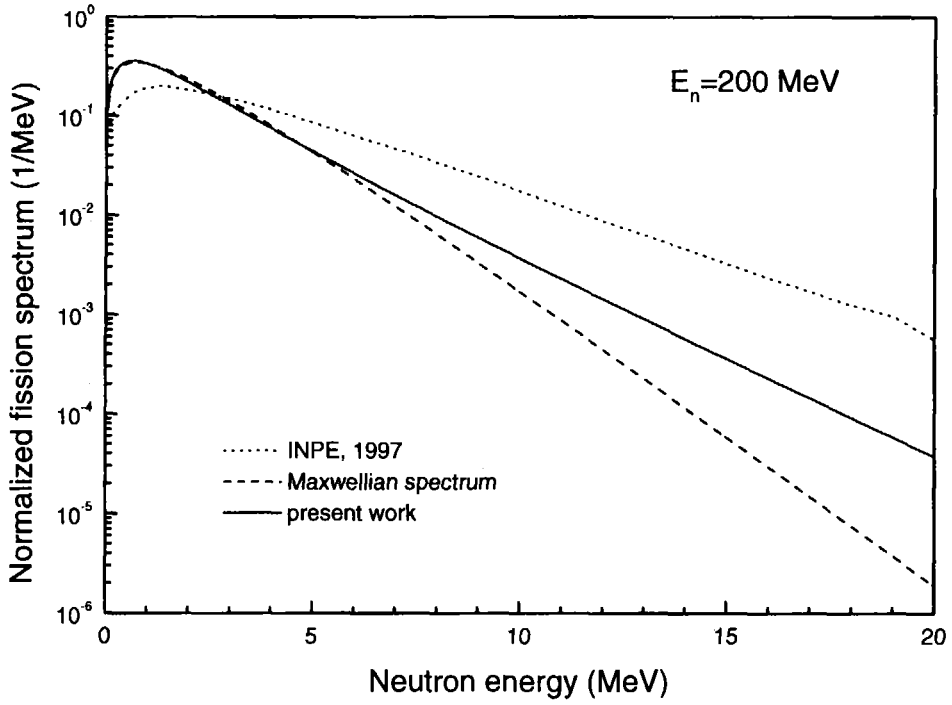

Fig.39 Example of the fission neutron spectra calculated in the present work for ^{235}U (solid line), in Ref.[62] (dotted line) and Maxwellian spectrum (dashed line) for a primary neutron energy equal to 200 MeV

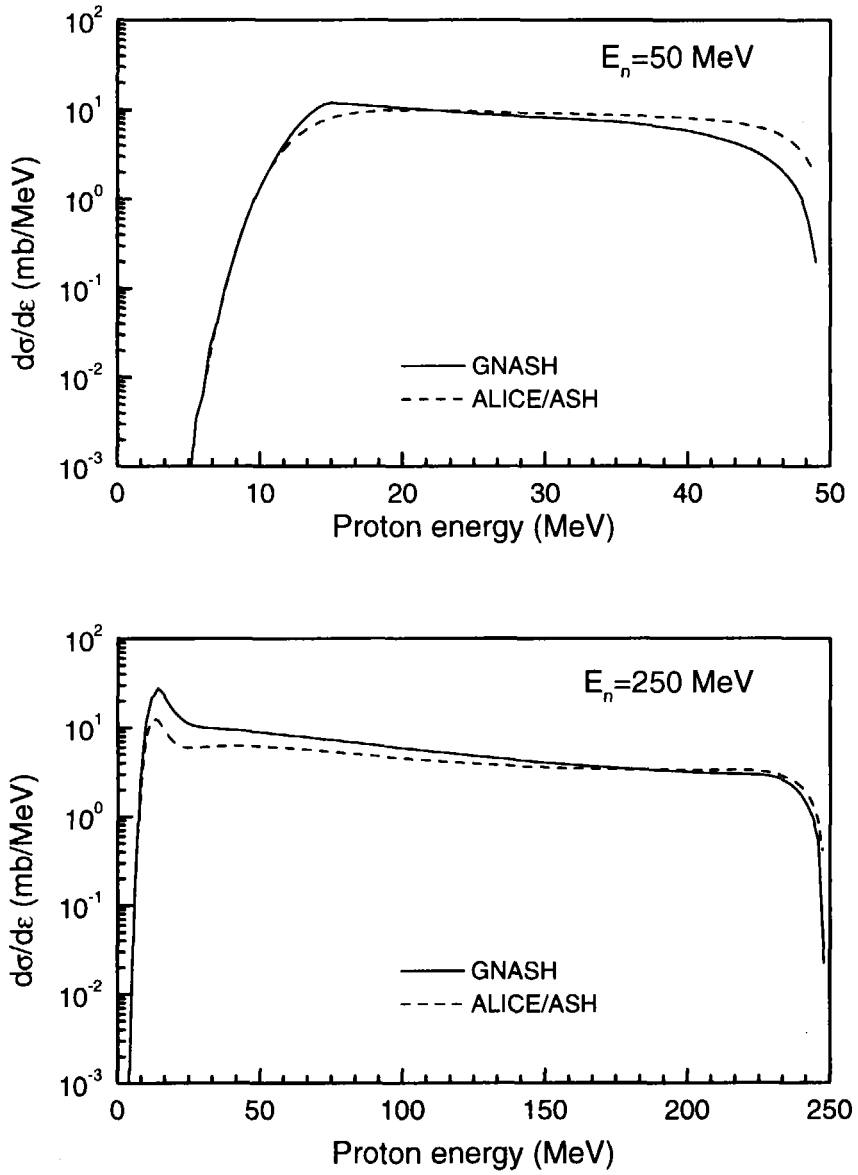

Fig.40 An example of the proton angle integrated spectra calculated using GNASH and ALICE/ASH codes for ^{235}U at incident neutron energies equal to 50 and 250 MeV.

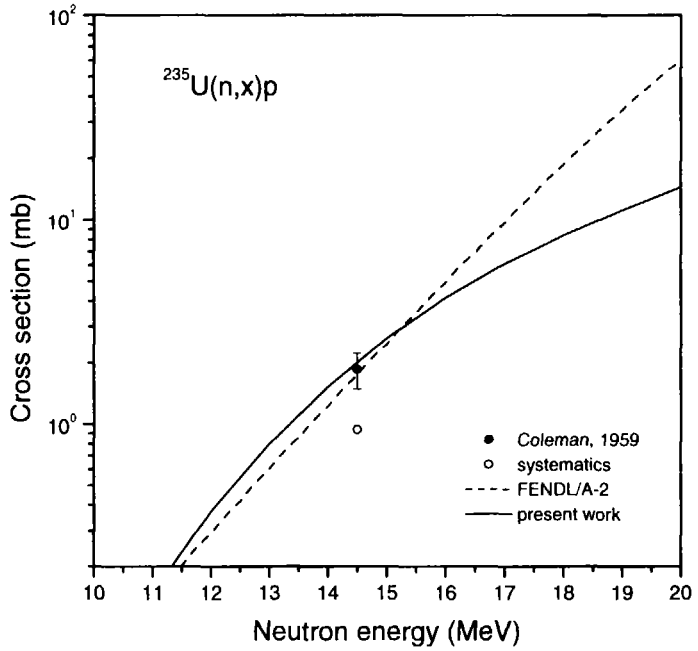

Fig.41 Comparison of the total proton production cross section for ^{235}U evaluated in the present work, taken from FENDL/A-2, measured in Ref.[58] and predicted by the systematics [55].

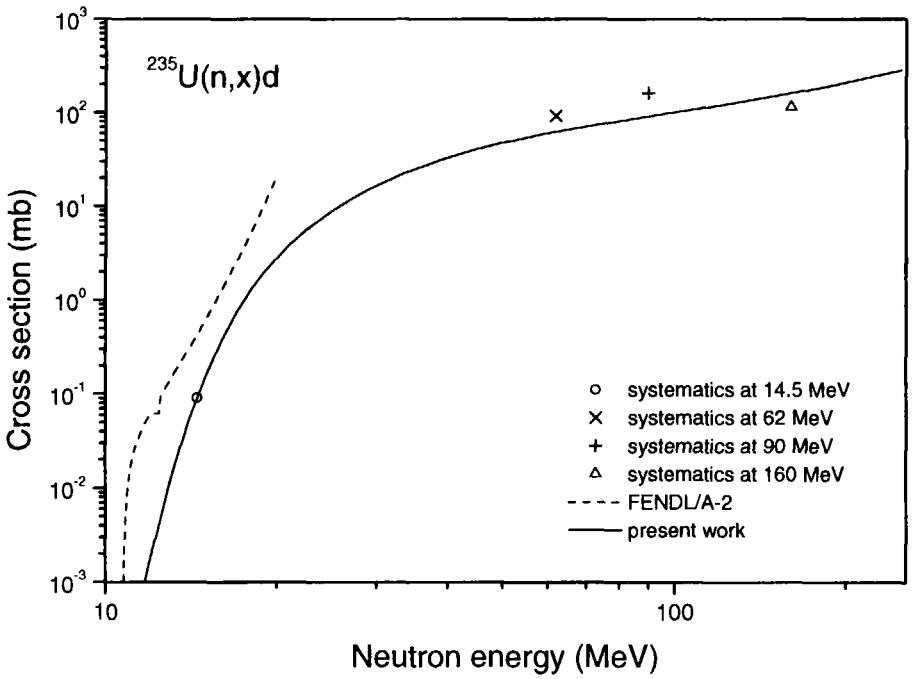

Fig.42 Comparison of the total deuteron production cross section for ^{235}U, evaluated in the present work, taken from FENDL/A-2 and predicted by the systematics.

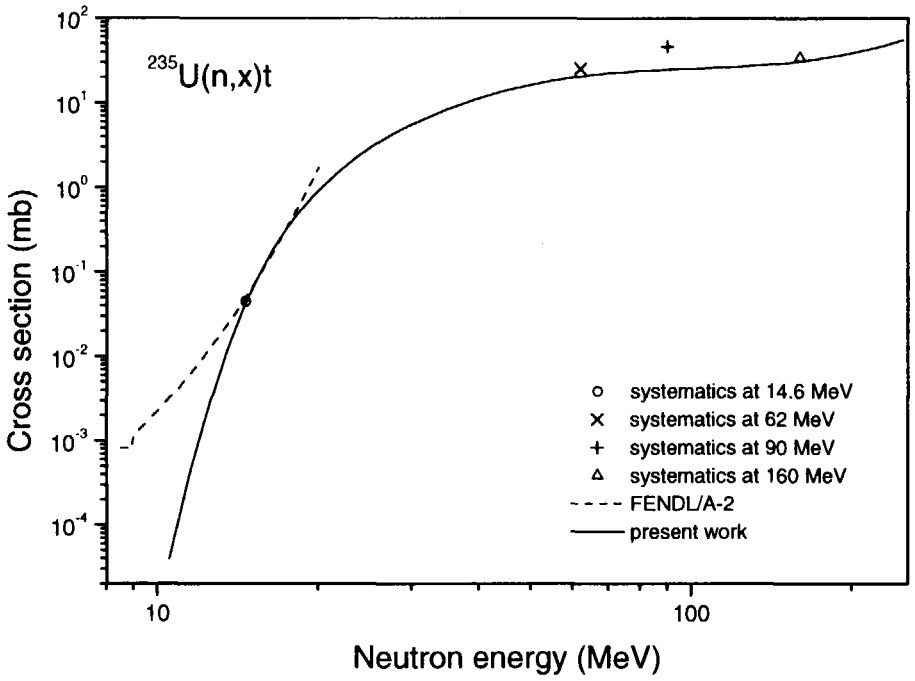

Fig.43 Comparison of the triton deuteron production cross section for ^{235}U, evaluated in the present work, taken from FENDL/A-2 and predicted by the systematics.

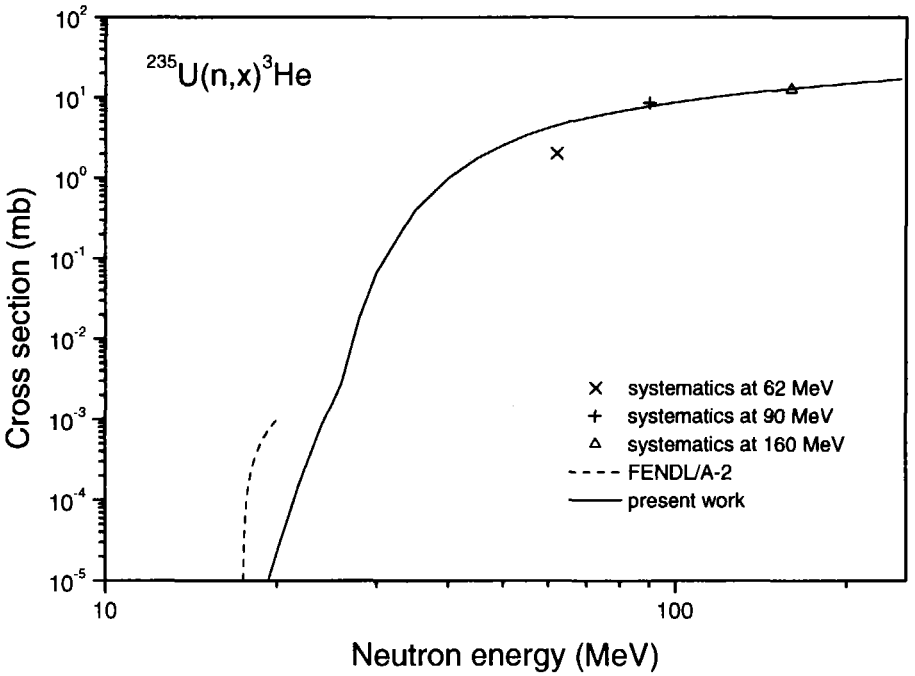

Fig.44 Comparison of the total ^{3}He production cross section for ^{235}U, evaluated in the present work, taken from FENDL/A-2 and predicted by the systematics.

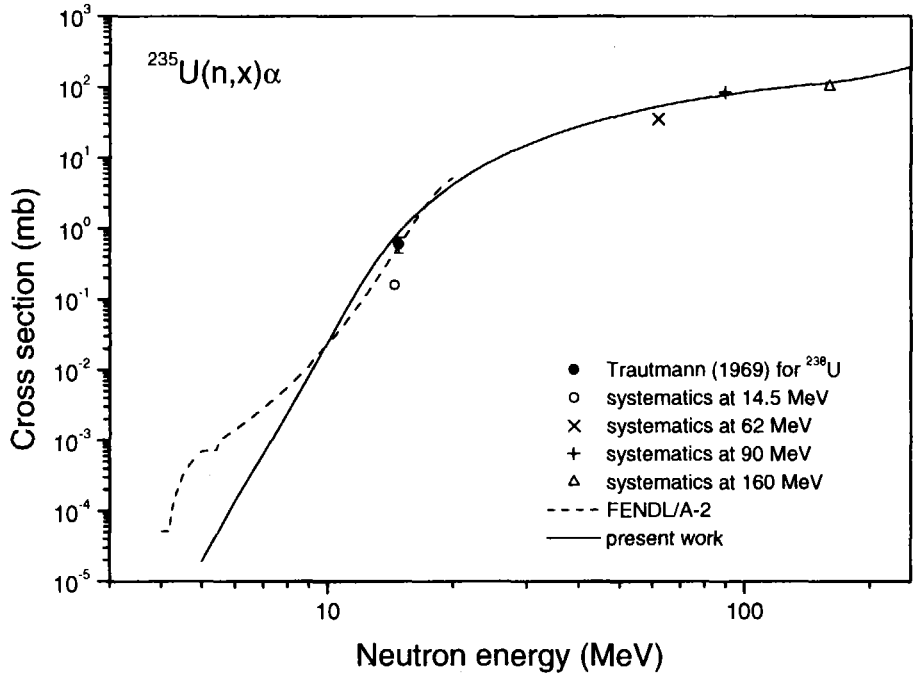

Fig.45 Comparison of the total α-particle production cross section for ^{235}U, evaluated in the present work, taken from FENDL/A-2, measured for ^{238}U [54] and predicted by the systematics.

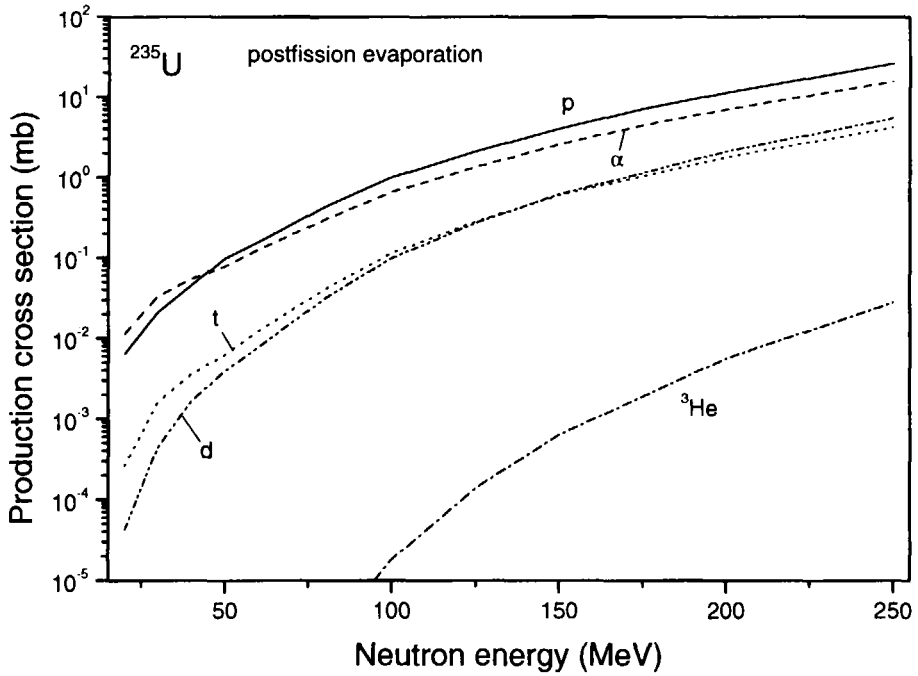

Fig.46 Calculated production cross sections for protons, tritons, ^{3}He- and α-particles emitted from excited fission fragments in n+^{235}U interactions.

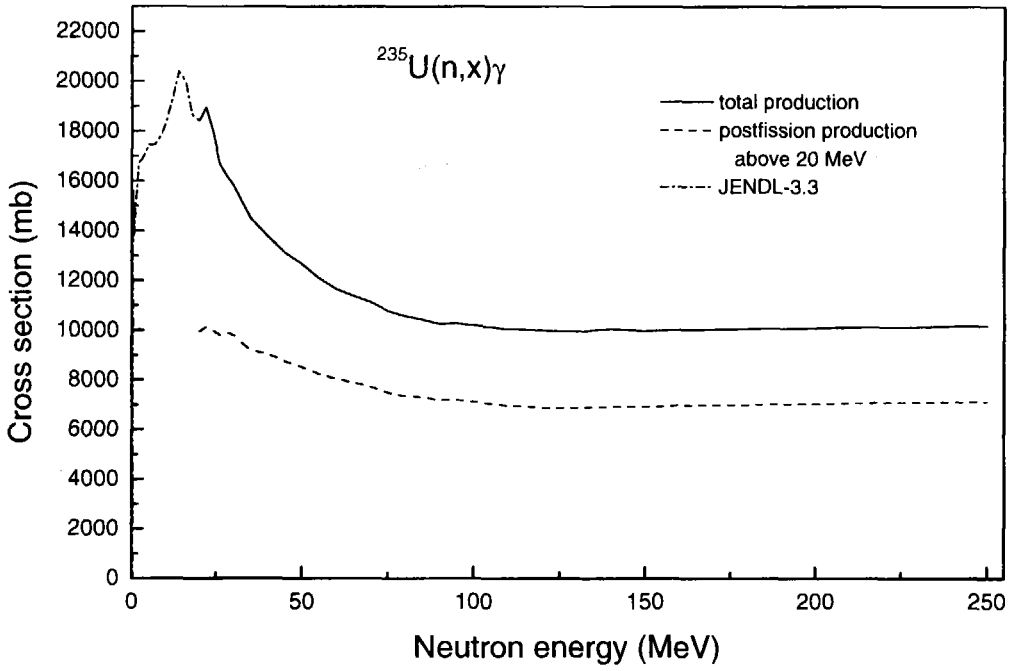

Fig.47 Total γ-production cross section, contribution of the post-fission emission and JENDL-3.3 data for ^{235}U.

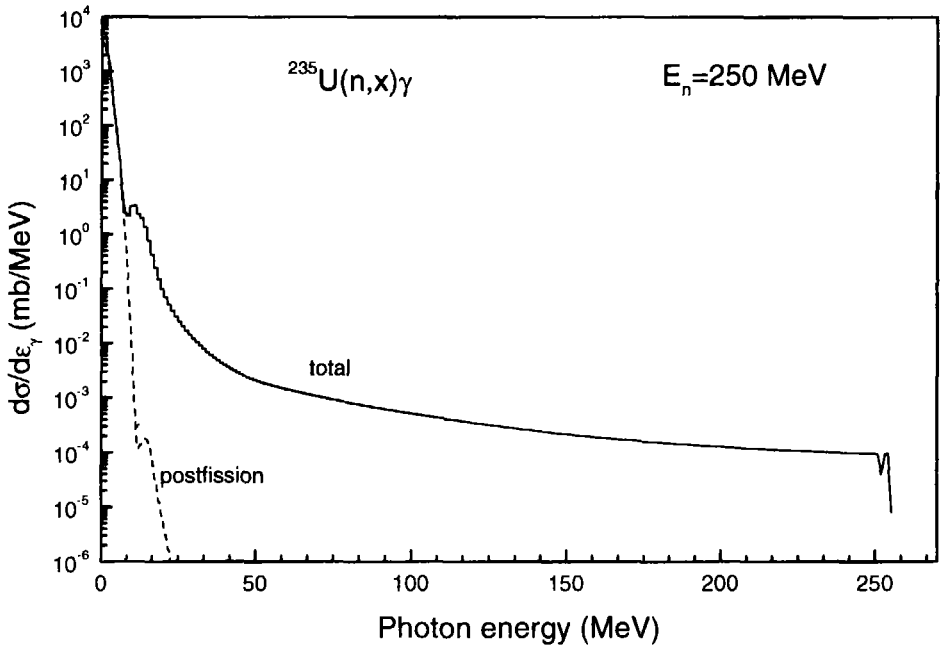

Fig.48 Total γ-spectrum and the post-fission contribution calculated for ^{235}U irradiated by 250 MeV-neutrons.

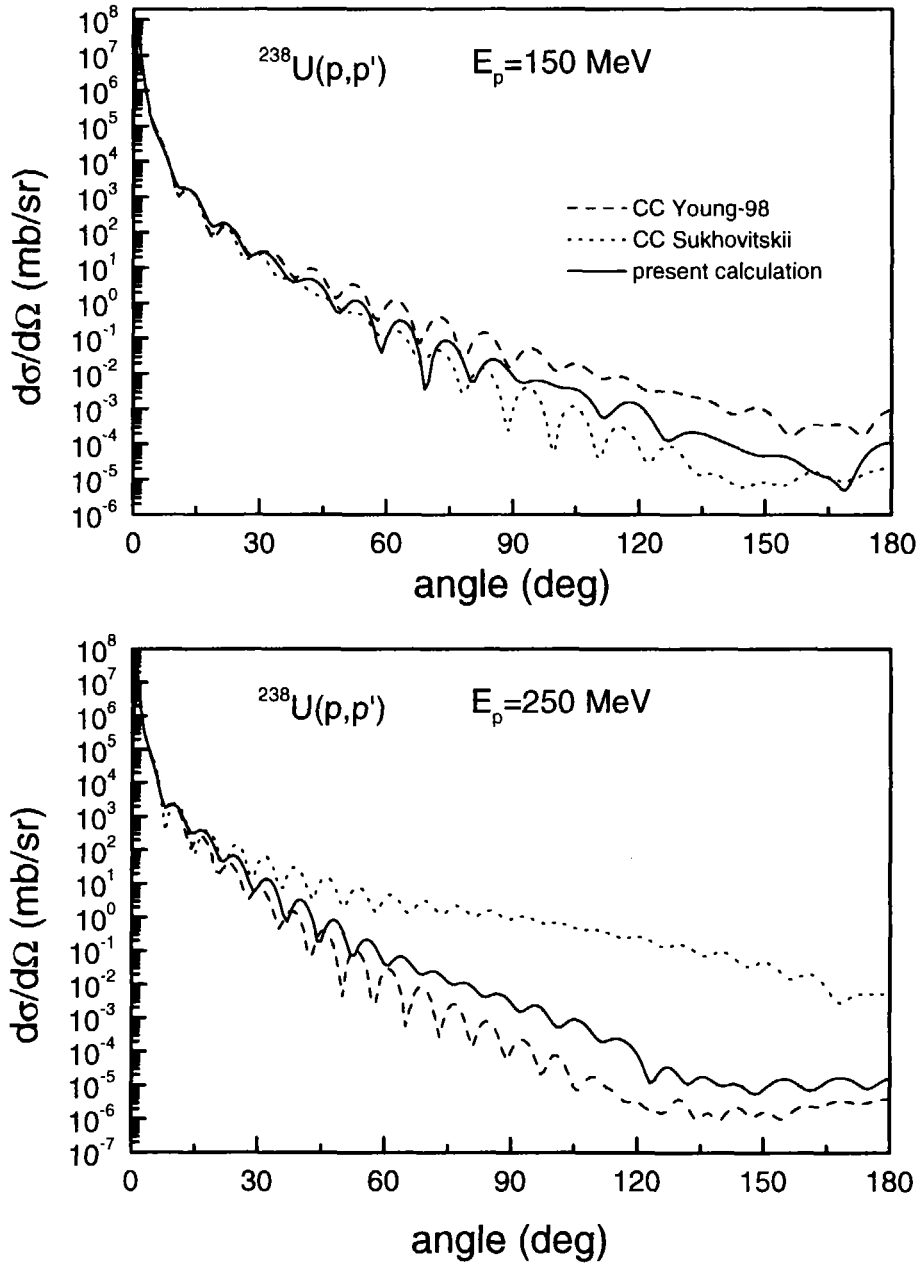

Fig.49 Angular distribution for elastic proton scattering on ^{238}U at incident energies equal to 150 and 250 MeV obtained using different sets of the coupled channel optical model parameters.

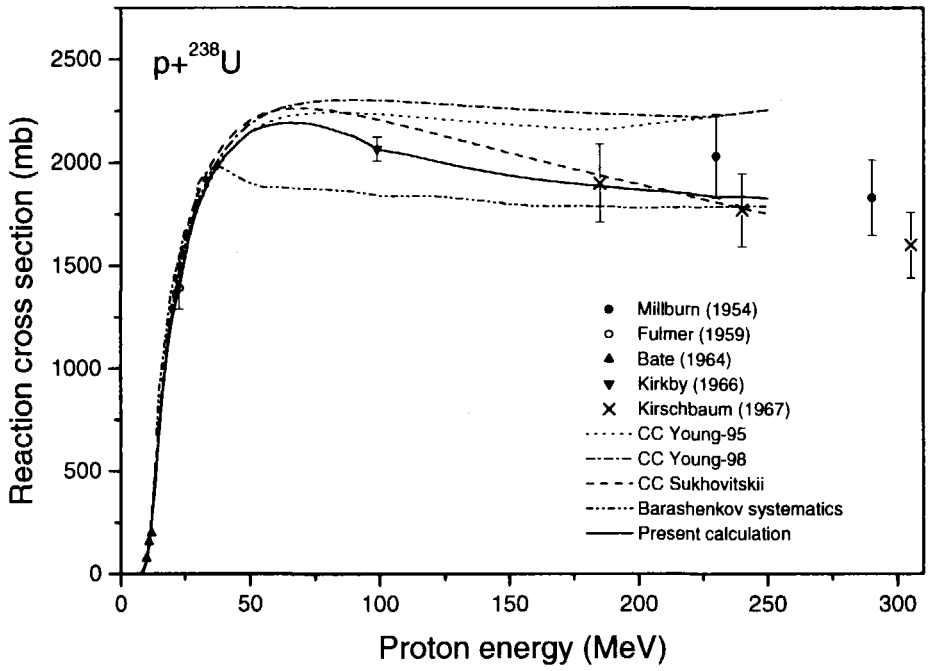

Fig.50 Proton reaction cross section for ^{238}U calculated using different sets of the coupled channel optical model parameters.

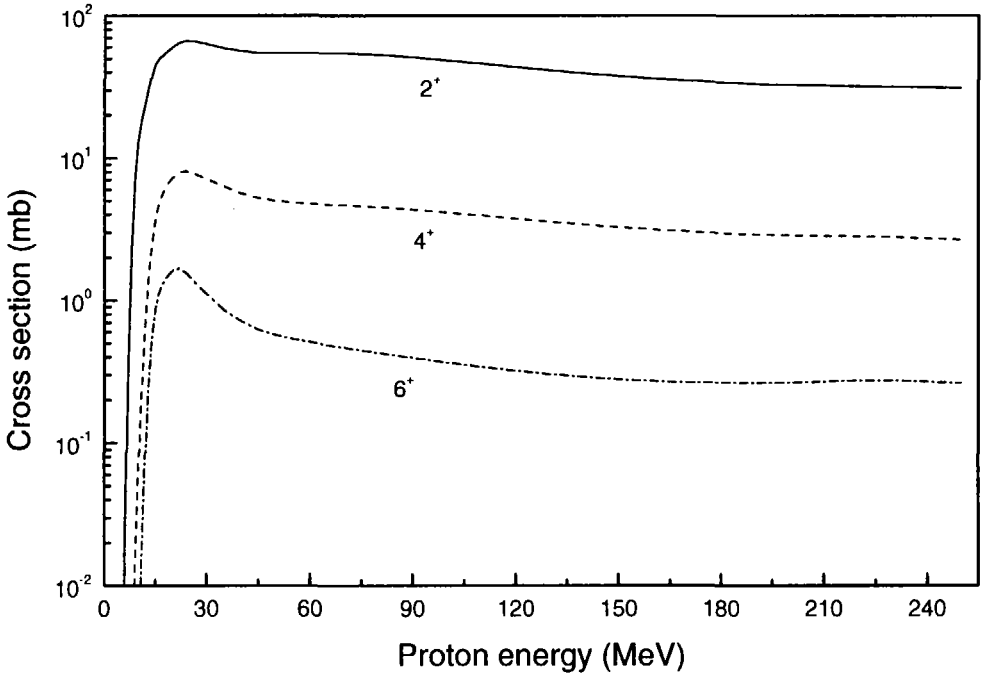

Fig.51 Direct proton inelastic scattering cross sections for the excited levels 2^+, 4^+, and 6^+ of ^{238}U.

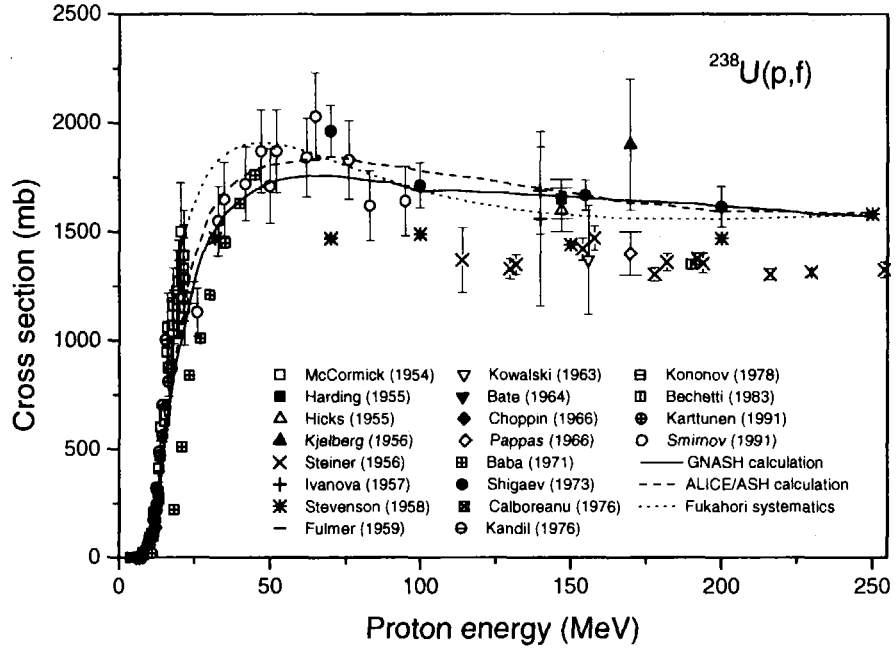

Fig.52 Fission cross section for ^{238}U calculated by GNASH code (solid line), ALICE/ASH code (dashed line) and evaluated by the systematics [103] (dotted lines) together with the experimental data.

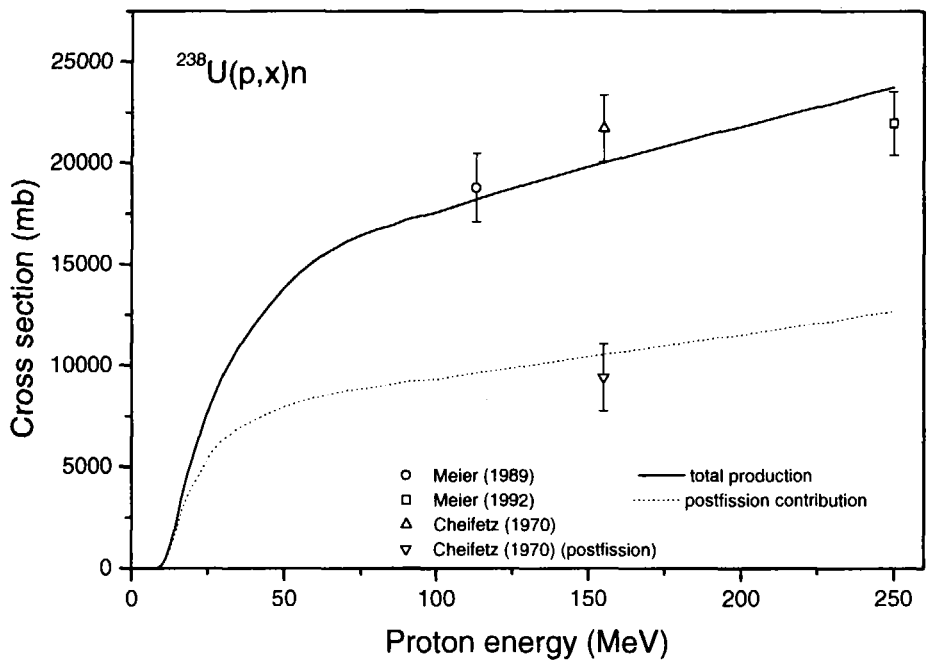

Fig.53 Total neutron production cross section and the contribution of the post-fission evaporation calculated in the present work for p+^{238}U interaction.

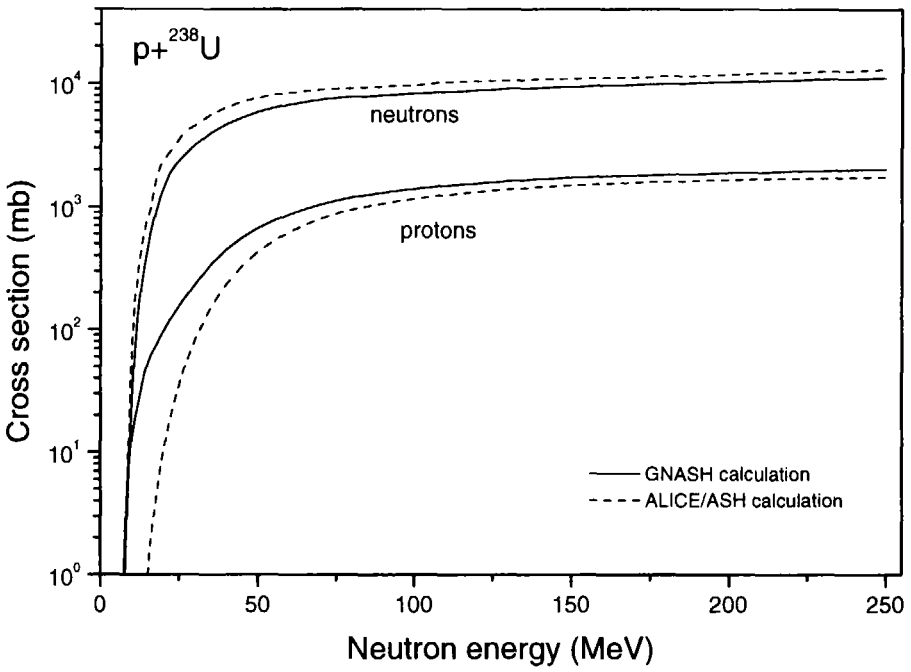

Fig.54 Comparison of the neutron and proton production cross sections calculated for irradiation of ^{238}U by protons with GNASH and ALICE/ASH codes without the contribution from the post-fission evaporation.

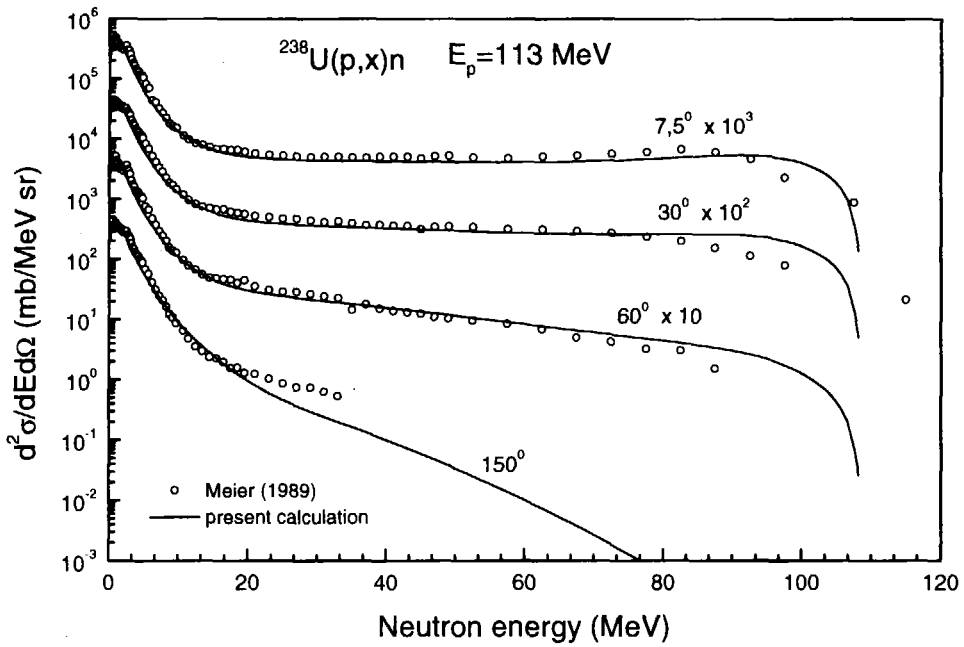

Fig.55 The neutron double differential cross sections calculated in the present work (solid line) and measured in Ref.[104] for p+^{238}U at the primary proton energy equal to 113 MeV.

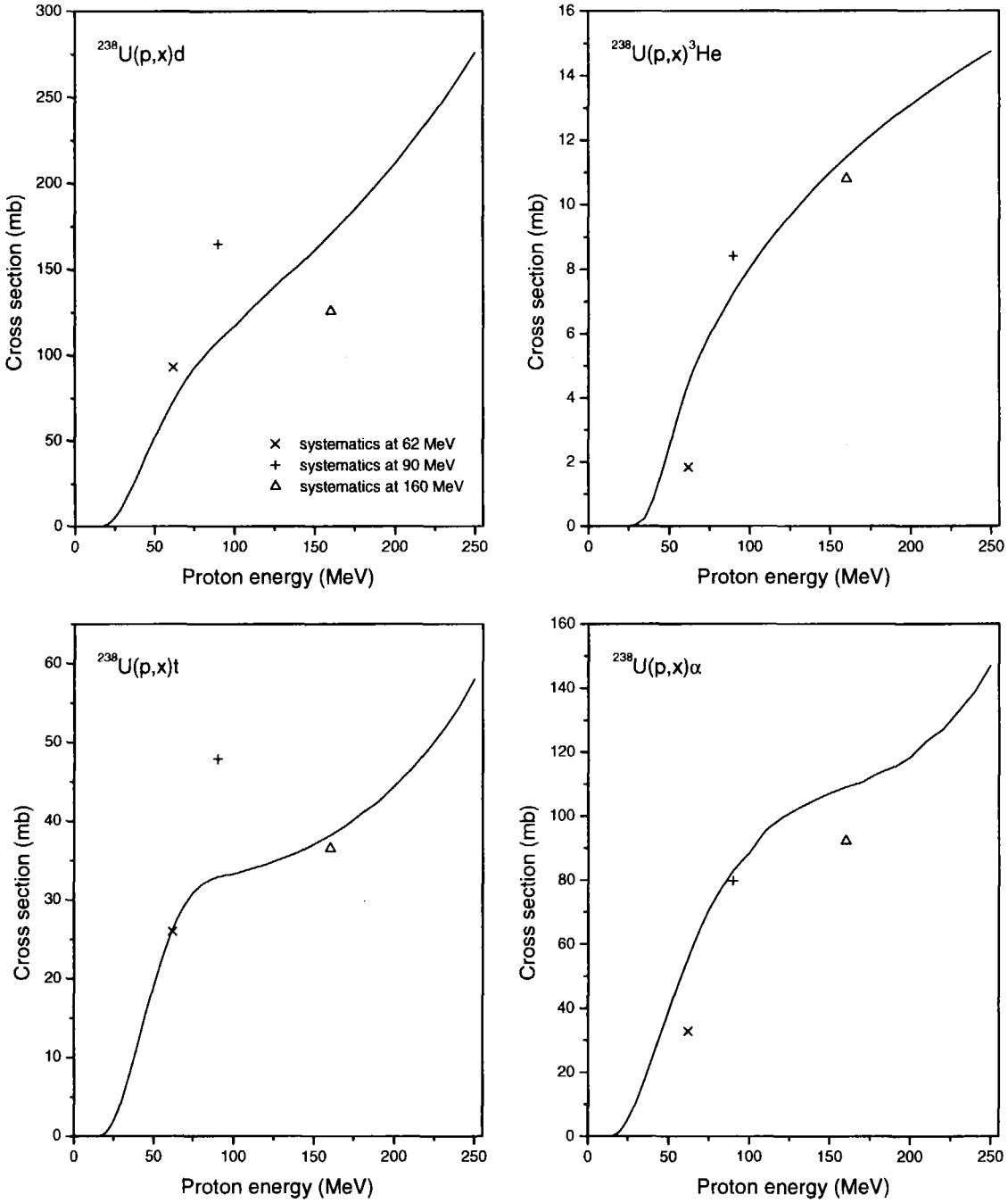

Fig.56 Evaluated d, t, ^{3}He and α-particle production cross section for p+^{238}U interactions and the systematics predictions at 62 MeV (×), 90 MeV (+) and 160 MeV (triangle).

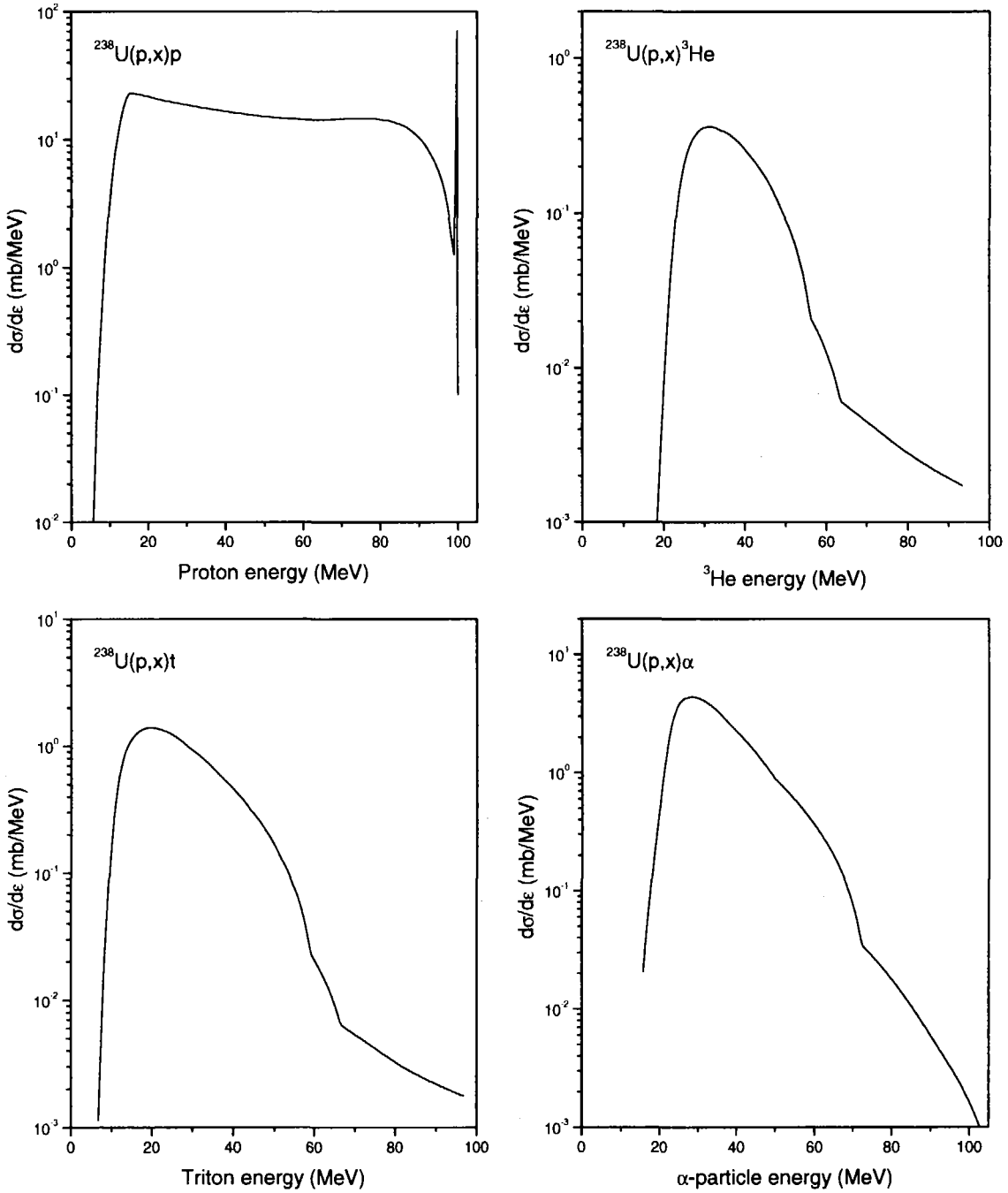

Fig.57 Calculated proton, triton, ^{3}He and α-particle spectra for ^{238}U irradiated by 100 MeV-protons.

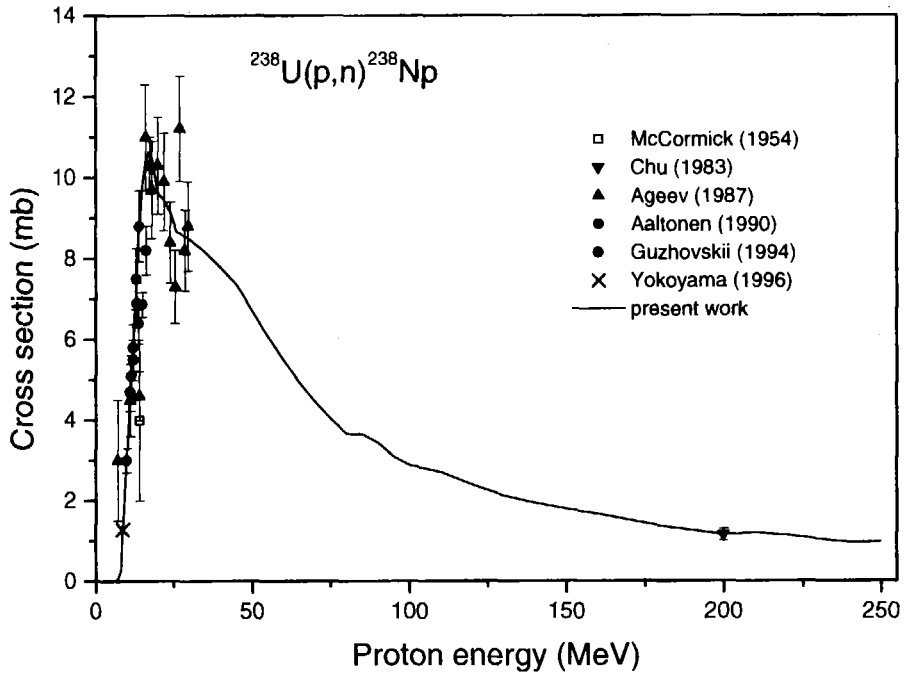

Fig.58 Evaluated (p,n) reaction cross section for ^{238}U and the experimental data from Refs.[78,109,110,112-114].

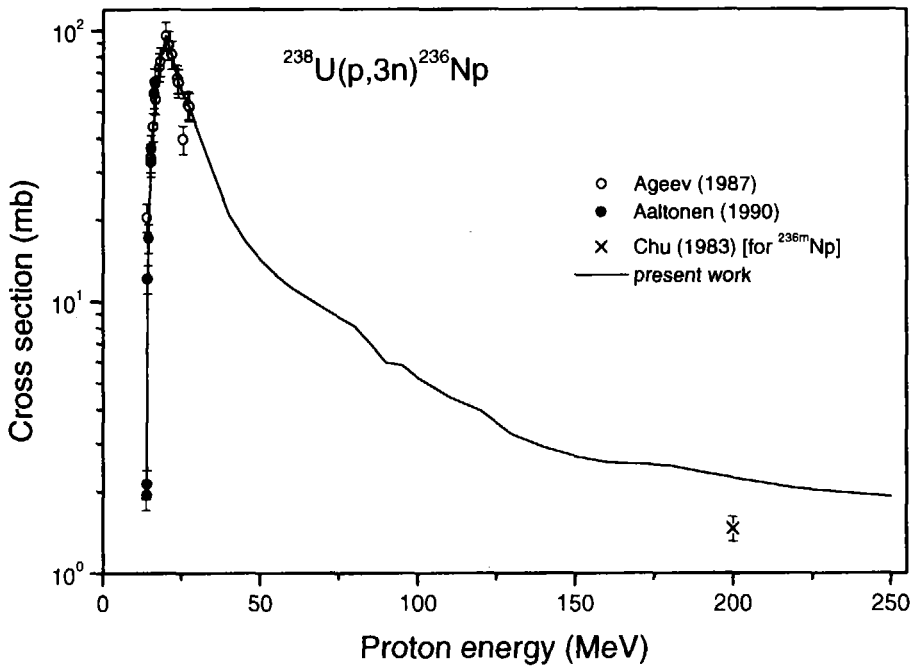

Fig.59 Evaluated (p,3n) reaction cross section for ^{238}U and the experimental data from Refs.[109,110,112]. Data from Ref.[110] are transformed as discussed in the text.

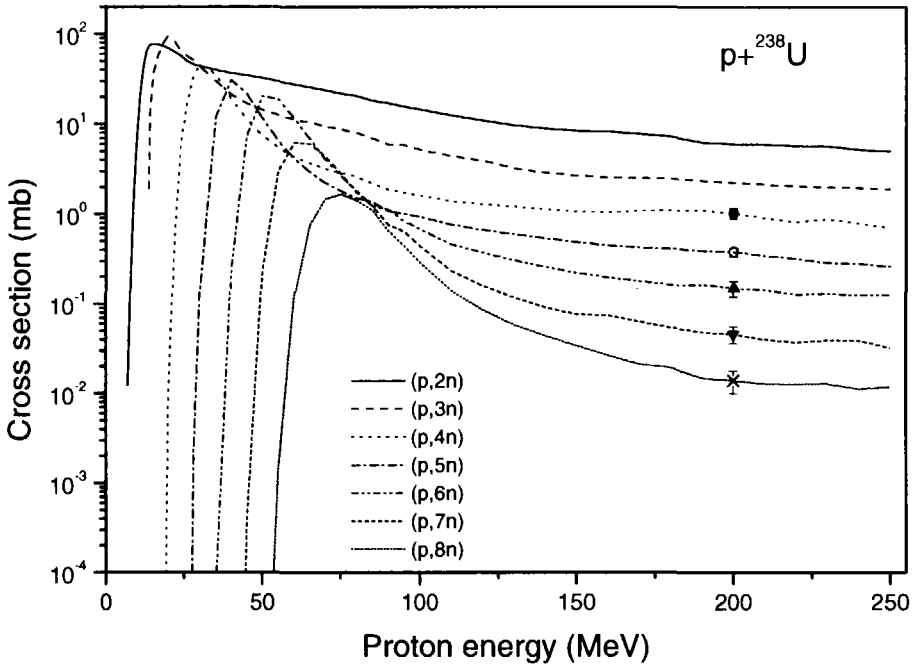

Fig.60 Evaluated (p,xn) reaction cross section for ^{238}U and the experimental data from Ref.[109].

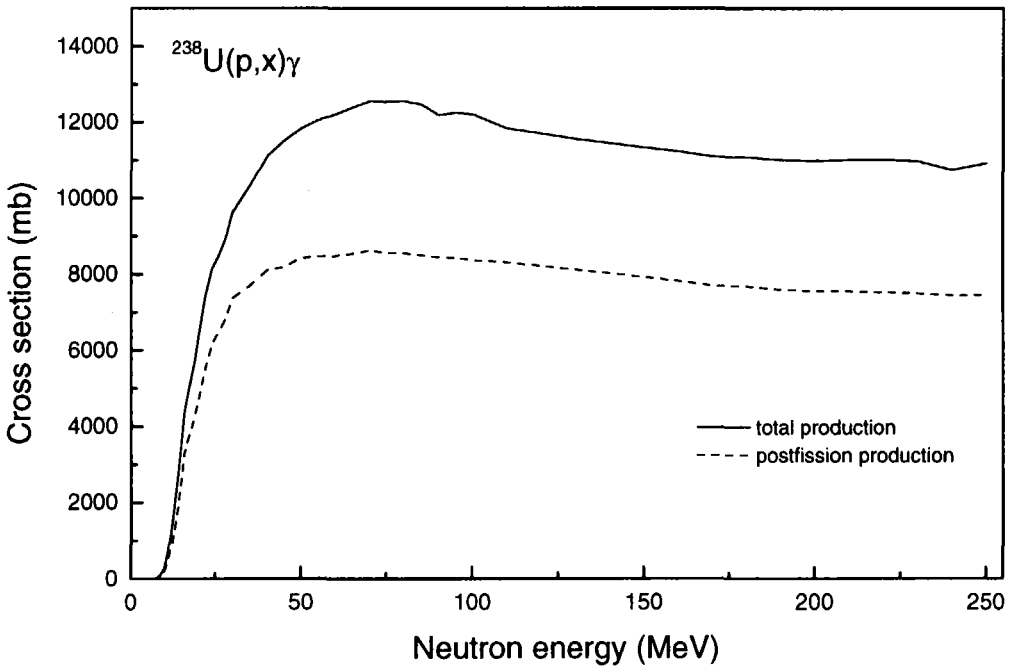

Fig.61 Total γ-production cross section and the contribution of the post-fission emission for p+^{238}U interactions.

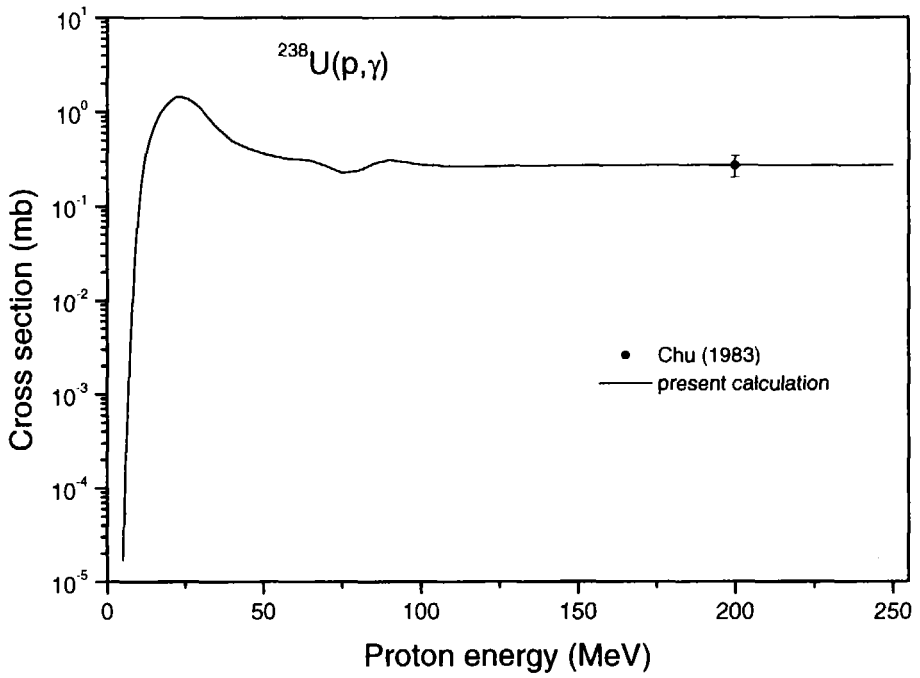

Fig.62 Evaluated (p,γ) reaction cross section for ^{238}U and the experimental data from Ref.[109].

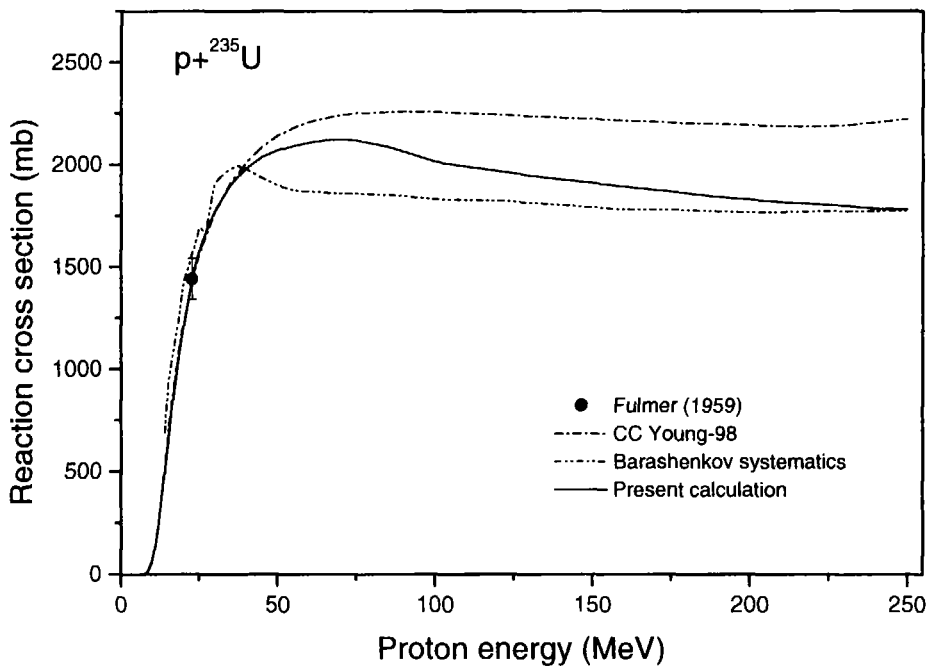

Fig.63 Proton reaction cross section for ^{235}U calculated using different sets of the coupled channel model parameters, predicted by the systematics [44] and measured in Ref.[69].

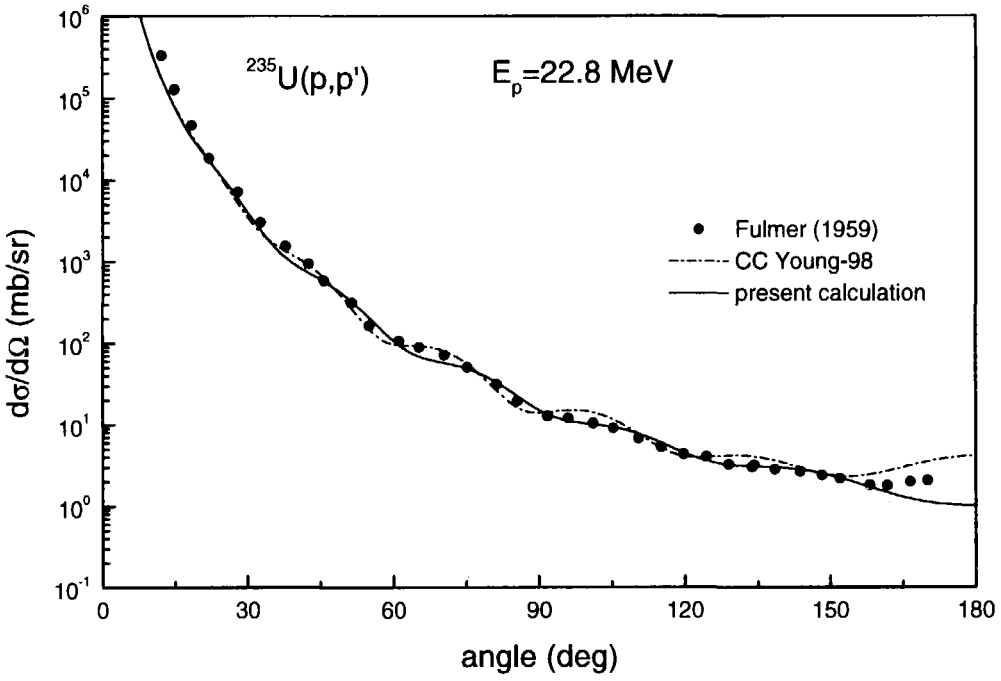

Fig.64 Calculated elastic angular distribution for ^{235}U and experimental data at a primary proton energy equal to 22.8 MeV from Ref.[69].

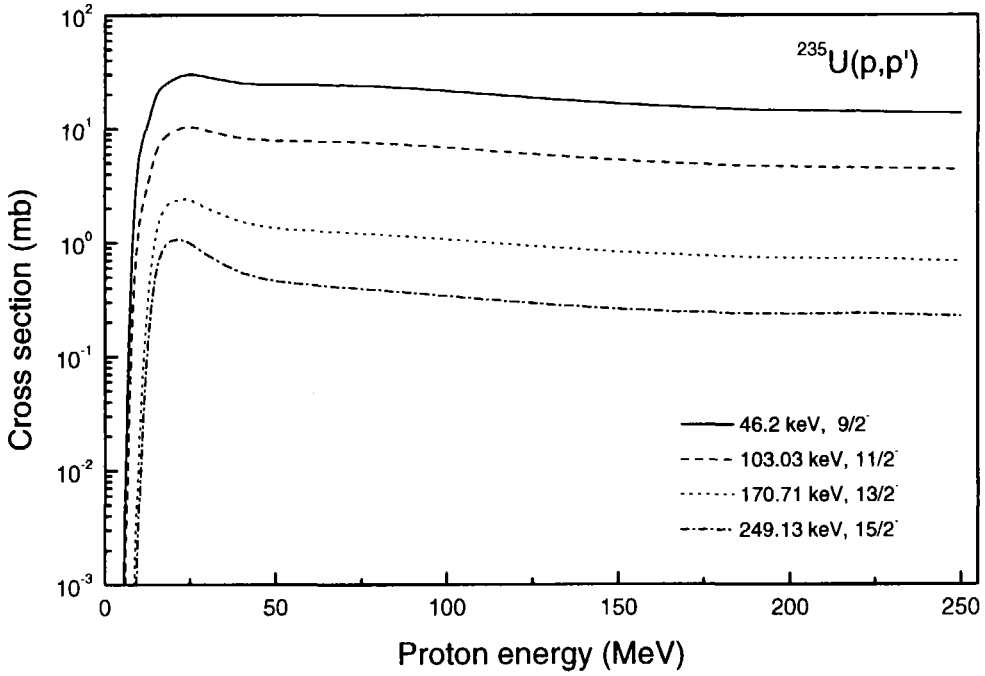

Fig.65 Direct proton inelastic scattering cross sections calculated for ^{235}U for the excited levels 9/2$^-$, 11/2$^-$, 13/2$^-$ and 15/2$^-$, members of the ground-state rotational band.

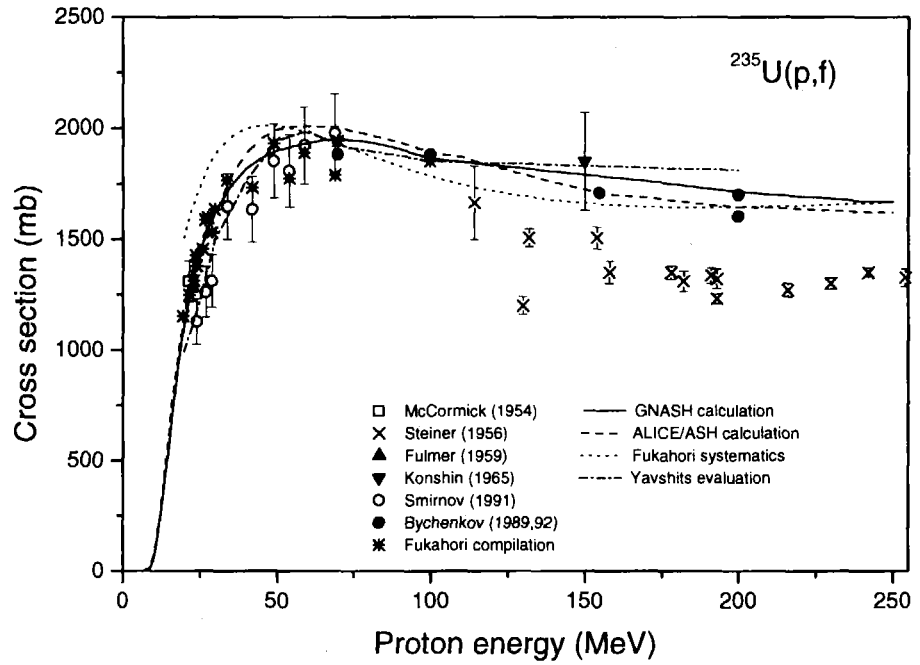

Fig.66 Fission cross section for ^{235}U calculated by GNASH code (solid line), ALICE/ASH code (dashed line), evaluated by the systematics [103] (dotted line), obtained in Ref.[118] (dotted-dashed line) together with the experimental data.

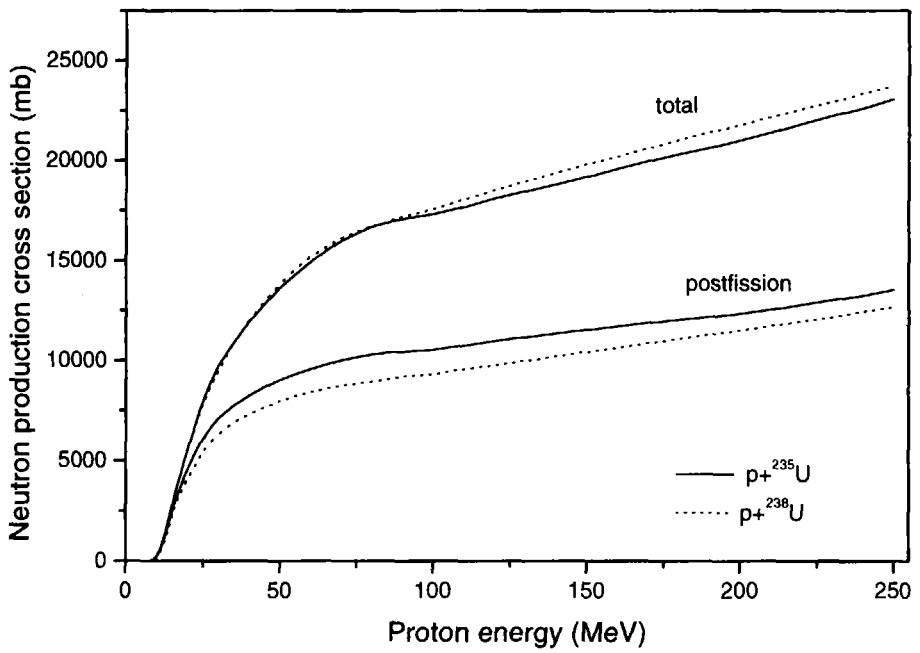

Fig.67 Total neutron production cross section and post-fission evaporation contribution for p+^{235}U (solid line) and p+^{238}U (dotted line) interactions.

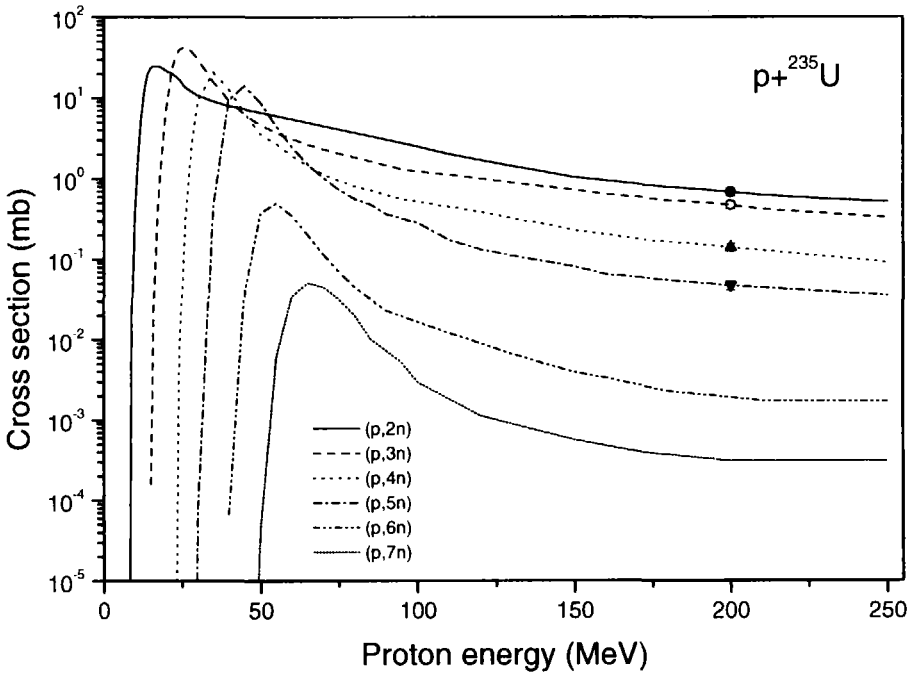

Fig.68 Evaluated (p,xn) reaction cross section for ^{235}U and the experimental data from Ref.[109].

This is a blank page.

国際単位系（SI）と換算表

表1　SI基本単位および補助単位

量	名称	記号
長さ	メートル	m
質量	キログラム	kg
時間	秒	s
電流	アンペア	A
熱力学温度	ケルビン	K
物質量	モル	mol
光度	カンデラ	cd
平面角	ラジアン	rad
立体角	ステラジアン	sr

表2　SIと併用される単位

名称	記号
分，時，日	min，h，d
度，分，秒	°，′，″
リットル	l，L
トン	t
電子ボルト	eV
原子質量単位	u

1 eV=1.60218×10^{-19}J

1 u=1.66054×10^{-27}kg

表3　固有の名称をもつSI組立単位

量	名称	記号	他のSI単位による表現
周波数	ヘルツ	Hz	s^{-1}
力	ニュートン	N	$m\cdot kg/s^2$
圧力，応力	パスカル	Pa	N/m^2
エネルギー,仕事,熱量	ジュール	J	N·m
工率，放射束	ワット	W	J/s
電気量，電荷	クーロン	C	A·s
電位，電圧，起電力	ボルト	V	W/A
静電容量	ファラド	F	C/V
電気抵抗	オーム	Ω	V/A
コンダクタンス	ジーメンス	S	A/V
磁束	ウェーバ	Wb	V·s
磁束密度	テスラ	T	Wb/m^2
インダクタンス	ヘンリー	H	Wb/A
セルシウス温度	セルシウス度	℃	
光束	ルーメン	lm	cd·sr
照度	ルクス	lx	lm/m^2
放射能	ベクレル	Bq	s^{-1}
吸収線量	グレイ	Gy	J/kg
線量等量	シーベルト	Sv	J/kg

表4　SIと共に暫定的に維持される単位

名称	記号
オングストローム	Å
バーン	b
バール	bar
ガル	Gal
キュリー	Ci
レントゲン	R
ラド	rad
レム	rem

1 Å=0.1nm=10^{-10}m

1 b=100fm^2=10^{-28}m^2

1 bar=0.1MPa=10^5Pa

1 Gal=1cm/s^2=10^{-2}m/s^2

1 Ci=3.7×10^{10}Bq

1 R=2.58×10^{-4}C/kg

1 rad=1cGy=10^{-2}Gy

1 rem=1cSv=10^{-2}Sv

表5　SI接頭語

倍数	接頭語	記号
10^{18}	エクサ	E
10^{15}	ペタ	P
10^{12}	テラ	T
10^{9}	ギガ	G
10^{6}	メガ	M
10^{3}	キロ	k
10^{2}	ヘクト	h
10^{1}	デカ	da
10^{-1}	デシ	d
10^{-2}	センチ	c
10^{-3}	ミリ	m
10^{-6}	マイクロ	μ
10^{-9}	ナノ	n
10^{-12}	ピコ	p
10^{-15}	フェムト	f
10^{-18}	アト	a

（注）

1．表1－5は「国際単位系」第5版，国際度量衡局1985年刊行による。ただし，1 eVおよび1 uの値はCODATAの1986年推奨値によった。

2．表4には海里，ノット，アール，ヘクタールも含まれているが日常の単位なのでここでは省略した。

3．barは，JISでは流体の圧力を表わす場合に限り表2のカテゴリーに分類されている。

4．EC閣僚理事会指令ではbar，barnおよび「血圧の単位」mmHgを表2のカテゴリーに入れている。

換算表

力	N(=10^5dyn)	kgf	lbf
	1	0.101972	0.224809
	9.80665	1	2.20462
	4.44822	0.453592	1

粘度　1 Pa·s(N·s/m^2)=10 P(ポアズ)(g/(cm·s))

動粘度　1m^2/s=10^4St(ストークス)(cm^2/s)

圧力	MPa(=10bar)	kgf/cm^2	atm	mmHg(Torr)	lbf/in^2(psi)
	1	10.1972	9.86923	7.50062×10^3	145.038
	0.0980665	1	0.967841	735.559	14.2233
	0.101325	1.03323	1	760	14.6959
	1.33322×10^{-4}	1.35951×10^{-3}	1.31579×10^{-3}	1	1.93368×10^{-2}
	6.89476×10^{-3}	7.03070×10^{-2}	6.80460×10^{-2}	51.7149	1

エネルギー・仕事・熱量	J(=10^7 erg)	kgf·m	kW·h	cal(計量法)	Btu	ft·lbf	eV
	1	0.101972	2.77778×10^{-7}	0.238889	9.47813×10^{-4}	0.737562	6.24150×10^{18}
	9.80665	1	2.72407×10^{-6}	2.34270	9.29487×10^{-3}	7.23301	6.12082×10^{19}
	3.6×10^6	3.67098×10^5	1	8.59999×10^5	3412.13	2.65522×10^6	2.24694×10^{25}
	4.18605	0.426858	1.16279×10^{-6}	1	3.96759×10^{-3}	3.08747	2.61272×10^{19}
	1055.06	107.586	2.93072×10^{-4}	252.042	1	778.172	6.58515×10^{21}
	1.35582	0.138255	3.76616×10^{-7}	0.323890	1.28506×10^{-3}	1	8.46233×10^{18}
	1.60218×10^{-19}	1.63377×10^{-20}	4.45050×10^{-26}	3.82743×10^{-20}	1.51857×10^{-22}	1.18171×10^{-19}	1

1 cal= 4.18605J（計量法）

= 4.184J（熱化学）

= 4.1855J（15℃）

= 4.1868J（国際蒸気表）

仕事率　1 PS(仏馬力)

= 75 kgf·m/s

= 735.499W

放射能	Bq	Ci
	1	2.70270×10^{-11}
	3.7×10^{10}	1

吸収線量	Gy	rad
	1	100
	0.01	1

照射線量	C/kg	R
	1	3876
	2.58×10^{-4}	1

線量当量	Sv	rem
	1	100
	0.01	1

（86年12月26日現在）

Neutron and Proton Nuclear Data Evaluation for ^{235}U and ^{238}U at Energies up to 250 MeV